GDAŃSK UNIVERSITY OF TECHNOLOGY

Faculty of Civil and Environmental Engineering

The author of the PhD dissertation: Mohamad-Javad Mehrani
Scientific discipline: Environmental Engineering, Mining and Energy

DOCTORAL DISSERTATION

Title of PhD dissertation: Application of mechanistic and data-driven models for nitrogen removal in wastewater treatment systems

Title of PhD dissertation (in Polish): Zastosowanie modeli mechanistycznych i opartych na danych do usuwania azotu w systemach oczyszczania ścieków

Supervisor *signature*	Co-supervisor *signature*
prof. dr hab. inż. Jacek Mąkinia	dr inż. Dominika Sobotka

Gdańsk, June 2022

GDAŃSK UNIVERSITY OF TECHNOLOGY

Faculty of Civil and Environmental Engineering

STATEMENT

The author of the PhD dissertation: **Mohamad-Javad Mehrani**

I, the undersigned, agree that my PhD dissertation entitled:
"Application of mechanistic and data-driven models for nitrogen removal in wastewater treatment systems" may be used for scientific or didactic purposes.[1]

Gdańsk June 2022 ..... *signature of the PhD student*

Aware of criminal liability for violations of the Act of 4th February 1994 on Copyright and Related Rights (Journal of Laws 2006, No. 90, item 631) and disciplinary actions set out in the Law on Higher Education (Journal of Laws 2012, item 572 with later amendments),[2] as well as civil liability, I declare, that the submitted PhD dissertation is my own work.

I declare, that the submitted PhD dissertation is my own work performed under supervision of **prof. dr hab. inż. Jacek Mąkinia** and **dr inż. Dominika Sobotka**.

This submitted PhD dissertation has never before been the basis of an official procedure associated with the awarding of a PhD degree.

All the information contained in the above dissertation which is derived from written and electronic sources is documented in a list of relevant literature in accordance with art. 34 of the Copyright and Related Rights Act.

I confirm that this PhD dissertation is identical to the attached electronic version.

Gdańsk June 2022 ..... *signature of the PhD student*

I, the undersigned, agree to include an electronic version of the above PhD dissertation in the open, institutional, digital repository of Gdańsk University of Technology, Pomeranian Digital Library, and for it to be submitted to the processes of verification and protection against misappropriation of authorship.

Gdańsk June 2022 ..... *signature of the PhD student*

[1] Decree of Rector of Gdansk University of Technology No. 34/2009 of 9th November 2009, TUG archive instruction addendum No. 8.

[2] Act of 27th July 2005, Law on Higher Education: Chapter 7, Criminal responsibility of PhD students, Article 226.

GDAŃSK UNIVERSITY OF TECHNOLOGY

Faculty of Civil and Environmental Engineering

DESCRIPTION OF DOCTORAL DISSERTATION

The Author of the PhD dissertation: Mohamad-Javad Mehrani

Title of PhD dissertation: Application of mechanistic and data-driven models for nitrogen removal in wastewater treatment systems

Language of PhD dissertation: English

Supervision: prof. dr hab. inż. Jacek Mąkinia

Co-supervision: dr inż. Dominika Sobotka

Date of doctoral defence:

Keywords of PhD dissertation in English: Mathematical modelling; data-driven; wastewater treatment; Comammox; nitrous oxide (N_2O); Nitrification, Deammonification, model development

Keywords of PhD dissertation in Polish: Modelowanie matematyczne; oparte na danych; oczyszczanie ścieków; Comammoks; podtlenek azotu (N_2O); Nitryfikacja, Amonifikacja, opracowanie modelu

Summary of PhD dissertation in English:

In this dissertation, the application of mechanistic and data-driven models in nitrogen removal systems including nitrification and deammonification processes was evaluated. In particular, the influential parameters on the activity of the *Nitrospira* activity were assessed using response surface methodology (RSM). Various long-term biomass washout experiments were operated in two parallel sequencing batch reactor (SBR) with a different temperature, aeration mode and substrates and were used for the modelling data source. In the next step, three extension models for the complete ammonia oxidation (comammox) process were developed using the GPS-X simulation software. The extensions were incorporated in the conventional two-step nitrification model. The developed comammox model accurately predicted nitrogen species, biomass concentrations and microbiological indexes. In addition, the contribution of the comammox in nitrogen conversion was generated using Sankey graphs under different operational conditions. Moreover, prediction of the N_2O emission in the liquid phase during the nitrification systems was evaluated using hybrid mechanistic/machine learning (ML) method (GPS-X and python programming). In addition, various feature selections (FS) was applied to figure out the effective factors on the production of the N_2O emission in the SBR nitrification systems. Finally, a model-based optimization of aeration was performed using GPS-X on the mainstream deammonification system was carried out, in which the DO value and on/off ratio were the variables and N removal rate (NRR) and N removal efficiency (NRE) were the target of optimization.

Summary of PhD dissertation in Polish:

W niniejszej rozprawie oceniono zastosowanie modeli mechanistycznych i opartych na danych w systemach usuwania azotu, w tym w procesach nitryfikacji i deamonifikacji. Następnie, za pomocą metodologii powierzchni odpowiedzi (RSM) oceniono czynniki mające wpływ na aktywność bakterii *Nitrospira*. W trakcie badań przeprowadzono serię eksperymentów, w których określono wpływ temperatury, sposobu napowietrzania oraz rodzaju substratu na proces częściowej nitryfikacji (czyli wymywania bakterii NOB) prowadzony w reaktorze sekwencyjnym (SBR). Uzyskane wyniki stanowiły źródło danych do modelowania matematycznego w programie GPS-X. W ramach przeprowadzonych badań opracowano trzy modele matematyczne procesu comammox uwzględniające jego rolę w konwersji azotu i włączono je do modelu konwencjonalnej dwustopniowej nitryfikacji. Opracowany model comammox dokładnie przewidywał stężenia poszczególnych form azotu, stężenia biomasy jak również wskaźniki mikrobiologiczne. W oparciu o wykresy Sankeya (sporządzone dla zróżnicowanych warunków eksploatacyjnych) określono udział procesu comammox w badanych procesach konwersji azotu. Dzięki zastosowaniu hybrydowej metody mechanistycznej/uczenia maszynowego (modelowanie w GPS-X i programowanie w Python), przeprowadzono modelowanie emisji N_2O (w fazie ciekłej) w procesie nitryfikacji. Określenie efektywnych współczynników emisji N_2O w reaktorach SBR pracujących w procesie nitryfikacji wykonano z zastosowaniem różnych metod selekcji cech (FS). W ostatnim etapie badań przeprowadzono optymalizację systemu napowietrzania w procesie deamonifikacji w ciągu głównym w oparciu o model sporządzony w programie GPS-X. Przyjęto, iż wartości stężenia tlenu rozpuszczonego i współczynnika włączenia i wyłączenia systemu napowietrzania (on/off) były zmiennymi, a szybkość i efektywność usuwania azotu były celem optymalizacji.

GDAŃSK UNIVERSITY OF TECHNOLOGY

Faculty of Civil and Environmental Engineering

Mohamad-Javad Mehrani

Application of mechanistic and data-driven models for nitrogen removal in wastewater treatment systems

DOCTORAL DISSERTATION

Supervisor:

prof. dr hab. inż. Jacek Mąkinia

Co-supervisor:

dr. inż. Dominika Sobotka

GDAŃSK, JUNE 2022

General Acknowledgments

*First, I am grateful to **God** for the good health and well-being .Moreover, I would like to warmly acknowledge my supervisor **Professor Mąkinia** for providing me with this opportunity to do my doctorate under his supervision. Indeed, his educational support and advice in every step, made me a professional researcher. Superior thanks to **Dr. Sobotka** for her support as my co-supervisor as well. She kindly helped me in this journey, especially in experimental works and analytical analysis.*

*I am also grateful to all my advisors and co-authors, especially **Professor Guo** and **Dr. Zheng** from **Queensland University, Australia,** together with **Professor Denecke** and **Dr. Azari** from **Duisburg-Essen University, Germany** that I had the chance to complete my internship under their supervision in the summer 2021.*

*I have to thank my colleagues who have helped me in different stages of this journey, especially **Dr. Kowal** for his contribution to the microbiological analysis, **Luci** for her help in modeling, and **Moji** for our firm friendship.*

*Most importantly, none of this could have happened without my family's reliance. I wish to express my sincere thanks to my **parents, two sisters,** and **my wife Niloo** for their encouragement, permanent support, and unconditional love. It was not possible to obtain this degree without their accompanying.*

I also place on record, my sense of gratitude to everyone who directly or indirectly supported or encouraged me in this venture.

Funding Acknowledgements

*Special acknowledgments are given to the **Polish National Science Center** for project no. UMO-2017/27/B/NZ9/01039 and the **Gdańsk University of Technology** for financial support in **Beta Scholarship** and **Young Scientists programs**. Moreover, I appreciate the support from the **Integrated development program** of the university for providing the grant under the **European Union Horizon 2020** for doing my internship at Duisburg-Essen University.*

Table of contents

Summary:

This comprehensive research study focused on the application of mechanistic and data-driven models in nitrogen removal systems and was carried out in four steps as follows.

First, the presence and role of *Nitrospira* in nitrogen removal systems, including nitrification and deammonification processes, were investigated based on literature data. This part of the study was focused on the present state of knowledge about the morphological, physiological, and genetic properties of the canonical and comammox *Nitrospira*. The functional characteristics of nitrogen removal have been noted as potential consequences of comammox by *Nitrospira* as well. To find particular variables and their combined interactions on *Nitrospira* abundance, a comprehensive meta-analysis of literature data was used using numerical analysis by response surface methodology (RSM) to investigate a relationship between individual or interaction of variables on the *Nitrospira* activity as one of the novelties of this research. More than 100 studies were evaluated and sufficient data were generated from the literature. Input independent variables were dissolved oxygen (DO) concentration, influent NH_4-N concentration, pH, and temperature and the response was activity (grow or suppression) of *Nitrospira* bacteria during the nitrification process. Results of the RSM showed that high DO (> 3.0 mg O_2/L) and high influent NH_4-N (> 20 mg N/L), as well as low temperature (15 °C) and pH (7) were expected to produce the highest *Nitrospira* abundances. On the contrary, the simultaneous criteria for the lowest *Nitrospira* abundances could not be defined without ambiguity. Hence, DO and influent NH_4-N concentrations in addition to temperature and pH can play an important role in increasing or suppressing *Nitrospira* activity.

In the second stage, three comammox models were proposed and the IWA Activated Sludge Model (ASM1) was expanded for the two-step nitrification and comammox model. The developed models were proposed in this study for the first time (to the best of our knowledge). Two series of long-term biomass washout experiments were carried out in a laboratory sequencing batch reactor (SBR) at 12 and 20 ℃ and were used for model calibration and validation. Based on the behaviour of Ammonia (NH_4-N), Nitrite (NO_2-N), and Nitrate (NO_3-N) in the bioreactor, the efficiency of the examined models was compared. The developed comammox model predicted nitrogen species, and biomass concentrations, with a high degree of accuracy (R^2=0.80). Furthermore, sensitivity and correlation research revealed that the maximum growth rates (μ), oxygen half-saturation (K_O), and decay rates (b) of the canonical nitrifiers and comammox were the most sensitive factors, with the highest correlation between b and all other kinetic parameters studied. In addition, Sankey graphs were generated to visualize the contribution of the comammox in nitrogen conversions. According to the simulation results, comammox could be responsible for converting more than 20% of the influent ammonia load. As a result, the importance of comammox in the nitrogen mass balance in activated sludge systems should not be overlooked, and more research is needed. For ammonia-oxidizing bacteria

(AOB), nitrite-oxidizing bacteria (NOB), and comammox bacteria, the best model estimated μ were 0.57d^{-1}, 0.11 d^{-1}, and 0.15 d^{-1} correspondingly.

Furthermore, the extended proposed model in the previous stage was applied for forecasting the N_2O production in an activated sludge bioreactor. According to a combined mechanistic and machine learning (ML) approach, a new technique for forecasting liquid N_2O generation during nitrification was developed. Two long-term nitrifying experiments in a sequencing batch reactor (SBR) were initially simulated using a mechanistic model (extended two-step nitrification and comammox model in the previous stage). Then, model predictions (NH_4-N, NO_2-N, NO_3-N, MLSS, MLVSS) were combined with recorded online observations (DO, pH, temperature) and used as input data for ML models. Three ML algorithms including the artificial neural network (ANN), the gradient boosting machine (GBM), and the support vector machine (SVM) were compared. Simulation results revealed that the ANN had the most accurate prediction model, and it was exposed to a 95% confidence interval analysis for calculating the data population error range. Various feature selection (FS) methods, such as Pearson correlation and random forest (RF), were also applied to find the most important characteristics driving liquid N_2O forecasts. The findings of the FS analysis revealed that NH_4-N concentration followed by NO_2-N concentration had the strongest link with the N_2O generation.

In the end, the application of the modeling in the real deammonification system was assessed. The model-based optimization was applied for the prediction and aeration optimization of mainstream deammonification in an integrated fixed-film activated sludge (IFAS) pilot plant under seasonal temperature changes. During a winter season and a transition phase to summer conditions, the influence of continuously decreasing temperature on the performance of the deammonification process was assessed, and the correlation of performance metrics was explored using principal component analysis (PCA). The N-removal rate (NRR) and N-removal efficiency (NRE) were maximized by optimizing the intermittent aeration in long-term (30 days) dynamic circumstances with on/off ratio and dissolved oxygen (DO) set-point management. Results of the optimization showed that the DO set-point of 0.2–0.25 mgO_2/L, and on/off ratio of 0.05 were the best pair variables for achieving the highest NRE and NRR in the system.

Summary (in Polish):

Niniejsze opracowanie stanowi kompleksowe badanie naukowe skupiające się na modelowaniu procesów usuwania azotu, które przeprowadzono w czterech etapach.

W pierwszej kolejności zbadano obecność i rolę procesu całkowitego utleniania amoniaku (comammox) przez pojedynczy mikroorganizm „*Nitrospira*" w systemach do biologicznego usuwania azotu, w tym w procesach nitryfikacji i deamonifikacji. W tej części badań skoncentrowano się na obecnym stanie wiedzy na temat właściwości morfologicznych, fizjologicznych i genetycznych bakterii *Nitrospira* kanonicznej i Comammox. Funkcjonalne cechy usuwania azotu zostały odnotowane jako potencjalne konsekwencje prowadzenia procesu comammox przez bakterie *Nitrospira*. Aby znaleźć poszczególne zmienne indywidualne oraz ich połączone interakcje dotyczące liczebności bakterii *Nitrospira*, zastosowano kompleksową meta analizę danych literaturowych przy użyciu analizy numerycznej metodą powierzchni odpowiedzi (RSM), co stanowi nowość w tego typu opracowaniach. W tym celu przeprowadzono obszerny przegląd literatury, liczący ponad 100 pozycji. Wejściowymi zmiennymi niezależnymi były stężenie rozpuszczonego tlenu (DO), stężenie NH_4-N na dopływie do reaktora, pH i temperatura, a odpowiedzią była aktywność bakterii *Nitrospira* podczas procesu nitryfikacji. Wyniki RSM wykazały, że wysokie stężenie DO (> 3,0 mg O_2/L) i NH_4-N na dopływie do reaktora (> 20 mg N/L), a także niska temperatura (15 °C) i pH (7) skutkowały najwyższą liczebnością bakterii *Nitrospira*. Przeprowadzona analiza nie umożliwiła jednoznacznego zdefiniowania kryteriów, przy których liczebność bakterii *Nitrospira* była najmniejsza. Dlatego też stężenia DO i NH_4-N na dopływie do reaktora, oprócz temperatury i pH, mogą odgrywać ważną rolę w promowaniu lub inhibitowaniu aktywności bakterii *Nitrospira*.

W drugim etapie zaproponowano trzy modele comammox w oparciu o jego rolę w systemie nitryfikacji. Opracowano model osadu czynnego (ASM1) do dwustopniowej nitryfikacji i modele procesu comammox. Opracowane modele comammox zostały zaproponowane w niniejszym opracowaniu po raz pierwszy (według naszej najlepszej wiedzy). Przeprowadzono dwie serie długoterminowych doświadczeń wymywania biomasy w laboratoryjnym reaktorze sekwencyjnym (SBR) w temperaturze 12 i 20 °C, które posłużyły do kalibracji i walidacji modelu. Na podstawie trendu zmian stężeń amoniaku, azotynów i azotanów w bioreaktorze porównano efektywności badanych modeli. Opracowany model comammox przewidział z dużą dokładnością (R^2=0,80) zarówno stężenia poszczególnych form azotu, jak i stężenia biomasy. Ponadto badania wrażliwości i korelacji wykazały, że maksymalna szybkość wzrostu (μ), stała nasycenia dla DO (K_O) i szybkość rozkładu (b) kanonicznych nitryfikatorów i bakterii comammox były najbardziej wrażliwymi czynnikami, przy czym najwyższa korelacja miała miejsce między b a wszystkimi innymi badanymi parametrami kinetycznymi. Ponadto wygenerowano wykresy Sankeya, aby obliczyć udział procesu

comammox w badanych procesach konwersji azotu. Zgodnie z wynikami symulacji, comammox może być odpowiedzialny za konwersję ponad 20% dopływającego ładunku amoniaku. W rezultacie nie należy pomijać znaczenia procesu comammox w systemach osadu czynnego, lecz prowadzić dalsze badania w tym zakresie. Dla bakterii utleniających amoniak (AOB), bakterii utleniających azotyny (NOB) i bakterii comammox najlepszy model oszacował parametry kinetyczne odpowiednio na 0,57 d^{-1}, 0,11 d^{-1} i 0,15 d^{-1}.

Ponadto do prognozowania produkcji N_2O zastosowano rozszerzony model zaproponowany w poprzednim etapie. Zgodnie z połączonym podejściem mechanistycznym i maszynowym (ML) opracowano nową technikę prognozowania emisji N_2O w fazie ciekłej podczas nitryfikacji. Dwa długoterminowe eksperymenty nitryfikacyjne w reaktorze sekwencyjnym (SBR) były początkowo symulowane przy użyciu modelu mechanistycznego (rozszerzony dwuetapowy model nitryfikacji i comammox w poprzednim etapie). Następnie, przewidywania modeli (NH_4-N, NO_2-N, NO_3-N, MLSS, MLVSS) połączono z zarejestrowanymi obserwacjami online (DO, pH, temperatura) i wykorzystano jako dane wejściowe dla modeli ML. Porównano trzy algorytmy ML, w tym sztuczną sieć neuronową (ANN), maszynę wzmacniającą gradient (GBM) i maszynę wektorów nośnych (SVM). Wyniki symulacji wykazały, że SSN miała najdokładniejszy model predykcyjny i została poddana analizie 95% przedziału ufności w celu obliczenia zakresu błędu populacji danych. W celu znalezienia najważniejszych cechy decydujące o prognozach N_2O wykorzystano różne metody selekcji cech (FS), takie jak korelacja Pearsona i klasyfikacja metodą lasu losowego (RF). Wyniki analizy FS wykazały, że stężenie NH_4-N, a następnie NO_2-N miało najsilniejszy związek z emisją N_2O.

Na koniec oceniono zastosowanie modelowania w rzeczywistym systemie deamonifikacji. Optymalizacja oparta na modelu została zastosowana do przewidywania i optymalizacji napowietrzania w procesie deamonifikacji w ciągu głównym w zintegrowanej pilotażowej instalacji osadu czynnego o stałej warstwie (IFAS) w warunkach sezonowych zmian temperatury. W sezonie zimowym oraz w fazie przejściowej do warunków letnich oceniono wpływ stale obniżającej się temperatury na efektywność procesu deamonifikacji, oraz zbadano korelację wskaźników efektywności przy użyciu analizy głównych składowych (PCA). Szybkość i efektywność usuwania azotu (odpowiednio NRR i NRE) zostały zmaksymalizowane poprzez optymalizację naprzemiennego napowietrzania w długoterminowych warunkach (30 dni) ze stosunkiem włączania/wyłączania (on/off) i zarządzaniem nastawą stężenia DO. Wyniki optymalizacji wykazały, że nastawa DO wynosząca 0,2–0,25 mg O_2/L oraz współczynnik on/off 0,05 były najlepszymi parami zmiennych do osiągnięcia najwyższych wartości NRE i NRR w systemie.

List of PhD papers

The following papers were derived from each step of this PhD dissertation as follows:

Paper I: M-J Mehrani, D Sobotka, P Kowal, S Ciesielski, J Makinia. 2020. The occurrence and role of *Nitrospira* in nitrogen removal systems, **Bioresource Technology,** 303, 122936. https://doi.org/10.1016/j.biortech.2020.122936

Paper II: M-J Mehrani, X Lu, P Kowal, D Sobotka, J Mąkinia. 2021. Incorporation of the complete ammonia oxidation (comammox) process for modeling nitrification in suspended growth wastewater treatment systems. **Journal of Environmental Management,** 297, 113223. https://doi.org/10.1016/j.jenvman.2021.113223

Paper III: M-J Mehrani, F Bagherzadeh, M Zheng, P Kowal, D Sobotka, J Makinia. 2022. Application of a hybrid mechanistic/machine learning model for prediction of nitrous oxide (N_2O) production in a nitrifying sequencing batch reactor. **Process Safety and Environmental Protection,** 162, 1015-1024. https://doi.org/10.1016/j.psep.2022.04.058

Paper IV: M-J Mehrani, M Azari, B Teichgraber, P Jagemann, J Schoth, M Denecke, J Mąkinia. 2022. Performance evaluation and model-based optimization of the mainstream deammonification in an integrated fixed-film activated sludge reactor. **Bioresource Technology,** 351, 126942. https://doi.org/10.1016/j.biortech.2022.126942

Journal metrics

The points value and basic journal metric based on Impact Factor for each journal are listed in the below table.

Table. Journal points and Impact Factor

Paper	Journal	Point value*	Impact Factor	Cite Score
I	Bioresource Technology	140	9.64	14.8
II	Journal of Environmental Management	100	6.78	9.8
III	Process Safety and Environmental Protection	100	6.15	8.9
IV	Bioresource Technology	140	9.64	14.8

**Points are represented based on the Polish Ministry of Science and Higher Education*

Copyrights

Authors contribution to the papers

Paper I:

MJ. Mehrani: Investigation, Formal analysis, Visualization, Software, Methodology, Writing - Original Draft, Data Curation.

D. Sobotka: Methodology, Writing – Original draft, review & editing.

P. Kowal: Methodology, Writing – review & editing.

S. Ciesielski: Writing – review & editing.

J. Mąkinia: Investigation, Supervision, Funding acquisition, Conceptualization, Writing – review & editing.

Paper II:

MJ. Mehrani: Investigation, Conceptualization, Software, Formal analysis, Methodology, Visualization, Writing – original draft.

X. Lu: Software, Formal analysis.

P. Kowal: Experimental and Data collection, Data Curation, Writing – review & editing.

D. Sobotka: Experimental and Data collection, Data Curation, Writing – review & editing.

J. Mąkinia: Supervision, Conceptualization, Funding acquisition, Writing – review & editing.

Paper III:

MJ. Mehrani: Investigation, Conceptualization, Software, Data Curation, Formal analysis, Methodology, Visualization, Writing – original draft.

F. Bagherzadeh: Data Curation, Visualization.

M Zheng: review & editing.

D. Sobotka: Data curation, Writing – reviewing & editing.

P. Kowal: Experimental and Data collection, Data curation, Writing – review & editing.

J. Guo: Supervision, Writing – review & editing.

J. Mąkinia: Conceptualization, Funding acquisition, Supervision, Writing – review & editing

Paper IV:

MJ. Mehrani: Investigation, Conceptualization, Software, Data Curation, Formal analysis, Methodology, Visualization, Writing – original draft.

M. Azari: Data curation, Methodology, Writing – reviewing & editing

B. Teichgraber: reviewing & editing.

J. Schoth: Experimental and Data collection.

P. Jagemann: Experimental and Data collection.

M. Denecke: Supervision, review & editing.

J. Mąkinia: Conceptualization, Funding acquisition, Supervision, review & editing

Other publications from my PhD study

-P Kowal, **MJ Mehrani**, D Sobotka, S Ciesielski, J Makinia. 2022. Rearrangement of the Nitrifying Bacteria Population in Activated Sludge Under Short Solids Retention Times, **Environmental Research**, (*accepted*).

- **MJ Mehrani**, P Kowal, D Sobotka, J Guo, J Makinia. 2022. New insights into modeling two-step nitrification in activated sludge systems – the effects of initial biomass concentrations, comammox, and heterotrophic activities, (*submitted*).

- **MJ Mehrani**, P Kowal, D Sobotka, J Guo, S Ciesielski, J Makinia. 2022. The coexistence and competition of canonical and comammox nitrite-oxidizing bacteria (NOB) in a nitrifying activated sludge system – experimental observations and simulation studies, (*submitted*).

International collaboration during my PhD study

-F. Bagherzadeh, **MJ. Mehrani**, M. Basirifard, J. Roostaei. 2021. Comparative study on total nitrogen prediction in wastewater treatment plant and effect of various feature selection methods on machine learning algorithms performance. **Water Process Engineering,** 41, 102033.

https://doi.org/10.1016/j.jwpe.2021.102033.

-F. Bagherzadeh, A. Shojaei Nouri, **MJ. Mehrani**, S. Thennadil. 2021. Prediction of energy consumption and evaluation of affecting factors in a full-scale WWTP using a machine learning approach. **Process Safety and Environmental Protection,** 154, 458–466.

https://doi.org/10.1016/j.psep.2021.08.040

-G. Kirim, et al. 2022. Mainstream short-cut N removal modelling: current status and perspectives. **Water Science & Technology**, (1), 325-332.

https://doi: 10.2166/wst.2022.131

-B. Szelag, **MJ. Mehrani**, J. Drewnowski, M. Majewska, G. Lagod, S. Kumari. 2021. Assessment of wastewater quality indicators for wastewater treatment influent using an advanced logistic regression model. **Desalination Water Treatment,** *232*, 421-432

Conference presentations during my PhD study:

MJ. Mehrani, D. Sobotka, J. Makinia. Modelling of NOB wash-out in nitrification process at low temperature. 11th Eastern European, Young Water Professionals Conference, 1-5 October 2019, Prague, **Czech Republic.**

MJ. Mehrani, D. Sobotka, J. Makinia. Modelling of wash-out process in the activated sludge system. 2nd IWA Polish Young Water Professionals Conference, 12-14 February 2020, Warsaw, **Poland.**

MJ. Mehrani, D. Sobotka,, P. Kowal, S. Ciesielski, J. Makinia. Modelling and experimental study of NOB wash-out at low temperature from an activated sludge system. IWA Nutrient Removal and Recovery Conference, 8 - 12 June 2020, Helsinki, **Finland**.

MJ Mehrani, D. Sobotka,, P. Kowal, J. Makinia. Model development for integration of complete ammonia oxidation (comammox) into the two-step nitrification activated sludge systems. EWWM virtual Conference 28-29 September 2021, Birmingham, **United Kingdom.**

MJ. Mehrani, M. Azari, M. Denecke, J. Makinia. Simulation and optimization of the deammonification process for treating mainstream WWTP under decreasing temperature. WRR modeling virtual conference, 21-25 August 2021, Arosa, **Switzerland**.

MJ. Mehrani, D. Sobotka,, P. Kowal, J. Makinia. Model development for complete ammonia oxidation (comammox) in the two-step nitrification activated sludge systems. IWA Wastewater, Water and Resource Recovery Conference, 10 – 13 April 2022, Poznan, **Poland.**

Nomenclature and abbreviations

Item	Description
ANN	Artificial Neural Network
AOB	Ammonia Oxidizing Bacteria
ASM	Activated Sludge Model
BNR	Biological Nutrient Removal
COD	Chemical Oxygen Demand
CMX	Complete Ammonia Oxidation
DHET	Denitrifying Heterotrophic Bacteria
FS	Feature Selection
GBM	Gradient Boosting Machine
GHG	Greenhouse Gas
HET	Heterotrophic Bacteria
SA	Sensitivity Analysis
SVM	Support Vector Machine
ML	Machine Learning
MLSS	Mixed Liquor Suspended Solids
MLVSS	Mixed volatile Liquor Suspended Solids
N	Nitrogen
N_2O	Nitrous oxide
NRE	Nitrogen Removal Efficiency
NRR	Nitrogen Removal Rate
NOB	Nitrite Oxidizing Bacteria
PCA	Principal Component Analysis
TN	Total Nitrogen
VSS	Volatile Suspended Solids
WWTP	Wastewater Treatment Plant

1 INTRODUCTION

The activated sludge process has been widely used to deal with a wide range of municipal and industrial sewage. This process has become essential in municipal & industrial wastewater treatment plants (WWTPs) (Makinia and Zaborowska, 2020). Nitrogen (N) removal is a vital process in the WWTP and is done by nitrification and denitrification processes which is a resource and energy-intensive processes. Nitrification requires oxygen and alkalinity, while denitrification requires carbon as either influent or supplementary carbon. Nitrification is a key process of N removal in municipal WWTPs, consisting of two steps: ammonia oxidation to nitrite (nitritation) followed by nitrite oxidation to nitrate (nitratation) (Ma et al., 2016; Zhang et al., 2020a).

Heterotrophic denitrifying bacteria (HDN) use electrons donated by organic materials to convert the nitrate (and nitrite) to nitrogen gas. This combined process requires a large amount of energy to provide oxygen for consumption by ammonium oxidation bacteria (AOB) and nitrite oxidation bacteria (NOB) during the nitrification, as well as organic matter for denitrification (Ma et al., 2016; Metcalf and Eddy, 2014).

Although nitrification has been known since the end of the 19th century, the process of understanding has changed dramatically in recent 30 years, which was reflected by the evolving descriptions in Metcalf and Eddy handbook series (Metcalf and Eddy, 2003; Metcalf and Eddy, 2014; Metcalf and Eddy, 1991). The improved understanding of the mechanisms of nitrification has been accompanied by growing attention to nitrite as a central component in the novel autotrophic N removal processes, including deammonification and a shortcut of nitrification-denitrification via nitrite ("nitrite shunt"). As a consequence, the role of NOB has received growing attention, but due to the limited knowledge of their metabolism, NOB remains a "*big unknown of the nitrogen cycle*" (Daims et al., 2016).

Very recent advances in modeling two-step nitrification include examination of the competition among the AOB and NOB species for different r/K strategist groups for AOB and NOB (Yu et al., 2020), and incorporation of comammox (Mehrani et al., 2021). The nitrification models should accommodate appropriately the behavior of AOB and NOB to understand factors influencing the competition between autotrophic N-converting microorganisms (Cao et al., 2017; Kaelin et al., 2009).

An efficient approach to investigate the nitrifier competition under selective pressures would be a combination of dedicated laboratory experiments with mathematical modeling and advanced microbiological analyses. Two-step nitrification models have been known for over 50 years (Knowles et al., 1965), but a simple Monod-type model for ammonia-oxidizing to nitrate (as a one-step conversion) was sufficient under typical operating conditions of activated sludge systems (Henze, 2000). Since the 2000s, with recognizing the central role of nitrite in the novel N removal systems, the interest in two-step models has been growing.

In particular, the recent discovery of complete ammonia oxidation (comammox) by a single *Nitrospira*-type microorganism (Daims et al., 2015; van Kessel et al., 2015) has overturned "*a century-old dogma of nitrification research*". However, the actual role of comammox-*Nitrospira* in full-scale WWTPs is ambiguous (Koch et al., 2019). Figure 1 shows the difference between conventional two-step nitrification and a model extension with comammox. Moreover, according to the r/K theory, the nitrifying bacteria can be divided into r- and K-strategists. The fast-growing r-strategists are represented by AOB *Nitrosomonas* and NOB *Nitrobacter*, whereas NOB *Nitrospira* is the K-strategist with a high substrate affinity (Yin et al., 2022; Yu et al., 2020). The assumptions of r/K theory are a base for the development of various NOB washout strategies in the novel N removal systems.

The controlled solids retention time (SRT), combined with dissolved oxygen (DO)-limited conditions and high residual ammonia, have been identified as the most common NOB wash-out strategies (Gustavsson et al., 2020; Regmi et al., 2014). However, low DO concentrations (<1.0 mg O_2/L) can be inefficient in the suppression of K-strategist NOB (*Nitrospira)* (Cao et al., 2017). Moreover, the low temperature has also been reported as a significant obstacle to NOB suppression (Gilbert et al., 2014; Laureni et al., 2016).

The occurrence and role of comammox in different N removal systems were investigated and the effect of influencing factors on the growing or suppression of the comammox *Nitrospira* was assessed together with the meta-analysis of literature between *Nitrospia* and the most influential parameters was carried out in the **Paper I**.

Mathematical models are commonly employed in the mainstream application of deammonification to simulate the behavior of biological processes under various operating

scenarios and cost-effectiveness. There are two kinds of models - including mechanistic (white box) and data-driven (black-box) models. Mechanistic models are developed using fundamental technical and scientific knowledge of a process that occurs within the represented system (Makinia and Zaborowska 2020) . When many of these assumptions are introduced only to simplify the theoretical description, the goal of these models is to predict behavior given assumptions about governing processes. The data-driven models can be used when mechanisms involved in a system are either scarce, non-existent, or unimportant. ANN and MVS are examples of such models that detect and quantify correlations between process variables without requiring knowledge of the process.

Incorporation of the comammox process into the two-step nitrification in three various scenarios was carried out using a mechanistic model in **Paper II** and the most accurate model in terms of N components and biomass concentration prediction was introduced for further investigation.

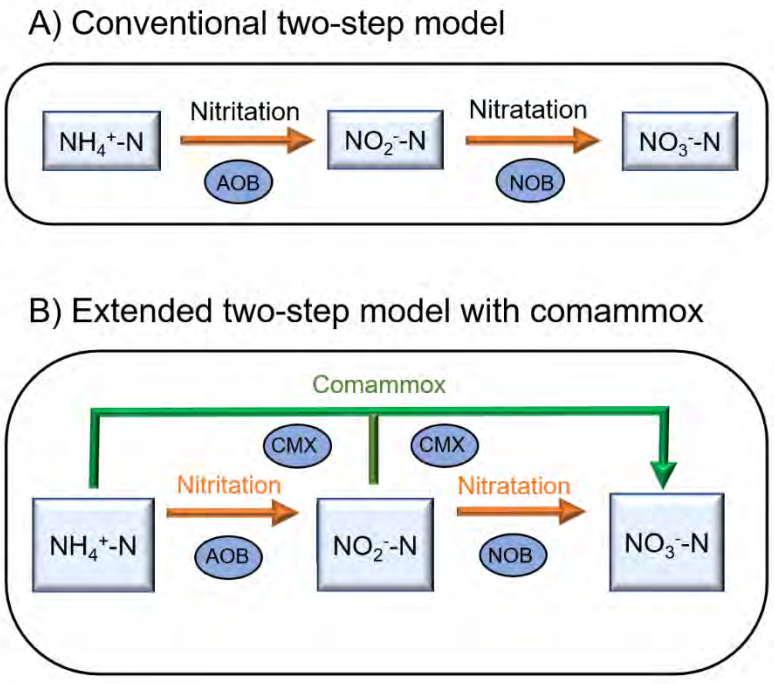

Figure 1- Conventional and extended twostep nitrification with comammox models

In WWTPs, part of the influent nitrogen load is transformed into nitrous oxide (N_2O) and released into the environment from the open-air treatment tank (Lin et al., 2018). N_2O is a major greenhouse gas (GHG) with a global warming potential (GWP) of 298 (Chen et al., 2020; IPCC, 2014). N_2O emissions have consistently been increasing in recent decades in WWTP,

accounting for 3.4% of the worldwide N_2O emissions (IPCC, 2014). As a result, minimizing N_2O generation in WWTPs is a novel research priority (Maktabifard et al., 2022; Vasilaki et al., 2019). AOB and HDN are the primary microorganisms that generate N_2O during biological nitrogen removal (Zaborowska et al., 2019).

To describe the N_2O production pathways in WWTPs, a variety of mathematical mechanistic models have been used. Models based on data-driven approaches have also been developed to incorporate N_2O production from various processes into the design, operation, and optimization of biological processes (Domingo-Félez et al., 2017; Duan et al., 2020). N_2O emission models have been introduced in biological nitrogen removal systems and have matured to the point where they can be used to help with process optimization in conventional N removal systems (Duan et al., 2020; Vasilaki et al., 2020a).

One of the most significant obstacles to using N_2O models, particularly datasets from large-scale demonstrations, is a shortage of data. As a result, in pilot and full-scale implementations, monitoring N_2O emissions is critical to improving the applicability of N_2O models in mainstream short-cut procedures (Hwangbo et al., 2021; Vasilaki et al., 2019). Hybrid models can also be utilized in the short-term laboratory or pilot-scale investigations with limited data, where mechanistic models can be used to simulate the biological process and the data collected can be fed into a data-driven model that can be used to predict N_2O (Vasilaki et al., 2020b).

Predictions of N_2O emission by mechanistic models require a time-consuming calibration process and sometimes the models become overparameterized under different operational conditions since it is an intermediate in nitrogen transformation pathways (Hwangbo et al., 2021). Furthermore, microbial communities engaged in N_2O synthesis are more complex than in traditional systems. On the other hand, machine learning (ML) is a data analysis tool that can learn from input data and make decisions based on that learning. For prediction and/or classification purposes, ML algorithms detect a certain pattern (during a training phase) based on defined data (input data), resulting in a more accurate output (Bagherzadeh et al., 2021). The ML technique can be combined with mechanistic models for increasing prediction accuracy (Li et al., 2022).

A hybrid mechanistic and ML approach to the prediction of the N_2O emission during the nitrification NOB washout process in the sequencing batch reactor (SBR) was evaluated in **Paper III**. The impact of the input parameters including the operational and environmental characteristics on the N_2O production was assessed as well. Short-cut N removal procedures in mainstream wastewater treatment have tremendous potential to conserve energy (oxygen demand), and resources (carbon demand), and pursue energy independence compared to the nitrification-denitrification process in WWTPs. Short-cut N removal (deammonification) has received a lot of interest from academics and the industrial sector in the recent decade (Kirim et al., 2022).

Deammonification is the nitrogen removal process by converting ammonium (NH_4-N) to nitrogen gas (N_2) through nitrite (NO_2-N). The procedure works by preventing nitrite from oxidizing to nitrate (NO_3-N) known as NOB washout and making nitrite accessible for "anaerobic" ammonia oxidation (anammox) bacteria (AnAOB) (Al-Omari et al., 2013; Feng et al., 2017). There are two strategies to make nitrite available: partial nitritation-anammox (PNA) and partial denitrification-anammox (PdNA). In full-scale applications, PNA and PdNA can be coupled to enhance the N removal efficiency (Gao and Xiang, 2021; O'Shaughnessy, 2016). PNA is an autotrophic process that involves partial oxidation of NH_4-N to NO_2-N (nitritation) and anammox, in which NH_4-N is oxidized under anaerobic conditions utilizing NO_2 -N as an electron acceptor without the use of organic carbon. As a result, the process requires collaboration between AOB and anammox bacteria, as well as NOB out-selection (Izadi et al., 2021).

Moreover, utilization of deammonification has been demonstrated for ammonium-rich wastewater, such as digested sludge dewatering, leachate, or industrial wastewaters. Despite all the efforts, stable NOB suppression, adequate anammox bacteria retention, a high carbon to nitrogen ratio (C/N), and the impact of low temperature are among the technical obstacles that mainstream applications face (Gu et al., 2020; Han et al., 2016). As a result, there are a few reported successful mainstream applications in WWTPs, and research on the utilization of deammonification in the mainstream as an energy-saving process is still ongoing (Izadi et al., 2021). In comparison with the conventional N-removal, the effective application of deammonification can cut the necessary oxygen input by 60%, remove the carbon source demand, and reduce sludge output by 90% (Gu et al., 2020; Miao et al., 2016).

Although experimental work in the laboratory and pilot-scale systems presently outnumbers mechanistic model analysis for short-cut processes (Zhang et al., 2020b), modeling efforts can aid in the acceleration of mainstream full-scale implementations. Simulation of the mainstream deammonification process and optimization of aeration parameters in a pilot plant of WWTP (Figure 2) to achieve a stable NOB washout was evaluated in **Paper IV**.

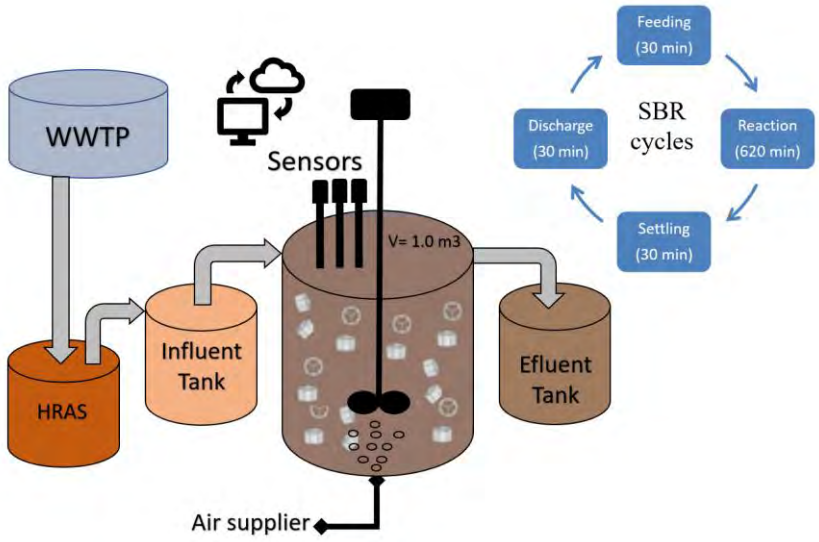

Figure 2- Deammonification system in the IFAS-SBR

2 OBJECTIVE AND SCOPE

The overall aim of using the mathematical modeling in WWTPs is to conceptualize and simulate the biological process to optimize them and save more energy and cost. Pure modeling, on the other hand, is not the complete solution. It should rather be utilized as a conceptual framework for future model development and implications (Henze, 2000).

The overall aim of this study was to evaluate important subjects that have recently appeared in the N removal systems, including **i)** evaluation of the role of comammox *Nitrospira* and incorporation of that into the two-step nitrification model (**Paper I and II**), **ii)** prediction and mitigation of N_2O production in a nitrifying system (**Paper III**), and **iii)** Long-term modeling and optimization of mainstream deammonification (**Paper IV**).

The comammox mechanism has drastically changed our knowledge of microbiologically mediated nitrogen removal processes including nitrification (Pinto et al., 2016). *Nitrospira* members' metabolism is not restricted to nitrite oxidation or comammox, but also includes functions outside of the nitrogen cycle, both aerobically (growth of formate and hydrogen) and anoxically (reduction of nitrate to nitrite) (Koch et al., 2019). The amount of published scientific papers each year on *Nitrospira's* involvement in WWTPs reflects the increased interest in that microorganism. The number of publications (based on the Scopus database) with the keywords of "*Nitrospira*" and "*wastewater*" has steadily increased over the previous decade.

Despite the numerous studies, many questions still remain unanswered about the importance and actual role of *Nitrospira* in N removal systems, effective suppression methods, particularly in deammonification systems, and comparison of the kinetic parameters of nitrifying bacteria groups, the coexistence of canonical and comammox *Nitrospira*, etc.

The physiological and microbiological properties of *Nitrospira*, their abundance in WWTPs, and variables influencing their proliferation were all investigated in the first step (**Paper I)**. This review was followed by a novel meta-analysis using the RSM method of over 100 case studies of various wastewater treatment systems that looked at the abundance of *Nitrospira* in terms of the combined effect and interaction of four process variables, including dissolved oxygen (DO), influent NH_4-N concentration, pH, and temperature. In addition, the detection

methods for microbiological diversity and abundance of *Nitrospira* were also discussed in **Paper I**.

Considering the expanding number of experimental research on comammox, it has not been considered in the nitrification modeling. Therefore, the aim of the second step of this dissertation (**Paper II**) was to assess the capabilities and limitations of three novel comammox model concepts (two-step nitrification with comammox), prediction of comammox and canonical AOB and NOB under highly dynamic conditions during biomass NOB washout experiments, and evaluate the role of comammox in ammonia conversion to nitrate using the process rates by Sankey graphs.

The goal of the study in **Paper II** was to add the possible comammox into nitrification modeling for converting NH_4–N to NO_3–N through NO_2-N. The possibility of growing comammox on NO_2-N was also considered which is very important in the deammonification systems. Moreover, the most influential kinetic parameters for extended model predictions were identified via sensitivity analysis and correlation matrix analysis, and experimental data from a laboratory-scale SBR with inoculum biomass from a full-scale WWTP were used to calibrate and verify the models. The newly proposed mechanistic comammox models were theorized to highlight the possible involvement of comammox in nitrifying systems and improve existing knowledge of N conversions in such systems.

Further, N_2O emission prediction and mitigation from WWTPs are among the hot topics of recent research worldwide. However, the pure mechanistic or ML modeling of N_2O has some limitations and difficulties. In step 3 (**Paper III**), based on data from a laboratory-scale nitrifying SBR system, a predictive hybrid model for liquid N_2O generation was developed. The newly developed model was able to overcome the restrictions of pure mechanistic models or machine learning methods. That modeling strategy consisted of two fundamental steps: **i)** data mining by the prediction of influential data on the N_2O production, such as N and biomass components, using the recently developed comammox model, and **ii)** liquid N_2O predictions using three powerful ML algorithms (ANN, SVM, and GBM) to achieve a highly accurate model by producing input data from the previous step.

The aims of the last step (**Paper IV**) were to model a long-term mainstream deammonification process (pilot-scale) to evaluate the following issues: **i)** estimation of the kinetic parameters for AOB, NOB, anammox, and heterotrophic bacteria under variable seasonal temperature and C/N ratio; **ii)** multi-objective optimization of the intermittent aeration strategy (DO concentration and on/off time) for maximizing the NRR and NRE, and **iii)** applying principal component analysis (PCA) to evaluate the correlation of the operational parameters on the system efficiency. Additionally, most of the past studies on aeration strategy optimization were carried out in short-term operational circumstances (batch tests or one cycle of a long-term experiment). The novelty of this study was to optimize the aeration parameters based on the long-term data from a mainstream deammonification system. Figure 3 represents the detailed issues addressed in each part of this dissertation.

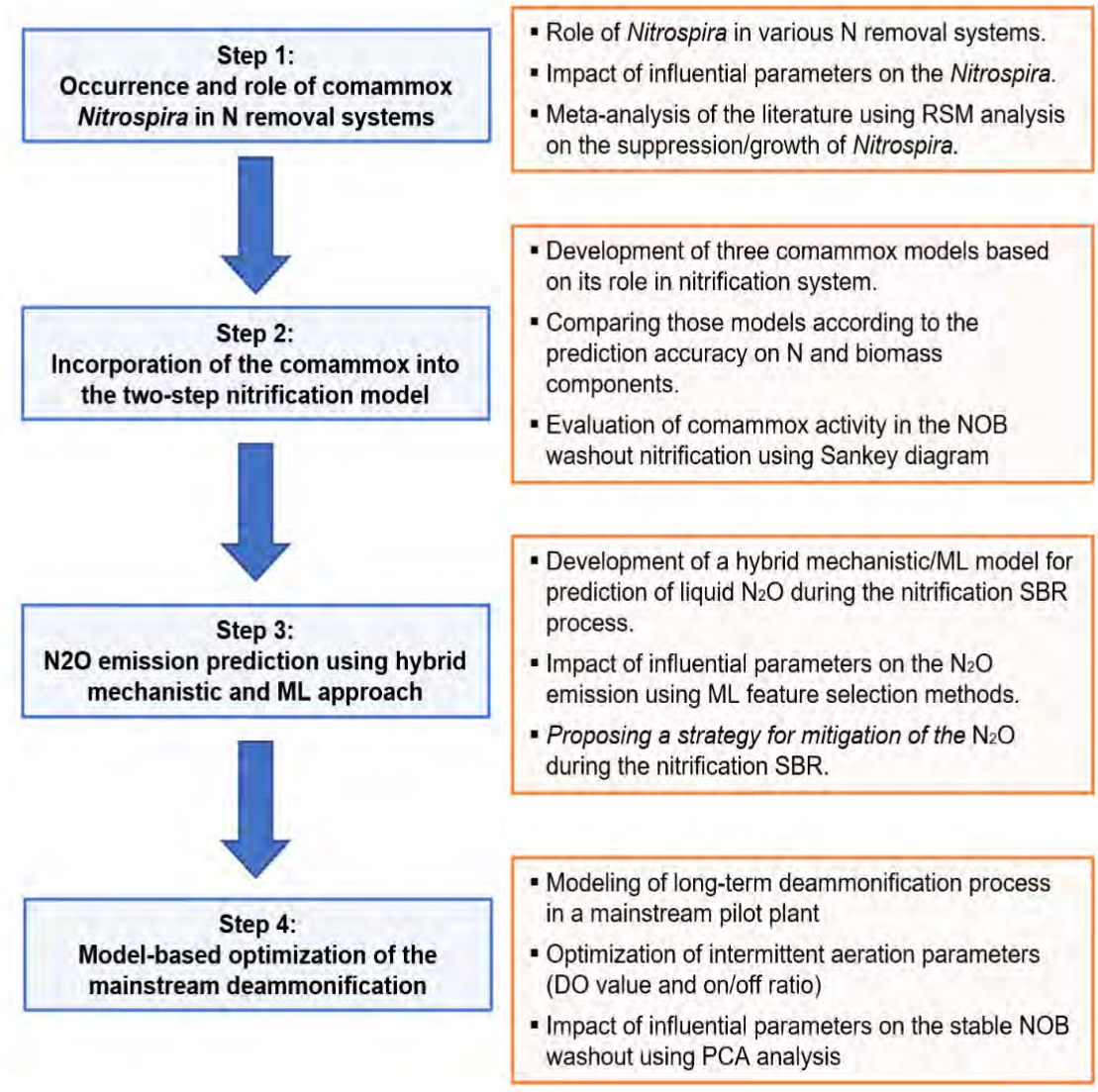

Figure 3. Division of the dissertation into 4 steps with indication of the publications in each part

3 DISSERTATION METHODOLOGY

3.1 Role of *Nitrospira* in the N removal processes (Paper I)

3.1.1 Impact of influencing data on *Nitrospira* activity

In this section, the reported occurrences of *Nitrospira* in the most common nitrogen removal processes in WWTPs, including nitrification-denitrification and deammonification, were summarized. *Nitrospira* abundances together with the most important operational constraints, including temperature, pH, DO, SRT, and nitrogen concentrations, were listed from over 100 technological studies (80 for nitrification-denitrification and 35 for deammonification systems).

Then, data has been classified into the scale of the studied system, feed characteristics, and reactor types. Most of the studied systems were fed with synthetic wastewater (48% for nitrification-denitrification and 59% for deammonification), while the nitrification-denitrification systems were also operated with real municipal and industrial wastewater.

3.1.2 Meta-analysis of the literature data

The Response Surface Methodology (RSM) is a method for examining a connection between numerous variables and one or more outputs. The RSM is beneficial in situations where statistical data are important and the influence of different factors and their interactions on each output may be identified (Anwar et al., 2015). The impacts and interactions of four process variables (factors) impacting *Nitrospira* abundance (output) in nitrogen removal systems were investigated using a standard RSM model implemented in Minitab (19.1) and DX (10.1) software (Stat-Ease, USA).

A relationship between the response Y (*Nitrospira* relative abundance) and four independent inputs x_i/x_j (pH, temperature, DO, and influent NH_4-N) was described by a second-order polynomial equation (Li et al., 2018) (Eq. 1):

$$Y = \beta_0 + \sum_{i=1}^{n} \beta_i x_i + \sum_{i=1}^{n} \beta_{ii} {x_i}^2 + \sum \sum_{i<j} \beta_{ij} x_i x_j + \epsilon \quad (1)$$

where β_0 is a constant coefficient, β_i are the linear coefficients, β_{ii} are the quadratic coefficients, β_{ij} are the interplay coefficients, x_i and x_j are the coded form of inputs, and ε is

the residual error. The analysis of variance was used to investigate the statistically significant of the model inputs ($p < 0.05$), followed by the importance level (Pareto analysis) to identify the level of significance of the response for input parameter and their interaction.

Four operational factors, including DO concentration, influent NH_4-N concentration, pH, and temperature, were employed as input independent variables. The values of those variables were calculated using the published range in the literature. The majority of the assessed data were within the pH range of 7–8, the temperature range of 20–25 °C, the DO concentration range of 0.2–4.0 mg O_2/L, and the influent NH_4-N concentration range of 5–60 mg N/L.

3.2 Incorporation of the comammox into the two-step nitrification model (Paper II)

3.2.1 Data collection for calibration and validation of the models

Biomass washout experiments were set at particular operational settings to remove NOB from a system. Long-term biomass cultivations were carried out in this investigation at decreasing SRTs. The inoculum biomass was obtained from the "Czajka" WWTP (N: 52.3509, E: 20.960) in Warsaw (Figure 4) during the winter and summer seasons. This WWTP is the largest facility in Poland with a hydraulic capacity of 435 000 m^3/d and a pollution load of nearly 2 million population equivalents (PE).

Figure 4- Czajka WWTP in Warsaw, Poland

The temperature was set to 12 and 20ºC, close to the actual process temperatures of WWTPs in winter and summer of Poland. During each series of the experiment, the inoculum biomass was diluted to approximately 2000 mg/L and poured into two parallel, fully automated plexiglass SBRs with a working volume of 10 L each (Figure 5). The reactors were placed in water coats, coupled with a thermostatic water bath, to keep the selected temperature setpoints. The reactors were equipped with an automated aeration control system, i.e. continuous aeration at the DO set point of 0.6±0.1 mg O_2/L. The pH was kept at 7.5±0.2 during all the experiments by automatically dosing NaOH (2M solution).

Each operational cycle lasted 8 h (480 min) and consisted of three phases: feeding (15 minutes), reaction (aeration) (450 minutes), and decantation (15 minutes). The SRT, equal to the hydraulic retention time (HRT), was aggressively decreasing from the initial 4 d to 1 d at the end of the trial. Each SRT condition (4, 3, 2, 1.5, and 1 d) was kept for one week during the experiments.

Figure 5- Experimental setup (SBR) at the laboratory of the university

During the experiments, mixed liquor samples were collected 3 times per week at the beginning and end of the reaction phases. The samples were filtered and analyzed in different forms of nitrogen (NH_4-N, NO_3-N, and NO_2-N). Also, mixed liquor suspended solids (MLSS) and mixed liquor volatile suspended solids (MLVSS) were measured at the beginning of the reaction phases. For microbiological analyses, duplicated biomass samples were collected from the reactors three times at 0 d (beginning), 20 d (middle), and 35 d (end).

3.2.2 Conceptual comammox models

The Activated Sludge Model No. 1 (ASM1) (Henze et al., 2000) was used as the core model to implement the three proposed mathematical comammox models in GPS-X 8.0. The nitrification process was divided into two stages (AOB and NOB), and the comammox was added as shown in Figure 6.

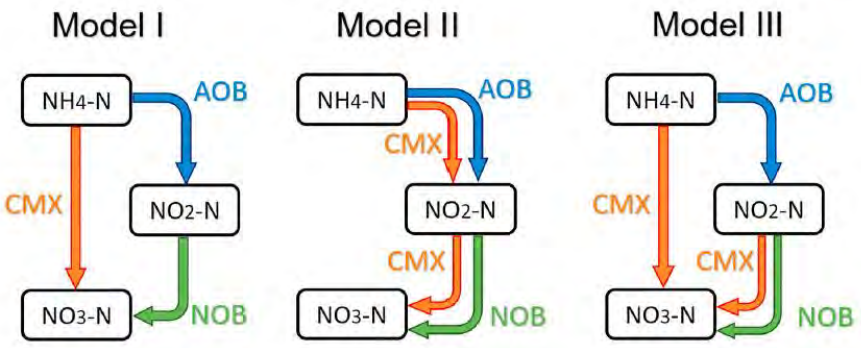

Figure 6- Three conceptual models of comammox as an extension of the two-step nitrification pathways

For calibration of those models, the most sensitive parameters were chosen using sensitivity analysis. Also, the correlation matrix was used to identify pairs of strongly associated parameters aiming at simplification of the calibration process. Each model was calibrated using the identical measurements (NH_4-N, NO_2-N, and NO_3-N) from the experimental data at 12°C and then verified using the experimental data at 20°C.

The models were compared in terms of the model efficiency (fitness-of-fit) (Hauduc et al., 2015). The coefficient of determination (R^2), root mean square error (RMSE), and mean absolute error (MAE) are the most frequent ones implemented in GPS-X. The RMSE measures the model's overall error in the same unit as the target variable, whereas the MAE assesses the quality of an estimated parameter's fluctuation and unbiasedness (Hauduc et al., 2015). R^2 and Janus coefficient (J^2) can measure the accuracy of prediction data vs. observation data. The following equations (2-5) define the metric values:

$$R^2 = 1 - \frac{\sum(P_0 - P_1)^2}{(P_0 - \sigma)^2} \quad (2)$$

$$MAE = \frac{\sum_{n_0}^{n}|(P_0 - P_1)|}{n} \quad (3)$$

$$RMSE = \sqrt{\frac{\sum_{n_0}^{n}(P_0 - P_1)^2}{n}} \quad (4)$$

$$J^2 = \frac{RMSE^2_{validation}}{RMSE^2_{calibration}} \quad (5)$$

where P_0 is the observed data in the data set, P_1 is the simulated data, σ is the mean value of observed data, and n is the number of observation samples.

3.2.3 Sankey Graphs for N conversion

Based on the predicted conversion rates (mg N/L.d) in the developed models, Sankey graphs were developed to identify the dominant N conversions at different stages and define the role of comammox in each proposed model under the dynamic biomass washout experiments.

3.3 Modeling N_2O emissions based on a hybrid modeling approach (Paper III)

3.3.1 Data collection for calibration and validation of the models

The N_2O liquid data was prepared by a sensor together with other operational data (pH, temperature, biomass, and N concentrations) during the washout experiments aimed at washing out NOB by applying specific operational conditions (various temperatures and decreasing SRTs).

The ML algorithms were trained and tested at experiments with temperatures of 20 °C and 12 °C, respectively. The volumetric nitrogen loading rates (NLRs) were held constant at 0.02±0.01 and 0.05±0.01 g N/(L·d), at 12 °C and 20 °C, respectively. Online sensors recorded pH, temperature, DO concentration, and liquid N_2O concentration every 30 seconds during the studies.

The biomass was prepared from Swarzewo WWTP (N: 54.7687, E: 18.4063), which is located in a touristic region on the Baltic Sea coast (Figure 7). The plant's hydraulic capacity is 18100 m^3/d, and the pollutant load is around 177000 PE. The plant treats up to 15000 m^3/d of wastewater during the summer months (June-September), and around 5000 m^3/d throughout the rest of the year. The plant also gets a 5% of nitrogen-rich wastewater from the fish industry in addition to household wastewater. It has six parallel SBRs in the biological stage.

Figure 7- Swarzewo WWTP in Swarzewo, Poland

3.3.2 Impact of input parameters on the N_2O liquid production

The Pearson correlation coefficient (PCC) is one of the feature selection (FS) filter methods that is a linear connection between two variables that range from + 1 to -1, with +1 being the entire positive correlation, 0 representing no correlation, and -1 representing negative correlation. Another filtering method for sorting input variables according to their relevance is the Random Forest (RF) containing several decision trees for the generation of utilizing random feature extraction and data set observations (Masmoudi et al., 2020).

3.3.3 Mechanistic Model

The developed two-step nitrification and comammox model was employed to expand the analytical data to a comparable interval period with the sensor data. Simulations using the mechanistic model were done using the GPS-X 8.0 software (Hydromantis, 2021) with a communication time of 30 seconds for both trials (similar to the online sensor data).

3.3.4 Data-driven (Machine Learning)

Among all ML models, the support vector machine (SVM), artificial neural network (ANN), and gradient boosting machine (GBM) were used in this study and will be described as follows.

3.3.4.1 Support Vector Machine (SVM)

The SVM regression is a supervised learning model that uses the same SVM (classification) manner with minor modifications. The SVM transforms an input matrix to a higher dimensional feature space via a kernel (Awad and Khanna, 2015). As shown in Figure 8, the data points outside of the decision boundary are ignored for developing the hyperplane (removing outliers). Similarly, the SVM model is only based on a subset of the training results, and any training data which are close to the model prediction (hyperplane) are ignored by the cost function method to prevent overfitting issues (Steinwart and Christmann, 2008).

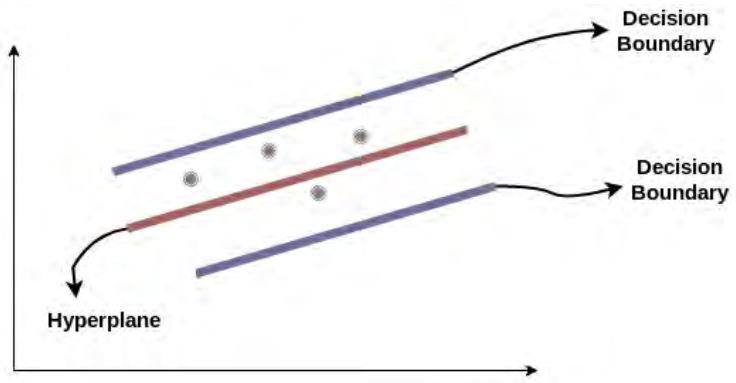

Fig. 8- SVM boundaries and hyperplane layers

3.3.4.2 Artificial Neural Network (ANN)

The ANN is a multilayer perceptron (MLP) with three layers: input, hidden, and output (Figure 9). Every neuron assumes a linear equation between its input and output with the help of hidden layers. Due to the unpredictability of a non-linear model, more neurons are expected to anticipate the objective variables with satisfactory accuracy (Ryan et al., 2004).

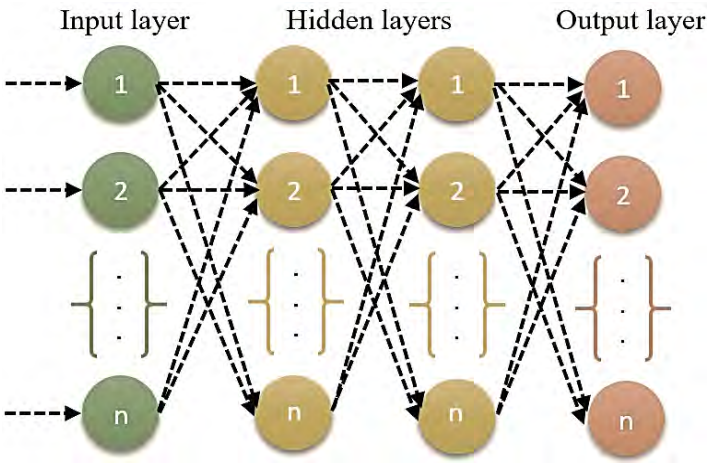

Figure 9- ANN model structure and layers

3.3.4.3 Gradient boosting machine (GBM)

The gradient boosting machine (GMB) is a machine learning model that consists of a set of decision trees, and it has a specific constructive strategy of ensemble formation. In a boosting approach, new trees are sequentially added to the ensemble according to the error of the whole ensemble prediction. As new trees are created with a constant learning rate, the estimation error is continuously reduced until reaching the maximum possible accuracy. Figure 10 indicates the ensemble model and aggregation of trees for the GBM model (Natekin and Knoll, 2013).

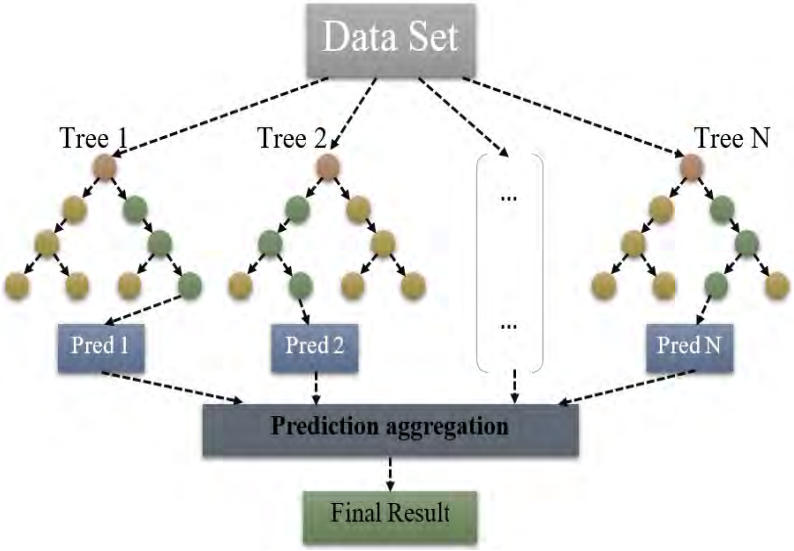

Figure 10- GBM model structure and layers

3.4 Modeling and optimization of mainstream deammonification process (Paper IV)

3.4.1 Data collection

Sufficient data were prepared from a pilot-scale deammonification system by the IFAS process. The reactor was employed at the Emschermündung WWTP in the vicinity of Dinslaken, Germany (EGLV) for the treatment of the municipal wastewater as shown in Figure 11.

Figure 11- Emschermündung WWTP in Dinslaken, Germany

The reactor was run for almost 12-hour cycles that included filling (30 minutes), reaction (620 minutes), sedimentation (30 minutes), and discharge (30 minutes) phases. In the initial phase, 120 L of wastewater was fed into the reactor for 30 minutes (Figure 12). Th reaction phase was divided into 20-minute on/off cycles to enable intermittent aeration. Based on a previous lab-scale investigation, the aeration was set on for 4 minutes and switched off for 16 minutes as the initial values. The DO concentration was initially fixed to 0.4 mg O_2/L during the aeration switched-on phase.

Moreover, the sedimentation phase with no aeration or mixing phases allowed to accomplish appropriate sludge settling and prevent biomass loss in the effluent. The reactor content was

released into the effluent container during the discharge phase (30 minutes). Regular sampling (three times per week) was performed in the influent and the effluent tanks.

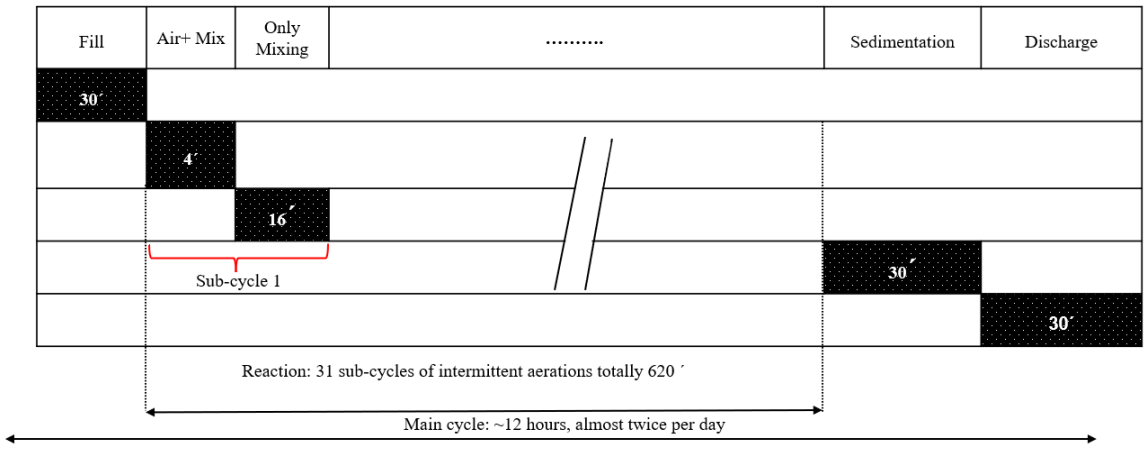

Figure 12- SBR phases in one cycle during the experiment

3.4.2 Modeling of the deammonification procedure

The Mantis2 model was used by GPS-X 8.0 to simulate the subjected deammonification system. The core model structure is based on the Activated Sludge Model No. 2d (ASM2d) (Henze et al. 2000) and the Anaerobic Digestion Model No. 1 (ADM1) (Batstone et al., 2002). The models have been combined and enhanced by Hydromantis to include the two-step nitrification and anammox processes.

3.4.3 Optimization of aeration

Optimization of the aeration strategy in order to maximize the NRR and NRE was carried out in the long-term process operation during the calibration period. Several scenarios for DO concentrations (0.2–0.4 mg O_2/L) and on/off ratio (0.02–0.3) were defined in the intermittent aeration. The sum of the aeration and non-aeration periods was fixed at 20 min in the 12-hours reaction cycle of SBR. The optimization target variable was evaluated in terms of maximizing the daily averages of NRR and NRE. All 18 defined scenarios for the analysis are presented in Table 1.

Table 1- Different scenarios for performance optimization

Scenario	On/Off ratio in a 20 minutes cycle			DO set-point,
	Off-time	On-time	On/Off ratio	mg O_2/L
1	15	5	0.33	0.4
2	16	4	0.25	0.4
3	17	3	0.17	0.4
4	18	2	0.11	0.4
5	19	1	0.05	0.4
6	19.5	0.5	0.02	0.4
7	15	5	0.33	0.3
8	16	4	0.25	0.3
9	17	3	0.17	0.3
10	18	2	0.11	0.3
11	19	1	0.05	0.3
12	19.5	0.5	0.02	0.3
13	15	5	0.33	0.2
14	16	4	0.25	0.2
15	17	3	0.17	0.2
16	18	2	0.11	0.2
17	19	1	0.05	0.2
18	19.5	0.5	0.02	0.2

3.4.4 Principal Component Analysis (PCA)

The PCA was used for the investigation of a relationship between process parameters and reactor performance. The PCA generated a new collection of variables while orthogonally transforming the previous data. The main purpose of PCA is to emphasize those variables that enhance a relative description of other objects, to create particular groups based on similarities, and to categorize variables (Ringnér, 2008). The output comprises two or three principal

components which are a linear combination of the original data plus orthogonal eigenvectors to examine statistical connections between operational parameters (MLSS, temperature, pH, and DO), influent/effluent NH_4-N, and effluent NO_3-N. OriginPro 2021 (OriginLab Corp) was used for generating the two-dimensional (2D) PCA at a statistically significant level (p 0.05).

4 RESULTS AND DISCUSSION

4.1 Role of *Nitrospira* in the N removal processes (Paper I)

4.1.1 Impact of influencing data on *Nitrospira* activity

The first part of **Paper I** was a review of the role of *Nitrospira* in different N removal systems and an evaluation of the effect of influential parameters on the growth/suppression of this bacteria. The relative abundance of *Nitrospira* increased in a reactor with a very low DO concentration (0.13 mg O_2/L) and a significantly decreased with a high DO concentration (8.7 mg O_2/L). Low DO concentrations are the most preferred strategy in WWTPs, especially for deammonification process, as one of the factors that can suppress NOB activity (Ma et al., 2016).

Furthermore, some publications have stated that the optimal temperature for *Nitrospira* growth is between 30 and 35 degrees Celsius (Yao and Peng, 2017). The ideal pH for *Nitrospira* is between 8.0 and 8.3. *Nitrospira* bacteria are sensitive to high pH (> 9.0) because it increases free ammonia (FA) concentration and inhibits their activity in both nitrification and anammox-based systems (Blackburne et al., 2007). (Camejo et al., 2017; Roots et al., 2019) discovered that reduced ammonia loading rates (ALR) had a beneficial effect on *Nitrospira* activity. Also, the *Nitrospira* abundance was able to achieve 53% of the whole microbial population with the combination of high nitrogen concentrations, low DO, and a long SRT (Roots et al., 2018).

4.1.2 Meta-analysis of the literature data

The RSM results in the second part of **Paper I** revealed that the highest *Nitrospira* activity can be expected under the following conditions when occurring simultaneously: high DO (> 3.0 mg O_2/L) and influent NH_4-N (> 20 mg N/L) as well as low temperature (< 15 °C) and pH (< 7).

A high value of the determination coefficient (R^2 = 0.86) and a low value of the standard deviation (σ = 0.5) confirmed the acceptability of goodness-of-fit. In addition, the results of the analysis of variance with low p-values indicated positive evidence against the null hypothesis. The level of importance of each input factor and the interaction between them was evaluated using the Pareto analysis.

4.2 Incorporation of the comammox into the two-step nitrification model (Paper II)

4.2.1 Conceptual comammox models

From the comparative results among three conceptual comammox models in the calibration procedure, the best goodness-of-fit was obtained by Model I. The R^2 values were 0.96, 0.92, and 0.93 for NH_4-N, NO_3-N, and NO_2-N, respectively. Moreover, the RMSE and MAE were also lower compared to the other two models. When comparing the values of model parameters adjusted during calibration (Table 2 in **Paper II**), it appears that there were only slight changes in μ_{AOB} and μ_{NOB} between the models. The optimized parameters of 0.55–0.60 d^{-1} for μ_{AOB} and 0.11 d^{-1} for μ_{NOB} were within the reported ranges (Park et al., 2017; Zheng et al., 2019). In Model I with a single substrate (NH_4–N), μ_{CMX} was 0.15 d^{-1} and lower than μ_{CMX} = 0.2–0.22 d^{-1} in Models II and III with two substrates (NH_4–N and NO_2-N).

4.2.2 Role of comammox in the N conversion

The nitrogen conversion pathways in the investigated models were also examined using Sankey graphs (Figure 8 of **Paper II**) based on the average values for the whole calibration period (30 d). The anticipated contribution of comammox bacteria was considerable but not as high as that of canonical nitrifiers. When the direct oxidation of NH_4-N to NO_3-N by comammox bacteria (Models I and III) was investigated, that pathway was responsible for 14% (Model I) and 11% (Model III) of the NH_4-N conversion, compared to 86% and 89%, respectively, when NO_2-N was oxidized by NOB. In Model II (considering the parallel oxidation of NH_4-N to NO_2-N by AOB and comammox), 21% of NH_4-N is oxidized by comammox, and the remaining 79% is converted by AOB. When oxidation of NO_2-N to NO_3-N by comammox was considered (Models II and III), that pathway was also less important than the oxidation by NOB. The contributions of commamox bacteria were 26% and 20% in Model II and Model III, respectively, with the remaining contributions of NOB.

4.3 Modeling N_2O emissions based on a hybrid modeling approach (Paper III)

4.3.1 Impact of input parameters on the N_2O liquid production

The results of Pearson Correlation showed that among pH, temperature, N (NH_4-N, NO_3-N NO_2-N), and biomass components, the N species (NH_4-N and NO_2-N) had the strongest

positive and negative correlations with the production of N_2O by 0.82 and 0.56, respectively. The biomass components (MLSS and MLVSS) were the second most connected variables, with a correlation factor of 0.48. The RF approach produced similar results to the Pearson method as well. The maximum levels of importance were obtained for NH_4-N (0.71) and NO_2-N (0.37), respectively. Moreover, DO concentration had the highest correlation with N_2O production among all other online measured data. Figure 5 in **Paper III** shows the importance level of the input variables for N_2O production.

4.3.2 N_2O prediction during the long-term nitrification system

Prediction results by the three powerful ML tools showed that the ANN has the most accurate prediction while SVM and GBM were overfitted even though they were able to capture the train data patterns. The ANN showed its adaptability under the different operational conditions. As shown in Figure 6 of **Paper III**, the SVM overestimated the N_2O peak with a 6-day delay, and the GBM failed to predict any distinguishable peak. Moreover, the model outputs showed significant inaccuracies at the start of the experimental trial (days 2–4) due to a fast spike in N_2O generation, as seen in Figure 7 of **Paper III**. When the N_2O production stabilized after 4 days, the errors were more stable (except for the SVM). In addition, the ANN model output error was less than the doubled standard deviation (2σ) throughout the experiment, indicating an accurate and correct prediction.

4.4 Modeling and optimization of mainstream deammonification process (Paper IV)

4.4.1 Intermittent aeration optimization

The model-based aeration optimization was done by two variables, i.e. DO concentration between 0.2 to 0.4 mg O_2/L and on/off ratio between 0.05 to 0.3 considering on daily average of NRR, NRE, NH_4-N, and COD removal efficiency as targets. Results (Figure 6 in **Paper IV**) showed that the optimum values for DO and on/off ratio were obtained at 0.2–0.25 mg O_2/L and 0.05, respectively. Hence, by declining the DO concentration to 0.2–0.25 mg O_2/L and on/off ratio down to 0.05, the current levels of NRE and NRR increased from the daily average of 30% to > 50% and from the daily average of 15 g $N/m^3 \cdot d$ to approximately 25 g $N/m^3 \cdot d$, respectively. On the other hand, the optimization did not have a significant individual effect on COD removal efficiency.

4.4.2 Impact of input variables on the stable NOB washout and N removal

The PCA results (Figure 5 in **Paper IV**) showed that the effluent NO_3-N value was highly associated with the DO concentration, demonstrating the significance of aeration for effective NOB suppression. The effluent revealed a direct negative association between NO_3-N and NH_4-N, while MLSS exhibited a positive correlation with NO_3-N. The effluent NO_3-N was less related to pH and temperature.

5 CONCLUSIONS

The following conclusions were derived from this PhD dissertation.

The effect of individual variables (pH, temperature, DO concentration, and influent NH_4-N concentration) and their combined interactions on the relative abundance of *Nitrospira* were determined by the meta-analysis of literature data. However, it is still necessary to apply other methods to validate the role and significance of *Nitrospira* in the N removal process.

Commamox could be responsible for the conversion of >20% of the influent NH_4-N load and the role of comammox *Nitrospira* in N conversion in activated sludge systems should not be neglected and requires further investigation. The initial biomass concentrations of AOB and NOB, combined with their maximum specific growth rates, had the highest importance level for nitrification model calibration.

Furthermore, a hybrid mechanistic and ML (ANN) model successfully predicted liquid N_2O concentrations during the nitrifying SBR system. This technique was innovative in comparison to previous attempts to develop a predictive model of N_2O production during nitrification with an appropriate coefficient of determination. The hybrid model correctly predicted unknown test data, demonstrating its adaptability in terms of different operating conditions and the capacity to generalize process patterns.

In addition, a mechanistic model for the mainstream deammonification process under fluctuated temperature conditions was validated using pilot-scale data. The DO set-point and on/off ratio were the most important factors for NOB suppression, according to the PCA results. The NRR and NRE can be increased to 25 g $N/m^3 \cdot d$ and > 50% by reduction of the DO set-point and on/off ratio to 0.2 mg O_2/L and 0.05, respectively, based on the aeration strategy optimization.

6 FUTURE RESEARCH

The discussion about modeling and mechanism of comammox, N_2O emission, and mainstream deammonification, is still ongoing with various experimental studies and model extensions. The use of proposed mathematical models for each part in this dissertation for continuous improvement, application, and comparison is strongly suggested. In addition to the standard prediction parameters (N species and biomass concentrations), microbiological indicators such as the relative abundance of comammox and the ratio of nitrifiers to heterotrophs can be added as targets of variables for calibration of mechanistic models.

Data-driven models are useful tools for turning WWTP processes into knowledge. These algorithms are gaining popularity in the prediction of WWTPs with operational and environmental characteristics as input data and effluent quality as output data. These models can also be integrated with mechanistic models to improve prediction. Data-driven models are highly efficient for online monitoring and decision support of such variables. This approach was used as a hybrid model for N_2O emission in this study and it is recommended to apply for other N components prediction.

Future studies should look deeper into the actual role of comammox in the N conversion. The results of this PhD study showed the potential importance of comammox in nitrification systems. Also, Quantitative Polymerase Chain (PCR) and multitranscript analysis can be used to examine the activity of functional genes involved in the nitrogen metabolism and N_2O generation during wastewater treatment.

A comparison between predictions of mechanistic models vs. ML models for N_2O production and emission using a larger data set is suggested. Future ML algorithms, rather than ANN, SVM, and GBM might be used to predict specific N_2O generation routes.

The developed activated sludge model with comammox can further be extended for calculation of the competition between two groups of canonical NOB based on their r/k strategy and comammox bacteria. Heterotrophic denitrification on Soluble Microbial Products (SMPs) can also incorporate into the model. Figure 13 represents a proposed conceptual model for further two-step nitrification model extension.

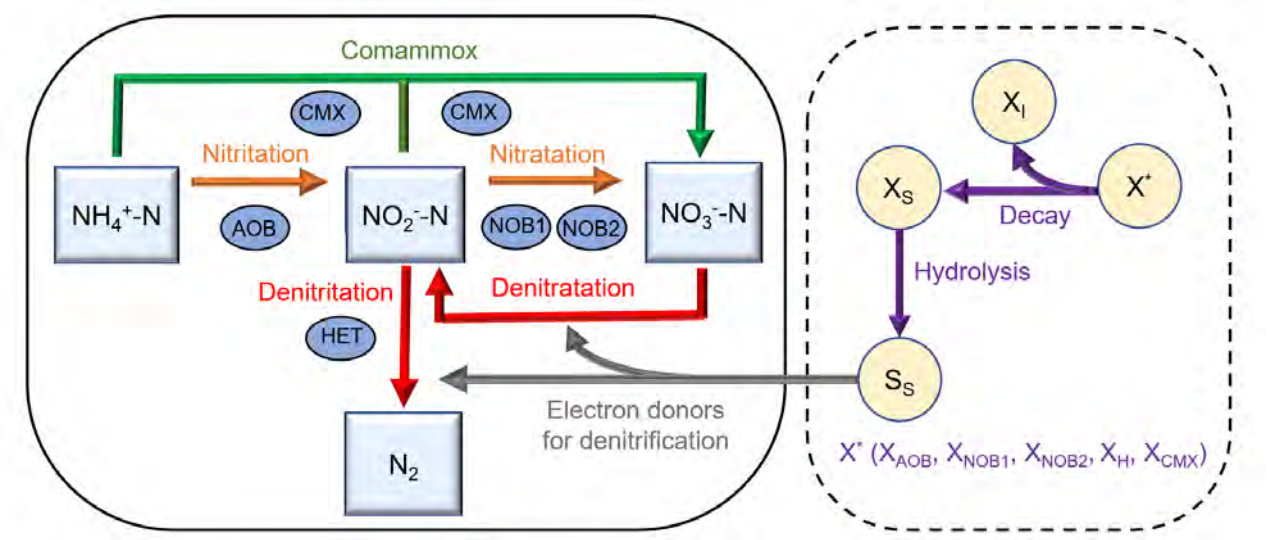

Figure 13- A concept of the extended two-step nitrification model including two NOB groups (r/k strategist) together with interactions of comammox and heterotrophic denitrification (Mehrani et al. 2022)

REFERENCES

Al-Omari A, Wett B, Han M, De Clippeleir H, Bott C, Nopens, I, Murthy S. Competition over Nitrite in Single Sludge Mainstream Deammonification Process. WEF/IWA Nutrient Removal and Recovery, Conference Proceedings. Water Environment Federation (WEF), International Water Association (IWA), 2013.

Anwar K, Mohamad said Ka, Afizal M, Amin M. Overview on the Response Surface Methodology (RSM) in Extraction Processes 2015; 2: 231-245.

Awad M, Khanna R. Support Vector Regression. In: Awad M, Khanna R, editors. Efficient Learning Machines: Theories, Concepts, and Applications for Engineers and System Designers. Apress, Berkeley, 2015.

Batstone DJ, Keller J, Angelidaki I, Kalyuzhnyi SV, Pavlostathis SG, Rozzi A, Sanders W, Siegrist HA., Vavilin VA. The IWA anaerobic digestion model no 1 (ADM1). Water Science and technology 2002; 45: 65–73.

Bagherzadeh F, Mehrani M-J, Basirifard M, Roostaei J. Comparative study on total nitrogen prediction in wastewater treatment plant and effect of various feature selection methods on machine learning algorithms performance. Journal of Water Process Engineering 2021; 41: 102033.

Blackburne R, Vadivelu VM, Yuan Z, Keller J. Kinetic characterisation of an enriched *Nitrospira* culture with comparison to *Nitrobacter*. Water Research 2007; 41: 3033-3042.

Camejo PY, Domingo JS, McMahon KD, Noguera DR. Genome-Enabled Insights into the Ecophysiology of the Comammox Bacterium "Candidatus *Nitrospira* nitrosa". mSystems 2017; 2: 14-17.

Cao S, Du R, Li B, Wang S, Ren N, Peng Y. Nitrite production from partial-denitrification process fed with low carbon/nitrogen (C/N) domestic wastewater: performance, kinetics and microbial community. Chemical Engineering Journal 2017; 326: 1186-1196.

Chen H, Zeng L, Wang D, Zhou Y, Yang X. Recent advances in nitrous oxide production and mitigation in wastewater treatment. Water Research 2020; 184: 116168.

Daims H, Lücker S, Wagner M. A New Perspective on Microbes Formerly Known as Nitrite-Oxidizing Bacteria. Trends in Microbiology 2016; 24: 699-712.

Domingo-Félez C, Pellicer-Nàcher C, Petersen MS, Jensen MM, Plósz BG, Smets BF. Heterotrophs are key contributors to nitrous oxide production in activated sludge under low C-to-N ratios during nitrification—Batch experiments and modeling. Biotechnology and Bioengineering 2017; 114: 132-140.

Duan H, van den Akker B, Thwaites BJ, Peng L, Herman C, Pan Y, et al. Mitigating nitrous oxide emissions at a full-scale wastewater treatment plant. Water Research 2020; 185: 116196.

Feng Y, Lu X, Al-Hazmi H, Mąkinia J. An overview of the strategies for the deammonification process start-up and recovery after accidental operational failures. Reviews in Environmental Science and Bio/Technology 2017; 16: 541-568.

Gao D, Xiang T. Deammonification process in municipal wastewater treatment: Challenges and perspectives. Bioresource Technology 2021; 320: 124420.

Gilbert EM, Agrawal S, Brunner F, Schwartz T, Horn H, Lackner S. Response of Different *Nitrospira* Species To Anoxic Periods Depends on Operational DO. Environmental Science & Technology 2014; 48: 2934-2941.

Gu J, Zhang M, Liu Y. A review on mainstream deammonification of municipal wastewater: Novel dual step process. Bioresource Technology 2020; 299: 122674.

Gustavsson DJI, Suarez C, Wilén B-M, Hermansson M, Persson F. Long-term stability of partial nitritation-anammox for treatment of municipal wastewater in a moving bed biofilm reactor pilot system. Science of The Total Environment 2020; 714: 136342.

Han M, Vlaeminck SE, Al-Omari A, Wett B, Bott C, Murthy S, et al. Uncoupling the solids retention times of flocs and granules in mainstream deammonification: A screen as effective out-selection tool for nitrite oxidizing bacteria. Bioresource Technology 2016; 221: 195-204.

Hauduc H, Neumann MB, Muschalla D, Gamerith V, Gillot S, Vanrolleghem PA. Efficiency criteria for environmental model quality assessment: A review and its application to wastewater treatment. Environmental Modelling & Software 2015; 68: 196-204.

Henze MG, W., Mino, T., van Loosdrecht, M.C.M. Activated sludge models ASM1, ASM2, ASM2d and ASM3. London, UK: IWA Publishing, 2000.

Hwangbo S, Al R, Chen X, Sin G. Integrated Model for Understanding N_2O Emissions from Wastewater Treatment Plants: A Deep Learning Approach. Environmental Science & Technology 2021; 55: 2143-2151.

Hydromantis C., (www.hydromantis.com/GPSX) Canada, 2021.

IPCC. Intergovernmental Panel on Climate Change Fifth Assessment Report, 2014.

Izadi P, Izadi P, Eldyasti A. Towards mainstream deammonification: Comprehensive review on potential mainstream applications and developed sidestream technologies. Journal of Environmental Management 2021; 279: 111615.

Kaelin D, Manser R, Rieger L, Eugster J, Rottermann K, Siegrist H. Extension of ASM3 for two-step nitrification and denitrification and its calibration and validation with batch tests and pilot scale data. Water Research 2009; 43: 1680-1692.

Kirim G, McCullough K, Bressani-Ribeiro T, Domingo-Félez C, Duan H, Al-Omari A, Mehrani M-J et al. Mainstream short-cut N removal modelling: current status and perspectives. Water Science and Technology 2022: 2022131.

Knowles G, Downing AL, Barrett MJ. Determination of Kinetic Constants for Nitrifying Bacteria in Mixed Culture, with the Aid of an Electronic Computer. Microbiology 1965; 38: 263-278.

Koch H, van Kessel MA, Lücker S. Complete nitrification: insights into the ecophysiology of comammox *Nitrospira*. Applied Microbiology and Biotechnology 2019; 103: 177-189.

Laureni M, Falås P, Robin O, Wick A, Weissbrodt DG, Nielsen JL, et al. Mainstream partial nitritation and anammox: long-term process stability and effluent quality at low temperatures. Water Research 2016; 101: 628-639.

Li K, Duan H, Liu L, Qiu R, van den Akker B, Ni B-J, et al. An Integrated First Principal and Deep Learning Approach for Modeling Nitrous Oxide Emissions from Wastewater Treatment Plants. Environmental Science & Technology 2022; 56: 2816-2826.

Lin Z, Sun D, Dang Y, Holmes DE. Significant enhancement of nitrous oxide energy yields from wastewater achieved by bioaugmentation with a recombinant strain of Pseudomonas aeruginosa. Scientific Reports 2018; 8: 11916.

Ma B, Wang S, Cao S, Miao Y, Jia F, Du R, et al. Biological nitrogen removal from sewage via anammox: Recent advances. Bioresource Technology 2016; 200: 981-990.

Makinia J, Zaborowska E. Mathematical Modelling and Computer Simulation of Activated Sludge Systems: IWA, UK, 2020.

Maktabifard M, Blomberg K, Zaborowska E, Mikola A, Mąkinia J. Model-based identification of the dominant N_2O emission pathway in a full-scale activated sludge system. Journal of Cleaner Production 2022; 336: 130347.

Masmoudi S, Elghazel H, Taieb D, Yazar O, Kallel A. A machine-learning framework for predicting multiple air pollutants' concentrations via multi-target regression and feature selection. Science of The Total Environment 2020; 715: 136991.

Mehrani M-J, Lu X, Kowal P, Sobotka D, Makinia J. Incorporation of the complete ammonia oxidation (comammox) process for modeling nitrification in suspended growth wastewater treatment systems. Journal of Environmental Management 2021; 297: 113223.

Mehrani M-J, Kowal P, Sobotka D, Guo J, Makinia J. The coexistence and competition of canonical and comammox nitrite-oxidizing bacteria (NOB) in a nitrifying activated sludge system – experimental observations and simulation studies 2022 (submitted).

Metcalf and Eddy. Wastewater engineering: treatment and reuse: Fourth edition / revised by George Tchobanoglous, Franklin L. Burton, H. David Stensel. Boston : McGraw-Hill, 2003.

Metcalf and Eddy. Wastewater Engineering: Treatment and Resource Recovery. United States: McGraw-Hill , New York, 2014.

Metcalf L, Eddy H, Tchobanoglous G, . Wastewater engineering: treatment, disposal, and reuse: McGraw-Hill, New York, 1991.

Miao Y, Zhang L, Yang Y, Peng Y, Li B, Wang S, et al. Start-up of single-stage partial nitrification-anammox process treating low-strength swage and its restoration from nitrate accumulation. Bioresource Technology 2016; 218: 771-779.

Natekin A, Knoll A. Gradient boosting machines, a tutorial. Frontiers in Neurorobotics 2013; 75-81.

O'Shaughnessy M. Mainstream Deammonification (WERF Report INFR6R11). VA (USA): Alexandria, 2016.

Park M-R, Park H, Chandran K. Molecular and Kinetic Characterization of Planktonic *Nitrospira* spp. Selectively Enriched from Activated Sludge. Environmental Science & Technology 2017; 51: 2720-2728.

Pinto AJ, Marcus DN, Ijaz UZ, Bautista-de lose Santos QM, Dick GJ, Raskin L. Metagenomic Evidence for the Presence of Comammox *Nitrospira* -Like Bacteria in a Drinking Water System. mSphere 2016; 11: 23-34.

Regmi P, Miller MW, Holgate B, Bunce R, Park H, Chandran K, et al. Control of aeration, aerobic SRT and COD input for mainstream nitritation/denitritation. Water Research 2014; 57: 162-171.

Ringnér M. What is principal component analysis? Nature Biotechnology 2008; 26: 303-304.

Roots P, Wang Y, Rosenthal AF, Griffin JS, Sabba F, Petrovich M, et al. Comammox *Nitrospira* are the dominant ammonia oxidizers in a mainstream low dissolved oxygen nitrification reactor. Water Research 2019; 157: 396-405.

Ryan M, Müller C, Di HJ, Cameron KC. The use of artificial neural networks (ANNs) to simulate N_2O emissions from a temperate grassland ecosystem. Ecological Modelling 2004; 175: 189-194.

Steinwart I, Christmann A. Support Vector Machines. New York: Springer, 2008.

Vasilaki V, Conca V, Frison N, Eusebi AL, Fatone F, Katsou E. A knowledge discovery framework to predict the N_2O emissions in the wastewater sector. Water Research 2020a; 178: 115799.

Vasilaki V, Danishvar S, Mousavi A, Katsou E. Data-driven versus conventional N_2O EF quantification methods in wastewater; how can we quantify reliable annual EFs? Computers & Chemical Engineering 2020b; 141: 106997.

Vasilaki V, Massara TM, Stanchev P, Fatone F, Katsou E. A decade of nitrous oxide (N_2O) monitoring in full-scale wastewater treatment processes: A critical review. Water Research 2019; 161: 392-412.

Yao Q, Peng D-C. Nitrite oxidizing bacteria (NOB) dominating in nitrifying community in full-scale biological nutrient removal wastewater treatment plants. AMB Express 2017; 7: 25.

Yin Q, Sun Y, Li B, Feng Z, Wu G. The r/K selection theory and its application in biological wastewater treatment processes. Science of The Total Environment 2022; 824: 153836.

Yu L, Chen S, Chen W, Wu J. Experimental investigation and mathematical modeling of the competition among the fast-growing "r-strategists" and the slow-growing "K-strategists" ammonium-oxidizing bacteria and nitrite-oxidizing bacteria in nitrification. Science of The Total Environment 2020; 702: 135049.

Zaborowska E, Lu X, Makinia J. Strategies for mitigating nitrous oxide production and decreasing the carbon footprint of a full-scale combined nitrogen and phosphorus removal activated sludge system. Water Research 2019; 162: 53-63.

Zhang M, Li N, Chen W, Wu J. Steady-state and dynamic analysis of the single-stage anammox granular sludge reactor show that bulk ammonium concentration is a critical control variable to mitigate feeding disturbances. Chemosphere 2020a; 251: 126361.

Zhang Z, Zhang Y, Chen Y. Recent advances in partial denitrification in biological nitrogen removal: From enrichment to application. Bioresource Technology 2020b; 298: 122444.

Zheng M, Wu S, Dong Q, Huang X, Yuan Z, Liu Y. Achieving mainstream nitrogen removal via the nitrite pathway from real municipal wastewater using intermittent ultrasonic treatment. Ultrasonics Sonochemistry 2019; 51: 406-411.

Paper I

M-J Mehrani, D Sobotka, P Kowal, S Ciesielski, J Makinia. 2020. The occurrence and role of *Nitrospira* in nitrogen removal systems, **Bioresource Technology**, 303, 122936.

https://doi.org/10.1016/j.biortech.2020.122936

Bioresource Technology 303 (2020) 122936

Contents lists available at ScienceDirect

Bioresource Technology

journal homepage: www.elsevier.com/locate/biortech

The occurrence and role of *Nitrospira* in nitrogen removal systems

Mohamad-Javad Mehrani[a], Dominika Sobotka[a], Przemyslaw Kowal[a], Sławomir Ciesielski[b], Jacek Makinia[a,*]

[a] Faculty of Civil and Environmental Engineering, Gdansk University of Technology, Narutowicza Street 11/12, 80-233 Gdansk, Poland
[b] Department of Environmental Biotechnology, Faculty of Environmental Sciences, University of Warmia and Mazury in Olsztyn, ul. Sloneczna 45G, 10-709 Olsztyn, Poland

GRAPHICAL ABSTRACT

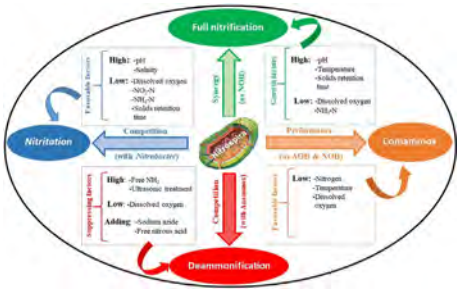

ARTICLE INFO

Keywords:
Comammox
Meta-analysis
Nitrite-oxidizing bacteria
Nitrospira
Nitrogen removal

ABSTRACT

Application of the modern microbial techniques changed the paradigm about the microorganisms performing nitrification. Numerous investigations recognized representatives of the genus *Nitrospira* as a key and predominant nitrite-oxidizing bacteria in biological nutrient removal systems, especially under low dissolved oxygen and substrate conditions. The recent discovery of *Nitrospira* capable of performing complete ammonia oxidation (comammox) raised a fundamental question about the actual role of *Nitrospira* in both nitrification steps. This review summarizes the current knowledge about morphological, physiological and genetic characteristics of the canonical and comammox *Nitrospira*. Potential implications of comammox for the functional aspects of nitrogen removal have been highlighted. The complex meta-analysis of literature data was applied to identify specific individual variables and their combined interactions on the *Nitrospira* abundance. In addition to dissolved oxygen and influent nitrogen concentrations, temperature and pH may play an important role in enhancing or suppressing the *Nitrospira* activity.

1. Introduction

Nitrification is a central process of the nitrogen (N) cycle in wastewater treatment plants (WWTPs), involving two consecutive steps, i.e. ammonia oxidation ($NH_4^+ \rightarrow NO_2^-$) (nitritation) followed by nitrite oxidation ($NO_2^- \rightarrow NO_3^-$) (nitratation). The nature of the process was already investigated in the second half of the 19th century (Dworkin and Gutnick, 2012).

Since nitrite accumulation was not normally observed in WWTPs, for a long time, nitrification research has primarily focused on ammonia-oxidizing bacteria (AOB). This also led to the discovery of new players of nitritation, such as ammonia-oxidizing archaea (AOA). In contrast, nitrite-oxidizing bacteria (NOB) were perceived as obligate chemo-lithoautotrophs with a physiological function strictly limited to

* Corresponding author.
E-mail address: jmakinia@pg.edu.pl (J. Makinia).

https://doi.org/10.1016/j.biortech.2020.122936
Received 27 November 2019; Received in revised form 27 January 2020; Accepted 29 January 2020
Available online 31 January 2020

nitratation (Daims et al., 2016).

The understanding of nitrification and nitrifying microorganisms has improved considerably over the last 20 years. Nitrite has been receiving growing attention as the pivotal component in a variety of novel nitrogen removal processes, including deammonification (known also as partial nitritation/anammox) or a shortened pathway of nitrification-denitrification via nitrite ("nitrite shunt"). As a consequence, the ecological importance of NOB has increased dramatically, but due to the limited knowledge on their biochemistry, NOB still remain a "big unknown of the nitrogen cycle" (Daims et al., 2016). Recent findings have suggested that uncultured members of the genus *Nitrospira*, rather than *Nitrobacter*, are the most diverse and abundant known NOB in municipal WWTPs (Gruber-Dorninger et al., 2014; Cao et al., 2017). Those bacteria (*Nitrospira*) were considered to be canonical NOB with the restricted metabolism (nitratation), however, recent findings identified a broader metabolic activity of *Nitrospira* (Koch et al., 2019).

The complete nitrification process by a single microorganism belonging to the genus *Nitrospira* has recently been discovered independently by two research groups (Daims et al., 2015; van Kessel et al., 2015). The process, known as comammox (complete oxidation of ammonia to nitrate), changes the current understanding of microbiologically mediated nitrogen removal processes involving nitrification (Pinto et al., 2016). The identification of the comammox bacteria overturned "a century-old dogma of nitrification research" (Koch et al., 2019). Metabolism of the members of *Nitrospira* genus is not limited to nitrite oxidation or comammox, but also comprise other functionalities beyond the N cycle, either under aerobic conditions (growth on formate and hydrogen) and anoxic conditions (reduction of nitrate to nitrite) (Koch et al., 2019).

The growing interest in the role of *Nitrospira* in WWTPs is reflected by the number of scientific papers published annually and focused specifically on that microorganism. In the Scopus database, the number of papers with the keywords "*Nitrospira*" and "wastewater" has continuously been increasing over the last decade from 6 (2010) to 89 (2019). Despite those numerous studies, there are still a lot of open questions concerning the importance and actual role of *Nitrospira* in nitrogen removal systems, effective methods of suppression, especially in deammonification systems, comparison of the kinetic parameters of these bacteria and *Nitrobacter*, coexistence of canonical and comammox *Nitrospira*, etc. These issues are addressed in this study by reviewing the physiological and microbial characteristics of *Nitrospira*, their abundance in WWTPs, and factors influencing their growth. The review is supported by meta-analysis of over 100 case studies of different wastewater treatment systems to investigate the *Nitrospira* abundance in terms of the combined effect and interaction of four process variables, such as dissolved oxygen (DO) concentration, influent NH_4-N concentration, pH, and temperature. Moreover, detection methods of the microbial diversity and abundance of *Nitrospira* are also summarized.

2. Physiological and morphological characteristics of *Nitrospira*

Currently, there are seven known NOB genera affiliated with four bacterial phyla, including *Proteobacteria* (*Nitrobacter, Nitrotoga, Nitrococcus*), *Nitrospinae* (*Nitrospina, 'Candidatus* Nitromaritima'), *Chloroflexi* (*Nitrolancea*) and *Nitrospirae* (*Nitrospira*) (Feng et al., 2017). *Nitrospira* are generally aerobic chemolithoautotrophic bacteria showing extraordinary diversity and plasticity. Members of the genus *Nitrospira* have been found in freshwater, soils, groundwater, geothermal springs and WWTPs. Moreover, *Nitrospira* colonize marine sponges, rhizospheres and leaf surface of plants (Daims and Wagner, 2018). Until now, *Nitrospira* have been divided into six phylogenetic lineages, which show different habitat preferences. In WWTPs, lineages I, II and IV have been detected (Lopez-Vazquez et al., 2014; Nowka et al., 2015), but most of *Nitrospira* were affiliated to the main lineages I or II, which could coexist together and dominate in both full-scale WWTPs and laboratory systems (Gruber-Dorninger et al., 2014). It is suggested that lineage II *Nitrospira* have higher affinity for nitrite and lower affinity for DO in comparison with these organisms in lineage I (Gruber-Dorninger et al., 2014; Park et al., 2017).

Nitrospira, like other NOB, is difficult to cultivate and thus growing sufficient amount of biomass for follow-up physiological studies remains challenging (Daims et al., 2016). Since most of *Nitrospira* genus members are uncultivated, and the obtained cultures are difficult to sustain, physiology of these bacteria is still not fully known. *Nitrospira* shows similar morphological properties to other NOB groups, i.e. the cell walls typical for gram-negative bacteria, and a helical to fibroid morphology (0.9–2.2 × 0.2–0.4 μm in size) or the average characteristic diameter of 1.3 ± 0.6 μm (Park et al., 2017). Most of *Nitrospira* species prefer to form biofilm structures and grow densely in microcolonies (Cao et al., 2017). In activated sludge, the reported *Nitrospira* enrichment cultures comprised either large cell aggregates in the range approximately 40–600 μm (Manser et al., 2005; Blackburne et al., 2007), smaller microcolonies (1–12 μm) (Koch et al., 2019) or even planktonic cells with small (3–4 μm) aggregates (Park et al., 2017). It should be noted that smaller floc sizes (< 40 μm) would significantly reduce any oxygen mass transfer limitation regardless of the bulk liquid DO concentrations (Blackburne et al., 2007).

Due to the difficulties in cultivation, information about the growth parameters, inhibitory compounds, and influence of environmental conditions on the *Nitrospira* activity are limited. Table 1 summarizes results of the studies on kinetic characterization of *Nitrospira* in terms of such parameters as the maximum specific growth rate (μ_{max}) and half-saturation (affinity) coefficients for DO (K_O) and nitrite (K_S). The only complete set of those parameters was reported by Park et al. (2017) in a study on the kinetic characterization of enriched *Nitrospira* from activated sludge.

3. Competition of *Nitrospira* with *Nitrobacter*

Two common NOB in WWTPs comprise *Nitrospira* and *Nitrobacter* and prediction of their dominance has commonly been based on the hypothesis that *Nitrospira* is a K-strategist with a high affinity with respect to nitrite and DO concentrations, while *Nitrobacter* is an r-strategist that prevails at higher concentrations of DO and nitrite (Blackburne et al., 2007; Huang et al., 2010; Persson et al., 2014; Wang and Gao, 2016; Cao et al., 2017; Kouba et al., 2017). The K-based selection is

Table 1
Review of most important kinetic parameters of *Nitrospira*.

μ_{max} d^{-1}	K_S mg N/L	K_O mg O_2/L	Remarks	Reference
0.69 ± 0.10	0.52 ± 0.14	0.33 ± 0.04	22 °C, Enriched culture	Park et al., 2017
NA	0.9–1.1	0.54	15–30 °C, Enriched culture	Blackburne et al., 2007
NA	0.11–0.50	0.47	20 °C, Mixed culture	Manser et al., 2005
0.45–0.52	0.13–0.39	NA	28–37 °C, Pure culture	Nowka et al., 2015
NA	0.16	NA	30 °C, Enriched culture	Schramm et al., 1999
0.18	NA	NA	20 °C, Pure culture	Watson et al., 1986

(μ_{max} – maximum specific growth rate, K_S – nitrite half-saturation (affinity) coefficient, K_O – dissolved oxygen half-saturation (affinity) coefficient).

associated with delayed reproduction, large cell size, and/or stable environments, while the r-selection regime is adopted with an early reproduction, small cell size, and/or variable environments (Andrews and Harris, 1986). Several studies have revealed that the competition between *Nitrospira* and *Nitrobacter* is primarily influenced by nitrite concentrations in the studied system. The growth of *Nitrospira* has been favored under low nitrite conditions, while *Nitrobacter* has been found the dominant NOB at higher nitrite concentrations (> 80 mg N/L) (Nogueira and Melo, 2006; Blackburne et al., 2007; Huang et al., 2010; Park et al., 2017; Wang et al., 2017). On the contrary, results of another study (Blackburne et al., 2007) showed that *Nitrospira* was the dominant NOB when nitrite concentrations were relatively high (> 100 mg N/L).

Another critical factor influencing the *Nitrospira* abundance in WWTPs is the operational DO concentration (Ushiki et al., 2017; Chang et al., 2019). Indeed, Park et al. (2017) attributed a high enrichment of *Nitrospira* in a DO- and nitrite-limited SBR to higher affinity for both DO (K_O = 0.5–0.6 mg O_2/L vs. 0.2–4.3 mg O_2/L) and nitrite (K_S = 0.1–1.1 mg N/L vs. 0.3–7.6 mg N/L) in comparison with *Nitrobacter*. The same authors postulated that there is another feature of *Nitrospira* that is advantageous for completion with *Nitrobacter* and other NOB under nitrite-limited conditions. *Nitrobacter* encodes for a cytoplasmic nitrite oxidoreductase (*nxr*), which requires the transport of nitrite and nitrate across the inner membrane in the reverse directions. In contrast, *Nitrospira* typically encodes for periplasmic *nxr*, which catalyses the second step of nitrification. The latter type of oxidation (periplasmic) is beneficial as a higher specific proton motive force is generated and the transmembrane exchange of nitrite and nitrate does not occur.

Table 2 shows a comparison of these two bacteria in terms of environmental factors which are important for the operation of biological wastewater systems. The maximum activity of *Nitrospira* is much lower than *Nitrobacter* measured as the rates of nitrite oxidation (Kim and Kim, 2006) and oxygen uptake (Blackburne et al., 2007). In addition to low nitrite and DO concentrations, *Nitrospira* may be better adapted to slightly higher pH (8–8.3 vs. 7.6–8.2) and temperatures (29–30 °C vs. 24–25 °C). However, the inhibition thresholds of free ammonia (FA) (0.04–0.08 mg NH_3-N/L) and free nitrous acid (FNA) (0.03 mg HNO_2-N/L) are significantly lower in comparison with *Nitrobacter* (10 mg NH_3-N/L and 0.2–0.4 mg HNO_2-N/L). This may provide another explanation why *Nitrospira* has been found a dominant NOB in low concentrations of ammonium and nitrite (Blackburne et al., 2007).

4. Comammox *Nitrospira*

The comammox process, shown in Fig. 1, is mediated by some members of the genus *Nitrospira*, including "*Candidatus N. nitrosa*", "*Candidatus N. nitrificans*", "*Candidatus N. inopinata*", and *strain Ga0074138* (Daims et al., 2015; van Kessel et al., 2015; Pinto et al., 2016; Camejo et al., 2017). While the canonical NOB possesses the gene *nxr* involved only in nitrite oxidation, the comammox *Nitrospira* possesses genes involved also in ammonia oxidation, i.e. ammonia monooxygenase (*amo*) and hydroxyloamine dehydrogenase (*hao*) (Santoro, 2016; Camejo et al., 2017; Hu and He, 2017; Annavajhala et al., 2018).

Costa et al. (2006) hypothesized the existence of a single microorganism capable of performing the two nitrification steps. The authors assumed that such a microorganism is slower-growing, but with a higher yield coefficient, in comparison with incomplete ammonia oxidizers (canonical AOB). Theoretical calculations revealed that the favorable conditions for the growth of complete oxidizers are provided in clonal clusters, such as biofilms, with low mixing conditions and low substrate diffusion gradients. In contrast, faster-growing canonical AOB could dominate in chemostats and other well-mixed systems.

Shortly after the discovery of comammox bacteria, Chao et al. (2016) reported the presence of those bacteria in a biofilm grown in aerobic reactors in WWTPs. Earlier studies on biomass distribution in fully nitrifying biofilm systems (Okabe et al., 1999; Schramm et al., 1999) revealed the highest NOB abundance in deeper zones of biofilms under DO limited conditions. Furthermore, Okabe et al. (1999) showed that *Nitrospira* was the dominant NOB, whereas *Nitrobacter* and other faster growing NOB species were hardly detected. This finding implicitly suggests that *Nitrospira* can adapt better to the limited DO availability. It may also explain the presence of "comammox" *Nitrospira* in the environments exposed to the DO concentration gradients, such as deeper zones of biofilms (Chao et al., 2016).

5. Methods of *Nitrospira* detection

5.1. Classical cultivation-based and biochemical techniques

In order to detect *Nitrospira* related bacteria in complex biomass matrix, such as activated sludge, a set of appropriately sensitive research tools should be applied. In the past, research on biomass samples from WWTPs were carried out using the classical microbiological methods, i.e. cultivation and light microscopy. These methods have allowed to identify many important groups of microorganisms in wastewater treatment processes. For example, the cultivation techniques developed in the early study by Winogradsky enabled to detect bacteria catalyzing both steps of nitrification (Nielsen and McMahon, 2014). Initially, biochemical and physiological studies were focused mainly on *Nitrobacter*, whereas other NOB were studied occasionally (Daims and Wagner, 2011). The progress in detection of the others nitrifying bacteria was linked with the development of a new generation of the biochemical techniques.

The first advanced method used for identification and differentiation of NOB was the whole cell fatty acid methyl esters (FAME) analysis. Lipski et al. (2001) showed that fatty acid profiles of four genera of NOB (*Nitrobacter, Nitrococcus, Nitrospina* and *Nitrospira*) were unique. Furthermore, it was proved that these profiles could also be used for single species (Gilbride, 2014) as well the whole microbial communities characterization (Huang et al., 2019).

Table 2
Comparison of the prevailing conditions for the competition of *Nitrospira* and *Nitrobacter* in biological wastewater treatment systems.

Factor	Unit	Prevailing range		References
		Nitrospira	*Nitrobacter*	
Maximum activity (rate):				
Nitrite oxidation	mg N/g NOB h	10.5	93.8	Kim and Kim, 2006
Oxygen uptake	mg O_2/g VSS h	32	289	Blackburne et al., 2007
pH	–	8–8.3	7.6–8.2	Grunditz and Dalhammar, 2001, Blackburne et al., 2007, Rodrigues et al., 2017
DO concentration	mg O_2/L	< 1.0	1.0	Huang et al., 2010, Liu and Wang, 2013
Temperature	°C	29–30	24–25	Huang et al., 2010, Courtens et al., 2016a
Inhibition threshold:				
Free ammonia	mg NH_3-N/L	0.04–0.08	10	Blackburne et al., 2007
Free nitrous acid	mg HNO_2-N/L	0.03	0.2–0.4	

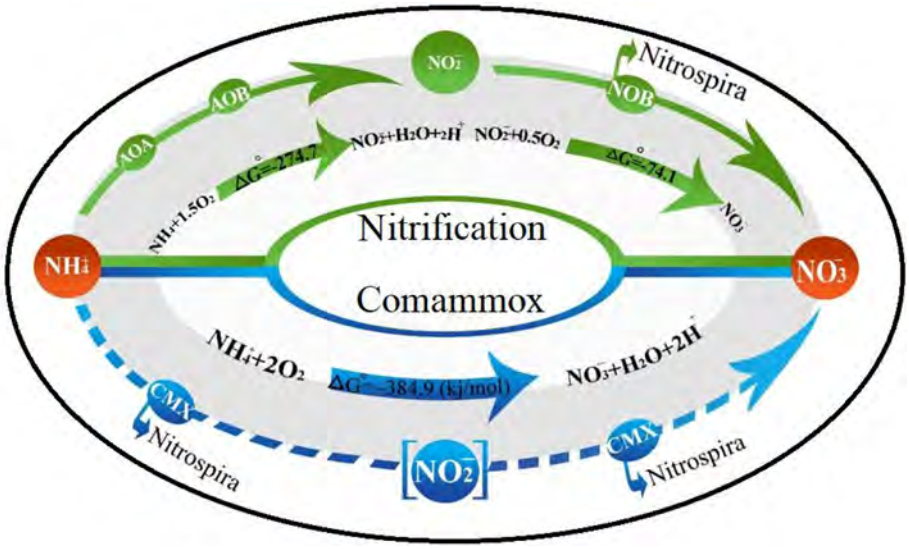

Fig. 1. The role of *Nitrospira* in the two-step nitrification and comammox processes.

The alternative way to identify NOB is based on an immunological approach. In this method, protein extract from enriched cultures is separated in is separated by electrophoresis in gel made of sodium dodecyl sulphate–polyacrylamide (SDS-PAGE) and then blotted onto a cellulose membrane and immune-stained using a protein specific antibody. Bartosch et al. (2002) used Mab 153–3 antibody to determine 13-subunit of the nitrite oxidizing system (β-NOS) of the known NOB. Due to the different mass of this protein, the immunological approach could be useful for differentiation of all major NOB (Bartosch et al., 2002).

The morphological and biochemical characteristics allow to detect individual, well characterized strains. However, in the case of comprehensive analysis of bacterial consortia composed of many different forms of microorganisms, the classical techniques are not practical due their prevailed low resolution and labor-intensity (Nemati et al., 2016). For example, application of the techniques based on the light microscopy is often limited for detection of *Nitrospira* due to the lack of specific phenotypic characters in the structure of their cells. On the contrary, the cultivation-based techniques focus on specific microorganisms, for which the knowledge about environmental parameters required for their growth is available (Salmonová and Bunešová, 2017).

5.2. Cultivation-independent techniques

A significant progress in the characterization of microbial communities, including the nitrifying bacteria, took place in the early 1990's along with the development of molecular techniques and their adaptation to the microbial ecology studies. The molecular techniques used in the phylogenetic studies of microorganisms are based on the nucleic acid sequences polymorphism analysis. Especially, polymerase chain reaction (PCR)-based methods, by application of the defined reaction primers, enables selective amplification of the targeted DNA sequences thus provide a fast and sensitive alternative to the biochemical and physiological methods (Gómez-Silván et al., 2014).

In the PCR-based methods, more often the genes incorporated in the operon responsible for the synthesis of ribosomal ribonucleic acids (rRNA) are applied as a molecular marker, due to their ubiquitous presence in the genomes of all types organisms and evolutionary properties, i.e. presence of the regions characterized by both significant degrees of conservation and high variation in the nucleotide composition. Other method that allows for bacteria species detection on site without the need of prior isolation is Fluorescence in Situ Hybridization (FISH). This semi-quantitative technique is used for specific detection of particular bacteria by hybridization of fluorescently labelled probes to complementary target rRNA sequences within intact cells. After hybridization, samples are analysed by the fluorescence microscopy (Wang et al., 2008). This technique, combined with flow cytometry, allows to enumerate the labelled cells (Lenaerts et al., 2007).

Currently, extensive databases containing 16S rRNA geneo sequences from almost all microorganisms known so far are widely available (e.g. SILVA database https://www.arb-silva.de, Genomic-based 16S ribosomal RNA Database – GRD https://metasystems.riken.jp/grd, Ribosomal Database Project – RDP https://rdp.cme.msu.edu) to conduct a comparative analysis to determine the phylogenetic position of isolates derived from the tested environmental samples (Tsukuda et al., 2017). Although the most commonly used gene for examination of microbial populations is the 16S rRNA, its use in the microbial ecology has some drawbacks. The main disadvantage is that it may not be related to the physiology of the target organisms (Kowalchuk and Stephen, 2001). Moreover, since comammox bacteria do not form a unique clade within *Nitrospira* lineage II, comammox and canonical *Nitrospira* NOB cannot be individually detected by 16S rRNA-based methods (Pjevac et al., 2017). Therefore, a preferred approach is based on the genes encoding key enzymes for a specific metabolic pathway (Wang et al., 2018).

The most widely applied molecular marker for *Nitrospira* detection is *nxr* gene which encodes nitrite oxidoreductase (NXR), which a key enzyme of nitritation. The possibility of using *nxr* gene as a functional marker for *Nitrospira* detection has first been described by Pester et al. (2014). This membrane associated enzyme are found in two recognizable forms. One is a cytoplasmic form found in *Nitrobacter, Nitrococcus and Nitrolancetus*, whereas the second is a periplasmic form found in *Nitrospira and Nitrospina*. The gene coding for NXR consists of alpha (*nxr*A), beta (*nxr*B) and gamma (*nxr*C) subunits. The *Nitrospira* NOB was successfully detected using PCR primers specific for nxrB gene (Pester et al., 2014).

The *nxr* genes sequences, derived from the canonical *Nitrospira* NOB, show a significant similarity to comammox *Nitrospira* (Daims et al., 2016). In addition, a comparative genomic analysis revealed low numbers of comammox-specific genes which are suitable for detection of comammox *Nitrospira* (Palomo et al., 2018). In order to perform a selective detection of these bacteria, the authors suggested to apply procedures based on the DNA sequences analysis of *amo* and *hao*) genes. These genes encode key enzymes of ammonium oxidation step in the comammox pathway. DNA sequences variants of the *amo* and *hao* genes obtained from the currently known comammox *Nitrospira,* are different from the homologs of the other groups. This reflects a high application

potential as a reliable molecular marker (Daims et al., 2015; van Kessel et al., 2015; Daims et al., 2016).

All the known comammox bacteria belong to sublineage II of the genus *Nitrospira* (Lawson and Lücker, 2018). *Amo* orthologs, which are encoded by comammox *Nitrospira*, are dissimilar to both each other and the other betaproteobacterial *amo* (Daims et al., 2015). This suggests that there are two distinct clades (clade A and B) of comammox *Nitrospira* and the pitfall of their detection with PCR results from the uniqueness of comammox-*Nitrospira* gene coding *amo*. Pjevac et al. (2017) and Koch et al. (2019) proposed a pair of PCR primers that would be the best available tool for fast identification of comammox *Nitrospira*.

The recently developed Next Generation Sequencing (NGS) technologies allow for complex analysis of particular bacterial genomes (metagenomics) or complex examination of microbial community genomes (metatranscrriptomics) without need of single strains isolation at high resolution level not available for the classical PCR-based methods (He et al., 2018). This approach was used by Annavajhala et al. (2018) to quantify the presence and elucidate the potential functionality of comammox bacteria in 16 full-scale mainstream and sidestream BNR reactors. The sequences specified for those bacteria constituted between 0.28 and 0.64% of the total coding DNA sequences in all the analyzed cases.

NSG and PCR based surveys provide crucial information about abundances and diversity of the key bacterial groups, but do not cover functionality aspects of the complex microbial communities. Therefore, the additional metatranscriptome i.e. profile of the overall gene expression of microorganisms in particular environments, should be implemented. Crovadore et al. (2018) analyzed metagenomes and metatranscriptomes of activated sludge bioreactors, with and without enrichment with aerobic granules. The analysis revealed that the bioaugmentation increased the expression level of genes involved in ammonia removal. Using a similar approach Yu et al. (2018) provided evidence for comammox in an enriched culture of tidal sediments.

Combination of the metagenomes and metatranscriptomes is currently most powerful approach for complex functional analysis of the microbial communities. The advantage of this approach is possible use of it for the measurement of in situ activity of comammox-*Nitrospira* that is extremely important for the understanding the role of this bacteria in wastewater treatment processes.

6. Occurrence of *Nitrospira* in nitrogen removal systems

The reported occurrences of *Nitrospira* in the most common nitrogen removal processes in WWTPs, including nitrification-denitrification (N-DN) and deammonification (PN-A), were summarized. *Nitrospira* abundances along with the most important operational parameters, such as pH, temperature, DO, solids retention time (SRT), nitrogen concentrations and removal efficiency/rates, were listed for approximately 100 technological studies (80 for N-DN and 35 PN-A systems). These data have been classified in terms of the scale of the studied system, feed characteristics and reactor types. Fig. 2 shows that the lab-scale studies constituted the majority (approximately 90%) of the analyzed N-DN and PN-A systems. Most of the studied systems were fed with synthetic wastewater (48% – N-DN and 59% – PN-A), while the N-DN systems were also operated with real municipal, domestic and industrial wastewater. Due to the nature of the PN-A process (treatment of high-loaded ammonia streams), the PN-A reactors were primarily operated with reject water from sludge dewatering processes (11%) or synthetic wastewater simulating the composition of reject water (59%). In both cases, the most popular reactor types were SBR/SBBR (42% – N-DN and 44% – PN-A).

In general, the studied systems were laboratory-scale SBRs fed with synthetic wastewater with respect to both N-DN and PN-A. Case studies with the highest observed relative abundances of *Nitrospira* in N-DN and PN-A systems are presented in Table 3. The highest abundance of *Nitrospira* (53%) was reported in a nitrifying SBR operated for more than one year at low DO concentrations (Roots et al., 2018).

In fully nitrifying systems, the theoretical ratio of NOB/AOB abundances corresponds to the ratio of their yield coefficients (Y_{NOB}/Y_{AOB}). When assuming the typical values of Y_{NOB} (= 0.09) and Y_{AOB} (= 0.15), the obtained ratio NOB/AOB = 0.6 suggests that AOB should dominate over NOB. In practice, the AOB and NOB abundances in nitrifying communities can shift and change depending on the local conditions (Cao et al., 2017). Significantly higher ratios of NOB/AOB have indeed been reported in both full-scale municipal WWTPs (0.8–1.5) (Harms et al., 2003; Ramdhani et al., 2013) and a lab-scale aerobic granular reactor (3–4) (Winkler et al., 2012). These deviations from the theoretical ratio NOB/AOB could be explained by the commamox process (Wang and Li, 2015; Daims et al., 2016).

In deammonification systems, the presence of *Nitrospira* has been observed in numerous studies (e.g. Malovanyy et al., 2015; Persson et al., 2014; Varas et al., 2015; Wang and Gao, 2016; Soliman and Eldyasti, 2016; Poot et al., 2016; Zhang et al., 2016). The presence of comammox *Nitrospira* seems to be undesirable in all anammox-based systems due to disturbance of nitrite production. However, the actual role of comammox *Nitrospira* in deammonification still needs to be evaluated (Cao et al., 2017), even though their coexistence with anammox bacteria has been reported (Van Kessel et al., 2015).

The out-selection of NOB is a critical factor for the efficient and stable deammonification (Zhang et al., 2016). The literature data (Varas et al., 2015; Poot et al., 2016; Soliman and Eldyasti, 2016; Wang and Gao, 2016) explicitly indicate that it is possible to suppress NOB activity, but without removing completely those bacteria from the system. For example, Wang and Gao (2016) observed this in a granular deammonification reactor, which had been deteriorated due to high abundances of *Nitrospira* and *Nitrobacter*. In the course of the experiment, the NOB activity was successfully suppressed by keeping low DO concentrations (< 0.13 mg/L) and high FA levels (5–40 mg N/L). After 2 months of the reactor operation, the ratio of produced nitrate/consumed ammonia decreased from 37% to 7%. However, the investigation of 16S rRNA gene copy numbers revealed that NOB were still highly abundant in the studied system. Only the copy numbers for *Nitrospira* increased approximately 50 times (from 2.63×10^6 to 1.06×10^8 copies/mg), while the copy numbers of *Nitrobacter* decreased approximately 5 times (from 4.52×10^7 to 2.17×10^6 copies/mg).

7. Factors influencing the *Nitrospira* activity and abundance in nitrification-denitrification and deammonification systems

A list of factors affecting the *Nitrospira* abundance (e.g. DO, temperature, pH, TNL, FA, SRT/HRT, time of reactor operation or salinity) in nitrification-denitrification and anammox-based systems, and their effect on the *Nitrospira* abundance are summarized Table 4. The effects of those factors on the *Nitrospira* activity and abundance are discussed in the following sub-sections.

7.1. Dissolved oxygen

Abundant amounts of *Nitrospira* have been maintained or even increased in low-DO nitrifying reactors (with DO concentration below 1.0 mg O_2/L) as reported by Huang et al. (2010), Liu and Wang (2013), Wang and Gao (2016), Zhou et al. (2018) and Roots et al. (2018). At the extreme case, *Nitrospira* reached 53% of the overall microbial relative during the operation at low DO concentration (0.2–1 mg O_2/L) in the nitrifying SBR (Roots et al., 2018). During the long term operation of the lab-scale SBR (DO = 0.5–1.0 mg O_2/L), Park et al. (2017) observed increased of the *Nitrospira* concentration from $7.0 \times 10^7 \pm 1.2 \times 10^6$ gen copies/mL to $7.7 \times 10^8 \pm 7.5 \times 10^7$ gen copies/mL. Zhou et al. (2018) gradually decreased DO concentration in a SBR from 3 to 0.5 mg O_2/L, which resulted in an increase in the *Nitrospira* abundance from

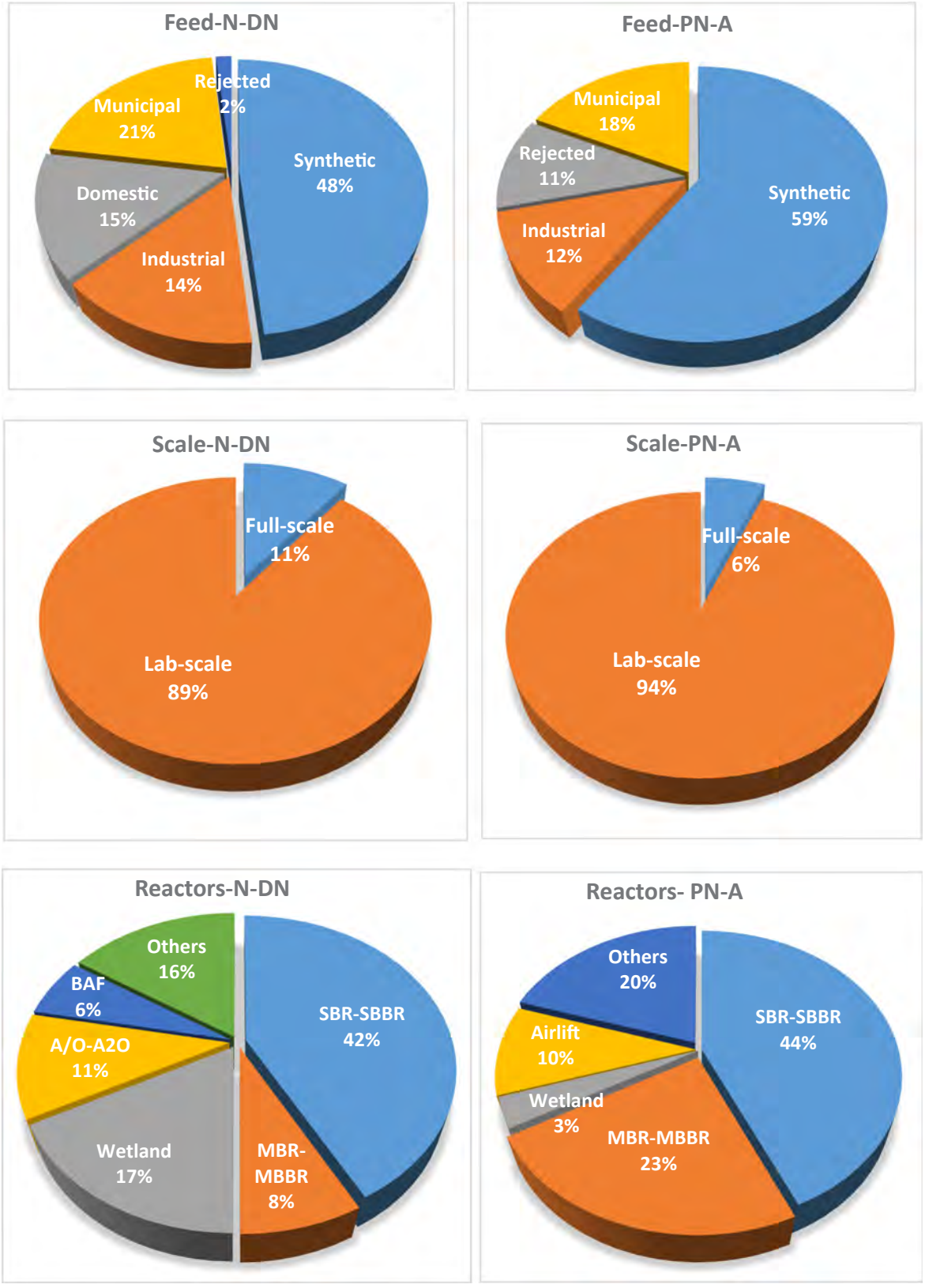

Fig. 2. Classifications of approximately 80N-DN systems and 35 PN-A systems in which *Nitrospira* were detected.

2.07×10^9 to 9.19×10^{10} copies/g MLSS during 114 days of operation. Moreover, Bao et al. (2016), Fitzgerald et al. (2015), and How et al. (2018) showed that efficient nitrification was possible also at even lower DO concentrations (0.3–0.5 mg O_2/L). Fitzgerald et al. (2015) divided *Nitrospira* into two groups: low-DO *Nitrospira* (represented by *Nitrospira moscoviensis*) and high-DO *Nitrospira* (represented by *Candidatus Nitrospira defluvii*). Experimental results confirmed an increase of the relative abundance of low-DO *Nitrospira* in a reactor with a very low DO concentration (0.13 mg O_2/L) and a significant decrease in the reactor with a high DO concentration (8.7 mg O_2/L). On the contrary, the

Table 3
Maximum relative abundances of *Nitrospira* reported for N-DN and PN-A systems.

System	Maximum relative abundance, %	Main operational conditions	References
N-DN	53	See Table 4 for details	Roots et al., 2018
N-DN	22	DO: 0.8–2.2 mg O_2/L, T: 30 °C, pH: 7.0–8.0, FA: 22 mg/L	Yang et al., 2018
N-DN	20	See Table 4 for details	Bhatia et al., 2017
N-DN	16	SRT: 18 d, NH_4-N: 30–40 mg/L,	Liu et al., 2018
N-DN	12	See Table 4 for details	Jia et al., 2017
N-DN	10	See Table 4 for details	Quartaroli et al., 2017
N-DN	9	See Table 4 for details	Song et al., 2017
N-DN	5	DO: 0.8 mg O_2/L, T: 22.54 °C, pH: 6.0–8.0, NH_4-N: 17 mg/L	Ouyang et al., 2017
N-DN	4.6	See Table 4 for details	Gao et al., 2017
N-DN	3.3	T: 25 °C, pH: 10, NH_4-N: 63 mg/L	Yuan et al., 2016
N-DN	3	See Table 4 for details	Dong et al., 2017
N-DN	2	See Table 4 for details	Tian et al., 2017
N-DN	2	See Table 4 for details	Luo et al., 2017
N-DN	2	DO: 2.5 mg O_2/L, T: 20 °C, SRT: 25 d, pH: 7.0–8.0, NH_4-N: 20 mg/L	Ma et al., 2017
PN-A	27.9	DO: 0.2 – 8.0 mg O_2/L, T: 16 °C, pH: 6.3–8.0, NH_4-N: 50 mg/L	Pedrouso et al., 2017
PN-A	10.5	See Table 4 for details	Wang et al., 2017
PN-A	7.5	DO: 1 mg O_2/L, T: 22 °C, pH: 7.2, NH_4-N: 45–68 mg/l,	Du et al., 2019
PN-A	5.35	See Table 4 for details	Mardanov et al., 2016
PN-A	4	See Table 4 for details	Liu et al., 2017

(N-DN – nitrification-denitrification, PN-A – partial nitritation/anammox).

relative abundance of high-DO *Nitrospira* increased in a reactor with a high DO concentration (8.5 mg O_2/L) and decreased in a reactor with a low DO concentration (0.12–0.24 mg O_2/L). The influence of DO concentration on the *Nitrospira* abundance in the partial nitrification SBR was investigated by Bao et al. (2016). A stable and complete nitrification was achieved at the DO concentration of 0.3 ± 0.14 mgO_2/L. The *Nitrospira*-like bacteria were the dominant NOB and their abundance increased from 1.03×10^6 to 2.64×10^6 cells/mL. When a higher DO concentration (1.8 ± 0.32 mgO_2/L) was applied, the *Nitrospira* abundance gradually decreased from 2.64×10^6 to 8.85×10^5 cells/mL. This explicitly suggests that high DO conditions may lead to continuous suppression of the Nitrospira activity.

Low DO concentrations are also the most preferred strategy in the wastewater treatment systems with partial nitrification process, as a one of the factors that selectively suppress NOB growth (Wang et al., 2017; Peng and Zhu, 2006; Ma et al., 2009, 2011). The lowest reported DO concentration (0.17 ± 0.08 mg O_2/L) was used in a PN-A SBR by Miao (2016). In that DO-limited system, *Nitrospira* was detected as a dominant NOB. The authors reported an increase in the *Nitrospira* gene copy number from 2.61×10^8 to 1.67×10^{10} copies/g MLSS. A slightly higher DO concentration (0.3 mg O_2/L) was used in the CANON process by Wang et al. (2017) and *Nitrospira* was detected as a dominant NOB in that system. Cao et al. (2018) observed that reduction of DO from 1.7 to 1.0 mg O_2/L in the aeration phases caused a shift of the dominant NOB from *Nitrobacter* to *Nitrospira*. Even more case studies for *Nitrospira* dominance (due to low DO) were reported for biofilm systems (Kindaichi et al., 2007; De Clippeleir et al., 2011; De Clippeleir et al., 2013; Gilbert et al., 2015) in comparison with the *Nitrobacter*-dominant cases (Isanta et al., 2015).

Opposite observations were made by Mardanov et al. (2016) and Qian et al. (2017). Mardanov et al. (2016) noted a decreased abundance of *Nitrospira* (from 5.35 to 3.34%) in the PN-A SBR operated with DO = 0.5 mg O_2/L. In the PN-A continuous reactor operated at DO in the range 0.8–1.5 mg O_2/L, the *Nitrospira* abundance was effectively inhibited (from 0.44 to 0.04%) with the increase of nitrogen removal efficiency (Qian et al., 2017).

In the partial nitrification systems, not only DO concentration but also aeration mode (continuous or intermittent) has a significant importance for the growth of NOB. The concept of intermittent aeration has recently been applied to effectively suppress nitrite oxidation primarily in lab-scale systems (Sun et al., 2018; Zhou et al., 2018; Roots et al., 2018; Bao et al., 2016; Ma et al., 2017; Park et al., 2017; Regmi et al., 2014; Zubrowska-Sudol et al., 2011; Li et al., 2011), but also in full-scale systems (Miao et al., 2018; Joss et al., 2009). Park (2008) found that DO substantially influenced a shift within *Nitrospira* between lineage I and II. Bao et al. (2016) found that a sudden switch to high DO conditions from a low DO level caused inhibition and gradually decreased the *Nitrospira* abundance from 2.64×10^6 to 8.85×10^5 cells/mL. The authors concluded that *Candidatus Nitrospira defluvii*-like bacteria favor limited DO conditions and cannot adapt to rapid transition to the high DO concentration. Sun et al. (2018) carried out four intermittent aerated reactors, two SBR operated under high DO = 2 mg O_2/L (SBR-H) and low DO = 1 mg O_2/L (SBR-L) and two continuous-flow multiple reactors (CMR) operated at the same conditions, i.e. DO = 2 mg O_2/L (CMR-H), and DO = 1 mg O_2/L (CMR-L). The authors observed (1) a higher abundance of *Nitrospira* in SBR-H (2.99%) compared to SBR-L (1.81%), and (2) higher abundance of *Nitrospira* in the SBR compared to the CMR (0.66% – CMR-H and 1.38% – CMR-L). Higher abundances of *Nitrospira* in the high-DO system is in contradiction to previously presented data. In deammonification systems, the successful NOB suppression was achieved with either short (Katsogiannis et al., 2003) or long aerobic periods (Mota et al., 2005; Zubrowska-Sudol et al., 2011; Li et al., 2011; Miao et al., 2016). During the SBR operation with intermittent aeration and low DO concentration (0.2–1.0 mg O_2/L), the *Nitrospira* abundance observed in 16S rRNA sequencing datasets increased from 3.1% (day 3) to 53% (day 407) (Roots et al., 2018). An appropriate configuration of the intermittent aeration system is challenging, and the recent discovery of the comammox *Nitrospira* might bring additionally challenges in implementation of that aeration mode.

7.2. Temperature

Several authors have reported that the optimum temperature for the growth of *Nitrospira* is in the range of 30–35 °C (Yao and Peng, 2017; Huang et al., 2010; Blackburne et al., 2007). Huang et al. (2010) analyzed the effect of temperature on the main representatives of NOB (including *Nitrospira*) in a biological reactor at a municipal WWTP. During one-year study, the temperature in the reactor was in the range 24–30 °C, depending on the season. The authors observed a strong effect of the temperature ($r = 0.59$, $P < 0.0001$) on the *Nitrospira* abundance. In their study, the peak concentrations were achieved

Table 4
Summary of influencing factors on growing of *Nitrospira* in nitrogen removal systems.

Main Factor	Value	Process	*Nitrospira* abundance	Other factors	Reference
DO	0.2 ÷ 1.0 mg O_2/L	PN-A	Increase from 3.1 to 53%	T: 20.3 ± 1.1 °C, SRT: 99 d, NH_4^+: 0–14 mg/L	Roots et al., 2018
	2.0 mg O_2/L	N	2.99%	T: 24 ± 0.5 °C, SRT: 15 d, HRT: 12 h,	Sun et al., 2018
	1.0 mg O_2/L	N	1.81%	NH_4-N: 43 ± 2.0 mg/L	
	Reduction from 1.7 to 1.0 mg O_2/L	PN-A	"Dominant" NOB	pH: 6.9 ± 0.2, SRT: 3–7 d	Cao et al., 2018
	0.8 ÷ 1.5 mg O_2/L	PN-A	Decrease from 0.44 to 0.04%	SRT: 33–56 d, NH_4^+: 105 mg/L	Qian et al., 2017
	0.5 mg O_2/L	PN-A	Decrease from 5.35 to 3.34%	SRT: 25 d, NH_4^+: 11 mg/L	Mardanov et al., 2016
Aeration to mixing ratio (aer:mix)	1 h : 1 h	N	1.6%	pH: 7.6–7.8, HRT: 3 d,	Mota et al., 2005
	0.5 h: 1.5 h		2.9%		
	2.5 h : 0.5 h	N	20%	DO: 3 mg O_2 L^{-1}, HRT: 11.1 h	Bhatia et al., 2017
	1.5 h : 1 h		8%		
Temperature	30 – 35 °C	PN	"Dominant" NOB	DO: < 1 mg O_2/L, SRT: 4.27 d,	Huang et al., 2010
				Long operational time (> 1 year),	
	38 – 50 °C	N	"Dominant" NOB	pH: 6.5–7.5, SRT: ~92 days	Courtens et al., 2016a
	Increase from 25 to 40 °C	N	Decrease from 2.02% to 0.09%	DO: 0.7 mg O_2/L, FA: 2.7 mg/L	Luo et al., 2017
	10, 17 and 28 °C	N	"Dominant" NOB in 17 °C	NH_4-N: 39.1 mg/L	Alawi et al., 2009
Temperature	10, 13, 16 and 19 °C	PN-A	"Dominant" NOB in 16 °C	DO: 0.5 mg O_2/L, HRT: 1.3 h,	Liu et al., 2016
				NH_4-N: 400 ± 8 mg/L,	
	15–17 °C	A	4.19%	DO: 0 mg O_2/L, pH: 7.5–7.8, HRT: 6–2 d,	Liu et al., 2017
				NH_4-N: 20–30 mg/L, NO_2-N: 22–30 mg/L	
	Reduction from 26 to 20 °C	PN-A	Decrease from 6.2% to 5.2%	DO: 0.2–1.5 mg O_2/L, pH: 7.4–8.5,	Zekker et al., 2017
				NLR: 0.5–2.2 g N (m^2·d)	
	Reduction from 25 to 15 °C	PN-A	Increased from 4.63 to 7.23%	DO: 0.2 μmol O_2/L, pH:	Akaboci et al., 2018
				7.54 ± 0.20 ÷ 8.45 ± 0.20, NLR:	
				612.5 ± 25.4 mg N/(L·d)	
Weather seasonality	Winter (9.2 °C)	N	4.14%	NH_4-N: 220–550 mg/L	Jia et al., 2017
	Summer (25.6 °C)		12.02%		
	Winter (24–25 °C)	N	"Nondominant" NOB	DO: 1.0 mg O_2/L, SRT: 4.27 ± 0.4 d,	Huang et al., 2010
	Summer (29–30 °C)		"Dominant" NOB	HRT: 4.38 ± 0.19 h,	
pH	6–9	N	The highest activity in range from 8.0 to 8.3	DO: 1.5 mg O_2/L, T: 22 ± 1 °C	Blackburne et al., 2007
	> 9	PN		T: 22.1 °C, pH: 7.2–8.8, SRT: 7d,	Rodrigues et al., 2017
				NH_4-N: 30 mg/L	
	6.4	N	"Dominant" NOB	T: 17 °C	Wegen et al., 2019
Low NLR	0.095 ÷ 0.238 kg/(m^3·d)	N	Increased from 1.5 to 2.0%	DO: 2–3 mg O_2/L, T: 25 ± 3 °C, SRT: 30 d, NH_4-N: 22.41–34.24 mg/L	Tian et al., 2017
High FA	49 mg/L	PN-A	< 0.5%	DO: < 1.0 mg O_2/L, pH: 8.2,	Wang and Gao, 2018
				T: 32 ± 1 °C, HRT: 0.83–2.5 h	
	85.7 ± 15.35 mg/L	PN	Wash out from the reactor	DO: 5.42 ± 0.72 mg O_2/L,	Liang et al., 2014, 2015
				T: 24.1–26.9 °C, HRT: 11.70 ± 1.72 h, NH_4^+: 800 mg/L	
	18.08–24.95 mg/L	N	4.78%	DO: 1–1.5 mg O_2/L, T: 25 °C,	Zhang et al., 2018
	36.06 – 50.66 mg/L	N	12.08%	pH: 8.1–8.2, HRT: 5 h	
FNA	3.64 mg N/L	PN-A	Decrease from 15.7 ± 3.9 to 0.4 ± 0.1%	T: 22 ± 1 °C, pH: 7.5–5.7, SRT: 12 d,	Wang et al., 2016
				HRT: 13.2 h, NH_4-N: 15–28 mg/L	
HRT	30 – 15 h	N	"Dominant" NOB	DO: 4 mg O_2/L, T: 20 °C, pH: 7.5–8.0,	Li et al., 2013
				NH_4-N: 500 mg/L	
	15 – 5 h	N	"Nondominant" NOB	DO: 4 mg O_2/L, T: 20 °C, pH: 7.5–8.0,	
				NH_4-N: 90 mg/L	
	1.7 – 2.3 h	N	"Dominant" NOB	DO: 7 mg O_2/L, T: 28 °C,	Winkler et al., 2017
	1.5 h		Wash out from the reactor	NO_2-N: 230 mg/(L·d)	
Organic compounds	Increase from 0.97 to 3.20 kg COD/(m^3·d)	PN-A	Decrease from 0.4% to undetected level	T: 26.1–32.0 °C, HRT: 3–4.8 h,	Watari et al., 2016
				NLR: 0.57–1.5 mg N/(L·d)	
	Increase C/N ratio from 10:1 to 30:1	N	Decrease from 9 to 4%	DO: 3.0–4.0 mg O_2/L, T: 25 °C, HRT: 10 h, NH_4-N: 20 mg/L	Song et al., 2017
	C/N	N	Increase from 0.58 to 4.6%	HRT: 1–3 d	Gao et al., 2017
	C/N = 1	N	3%	T: 30.0 °C, HRT:20–44 h	Dong et al., 2017
	C/N = 2		Undetected level		
Salinity	25 mg Cl/L	N	10%	DO: 2 mg O_2/L, T: 30.0 °C, pH: 6.5–7.5,	Quartaroli et al., 2017
	125 mg Cl/L		Undetected level		
	0 mg Cl/L	PN-A	2.5%	DO: 0.3 mg O_2/L, pH: 8.0 ± 0.2,	Wang et al., 2017
	15 mg Cl/L		10.5%	HRT: 16 h, NH_4-N: 200 mg/L	
Tetracycline	10 mg/L	N	1.6%	DO: 2 mg O_2/L	Zheng et al., 2016a
	35 mg/		1.2%		
	20 μg/L	N	5–7%	SRT: 18 d, HRT: 16.5 h,	Liu et al., 2018
	2 mg/L		3.5–4.9%		
	50 μg/L	N	15–16%		
	5 mg/		10.5–11.2%		

(DO – dissolved oxygen, FA – free ammonia, FNA – free nitrous acid, HRT – hydraulic retention time, N – nitrification, NLR – nitrogen loading rate, PN-A – partial nitritation-anammox, PN – partial nitritation, A – Anammox, SRT – solids retention time, T – temperature)

during the periods of the highest process temperatures. Moreover, during pure culture studies on *Nitrospira*, the authors showed that these bacteria thrived between 30 and 35 °C. The impact of seasonality on the growth of *Nitrospira* was also observed by Jia et al. (2017). In a lab-scale wetland system, *Nitrospira* (the most dominant genus) was always higher in summer (12.0%) than in winter (4.1%). The average temperatures in these seasons were 25.6 and 9.2 °C, respectively. Blackburne et al. (2007) investigated short-term effects of temperature in the range 14–40 °C on the oxygen uptake rate (OUR) of *Nitrospira*. In the temperature range from 14 to 35 °C, the OUR increased from 11 to 32 mg O_2/(g VSS · h), while between 35 and 40 °C, the activity of *Nitrospira* decreased almost twice. Based on these results, Blackburne et al. (2007) determined the optimum temperature range for *Nitrospira* as 30–35 °C, whereas the inhibitory effect at 40 °C was either reversible or irreversible, depending on the exposure period. The negative effect of high temperatures (above 40 °C) was also found by Luo et al. (2017). The increase in the process temperature from 25 to 40 °C resulted in a decreasing ammonia utilization rate (AUR). A high FA concentration (about 2.7 mg NH_3-N/L) at T = 40 °C, combined with a low DO concentration (0.07 mg O_2/L), inhibited the growth of *Nitrospira* which resulted in the decrease of its abundance from 2.02 to 0.09%. Zekker et al. (2017) observed that after a reduction of the process temperature from 26 to 20 °C in a PN-A moving bed biological reactor (MBBR), a relative abundance of *Nitrospira* (dominant NOB) slightly decreased from 6.2 to 5.2%. The positive effect of high temperature on the *Nitrospira* was also observed in a deammonification system by Miao et al. (2016). The authors observed that in the high temperature (32 ± 1 °C) even a very low DO concentration was not able to suppress NOB (represented by *Nitrospira*) activity.

Courtens et al. (2016b), Edwards et al. (2013), and Lebedeva et al. (2008, 2011) showed that *Nitrospira* was the dominant NOB also in the thermophilic conditions (38–50 °C). Edwards et al. (2013) successfully enriched *Nitrospira calida* and *Nitrospira moscoviensis* with similar physiological properties, temperature optimum of 45–50 °C and an upper-temperature limit between 60 and 65 °C. Lebedeva et al. (2011) and Lebedeva et al. (2008) isolated *Nitrospira calida* and *Candidatus Nitrospira bockiana* with the growth temperature ranges of 46–58 °C and 28–44 °C, respectively.

Ambiguous results regarding the optimum temperature for *Nitrospira* growth were presented by Chen et al. (2018) and Alawi et al. (2009). Chen et al. (2018) observed that *Nitrospira* were more preferable at low-temperature conditions (10–20 °C). Alawi et al. (2009) compared the NOB communities grown at different temperatures (10, 17 and 28 °C). *Nitrospira defluvii* genus was detected in all samples, dominating at T = 17 °C. After the temperature decrease from 25 to 15 °C, the relative abundance of *Nitrospirae* increased from 4.6 to 7.2% (Akaboci et al., 2018). Persson et al. (2014) decreased the process temperature in a PN-A MBBR from 19 to 10 °C. Although *Nitrospira* was not the dominant NOB, the authors reported a significantly higher abundance at 16 °C than at 19, 13 or 10 °C. Moreover, during the 300 days of the reactor operation at a temperature of 13 °C, there was no significant change in the abundance of *Nitrospira*. *Nitrospira* was also the dominant NOB in the anoxic anammox reactor operated at low temperatures (15–17 °C), with the maximum relative abundance 16.34% in the biomass fraction of 200–400 μm (Liu et al., 2018).

The relationship between microbial growth and temperature in the entire physiological range can be described by the modified Ratkowsky equation (Ratkowsky et al., 1983):

$$\sqrt{r} = b(T - T_{MIN})\left(1 - e^{(c(T-T_{MAX}))}\right) \quad (1)$$

where T is the absolute temperature in K, r is the growth rate constant, T_{MIN} and T_{MAX} are the minimum and maximum temperatures, respectively, at which the growth rate is zero, and 'b' and 'c' are the fitting parameters. For *Nitrospira*, the effect of temperature on the normalized reaction rate could be accurately described by that equation (Fig. 3). The data in the temperature range 15–30 °C were developed based on the exponential equation of Blackburne et al. ($0.44e^{0.055(T-15)}$), while the actual experimental data were used for the temperatures > 30 °C.

7.3. pH

Nitrospira-like bacteria are sensitive to the high pH (> 9.0) because of growing the FA content and inhibiting their activity in both nitrification (Grunditz and Dalhammar, 2001; Blackburne et al., 2007) and anammox based systems (Rodrigues et al., 2017). According to Blackburne et al. (2007), the optimum pH for *Nitrospira* is in the range 8.0–8.3. A similar optimum pH (8.1 ± 0.1) was found by Zhang et al. (2018) in a nitrifying reactor. A lower range (7.6–8.0) was found for isolated pure cultures of *Nitrospira moscoviensis* sp. (Ehrich et al., 1995). Similar pH values (7.6–7.8) were kept by in five nitrifying intermittently aerated reactors (Mota et al., 2005). In all the reactors *Nitrospira* was the dominant NOB and accounted for > 73% of the total NOB population. Lower pH values (7.0–7.6) were selected in the studies of Park et al. (2017) and Blackburne et al. (2008), and *Nitrospira* was found to be the dominant NOB at pH 6.4 at T = 17 °C (Wegen et al., 2019).

7.4. Nitrogen concentration

The concentration of inorganic forms of nitrogen, such as ammonium, nitrite, nitrate as well as FA in the reactor, have a significant impact on the activated sludge composition. A positive influence of low ammonia loading rate (ALR) on the *Nitrospira* growth was found by Roots et al. (2018) and Camejo et al. (2017). The ALR were 0.0401 and 0.024 kg NH_4-N/(m^3·d), respectively. In both systems, nitrogen concentrations in the reactors were in the range of 0–12 mg N/L of NH_4 , NO_3, and NO_2 (Camejo et al., 2017), and 0–14 mg N/L of NH_4 and NO_3, 0–0.2 mg N/L of NO_2 (Roots et al., 2018). The combination of those nitrogen concentrations, a low DO concentration and sufficiently long SRT, allowed *Nitrospira* to reach 53% of the overall microbial population. The opposite approach was proposed by Tian et al. (2017) who conducted research in a highly loaded and aerated reactor. The *Nitrospira* abundance increased (from 1.5 to 2%) with the increase of the ALR from 0.095 to 0.238 kg NH_4-N/(m^3·d) in a short operational time (30 d), DO of 2–3 mg O_2/L, temperature of 25 ± 3°C, and influent NH_4-N of 22.4–34.2 mg N/L.

It well known that FA inhibits the activity of NOB (Ushiki et al., 2017). Recently, the influence of FA specifically on *Nitrospira* was investigated by Blackburne et al. (2007), Simm et al. (2006) and Ushiki et al. (2017). Simm et al. (2006) carried out two kinds of inhibitory tests, first with mixed microbial culture from a bench scale reactor and second with a pure culture of *Nitrospira moscoviensis*. The tests conducted with the mixed microbial population did not show classical FA inhibition of NOB at FA concentrations as high as 14.8 mg N/L. FA concentrations up to 10 mg N/L did not inhibit the activity of pure cultures of *Nitrospira moscoviensis* growth in batch cultures. Blackburne et al. (2007) estimated the inhibition thresholds of *Nitrospira* by FA at 0.04–0.08 mg N/L. For pure cultures, Ushiki et al. (2017) found that *Nitrospira* sp. Strain ND1 and *Nitrospira japonica* strain NJ1 were inhibited by FA 0.85 and 4.3 mg N/L, respectively. Zhang et al. (2018) concluded that the low levels of FA (18–25 mg N/L) had a limited effect on *Nitrospira,* while the higher levels of FA (36–50 mg N/L) had a evidently negative effect on *Nitrospira*. Wang and Gao (2018) suppressed the activity of *Nitrospira* (< 0.5%) in lab-scale anammox reactor by high FA of 49 mg N/L and limited DO (< 0.6 mg O_2/L). Liang et al. (2015b) observed successful suppression of *Nitrospira* in the CANON process with FA of 85.7 mg N/L.

Nitrospira is also sensitive to high nitrite levels. Wagner et al. (2002) observed suppression of the growth of *Nitrospira* at nitrite concentrations above 80 mg N/L. Kinnunen et al. (2017) analyzed the influence of nitrite on the NOB guild composition in a biofilm. They observed a

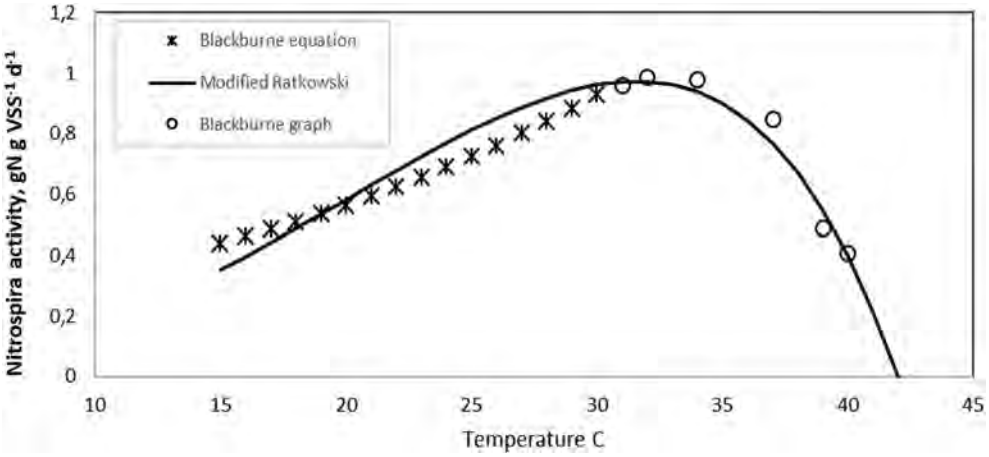

Fig. 3. Effect of temperature on the activity of *Nitrospira* described by the modified Ratkowsky equation (Eq. (1)) based on the data from the study of Blackburne et al. (2007) (R^2 = 0.93, c = 0.07457, b = 0.04252, T_{MIN} = 0, T_{MAX} = 42).

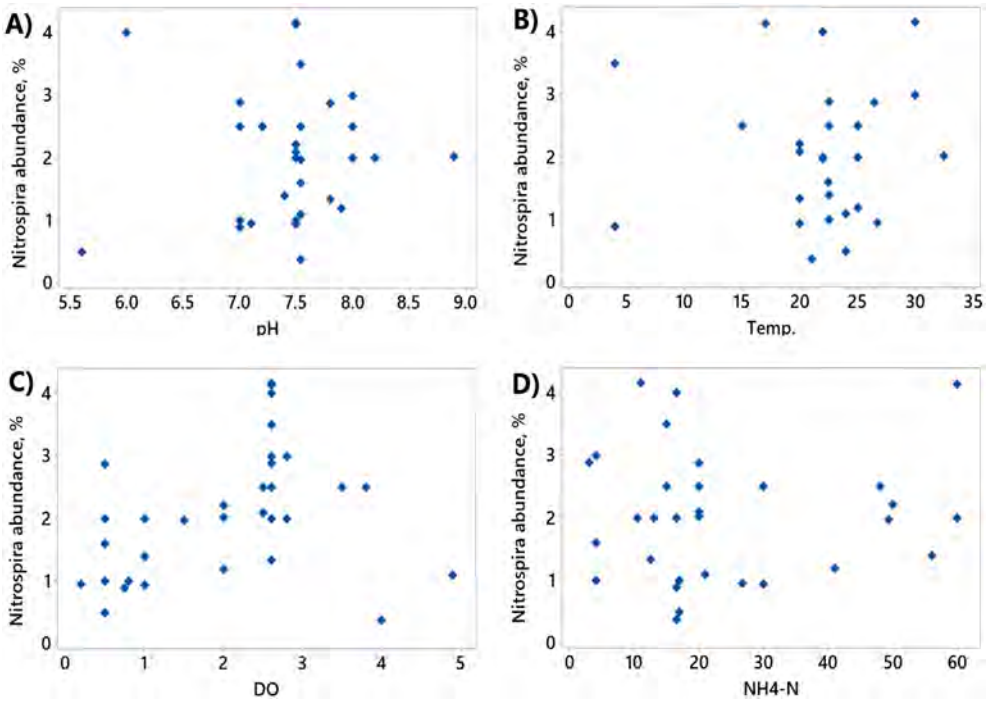

Fig. 4. Scatter plot of variables versus the *Nitrospira* abundance.

low abundance of *Nitrospira* in the source community and its dominance in the low nitrite loading biofilm (18.7%). In the high nitrite loading biofilm, the guild composition was dominated by *Nitrotoga* genus. With half-saturation constants (K_s) between 1.4 and 4.1 mg N/L *Nitrospira* bacteria are adapted to substrate limited conditions (Nowka et al., 2015). While *Nitrobacter* prevails in high-strength systems, *Nitrospira* predominates under mainstream conditions due to a higher affinity for nitrite (and DO) (Law et al., 2019). According to Park et al. (2017), *Nitrospira* could be enriched from the activated sludge through a long-term cultivation in a continuous-flow reactor operated under nitrite- and DO-limited conditions. The authors noted that the increased *Nitrospira* abundance resulted from the increased influent nitrite concentration. The enriched *Nitrospira* reflected 97% similarity of 16S rRNA sequence to *Candidatus Nitrospira defluvii*, which belongs to *Nitrospira* lineage I. Furthermore, *Nitrospira defluvii* (lineage I) displayed a higher resistance to nitrite inhibition than the members of lineage II, which may suggest that elevated nitrite concentrations influence the niche differentiation between the lineages of *Nitrospira* genus (Nowka et al., 2015).

7.5. Solids and hydraulic retention times

The SRT and HRT are important operating parameters influencing the diversity of the microbial community in biological reactors, especially in membrane reactors (Silva et al., 2016). As the literature data show, there is a very wide range of SRT (10–99 d), allowing for an increase of the *Nitrospira* abundance (Roots et al., 2018; Bao et al., 2016; Park et al., 2017; Courtens et al., 2016a; Fitzgerald et al., 2015; Regmi et al., 2014; Liu and Wang, 2013). Pongsak et al. (2017) found *Nitrospira* at four WWTP with SRT ≥ 6 days. On the other hand, Liu and Wang (2013) observed that *Nitrobacter* and *Nitrospira* were the superior competitors at short SRTs (5 d) and long SRT (10–40 d), respectively. The authors suggested that nitrite concentration was a more important factor than SRT for the competition between *Nitrobacter* and *Nitrospira*.

Based on the maximum growth rate of *Nitrospira defluvii*, Winkler et al. (2017) determined the minimum HRT between 0.6 and 0.67 d.

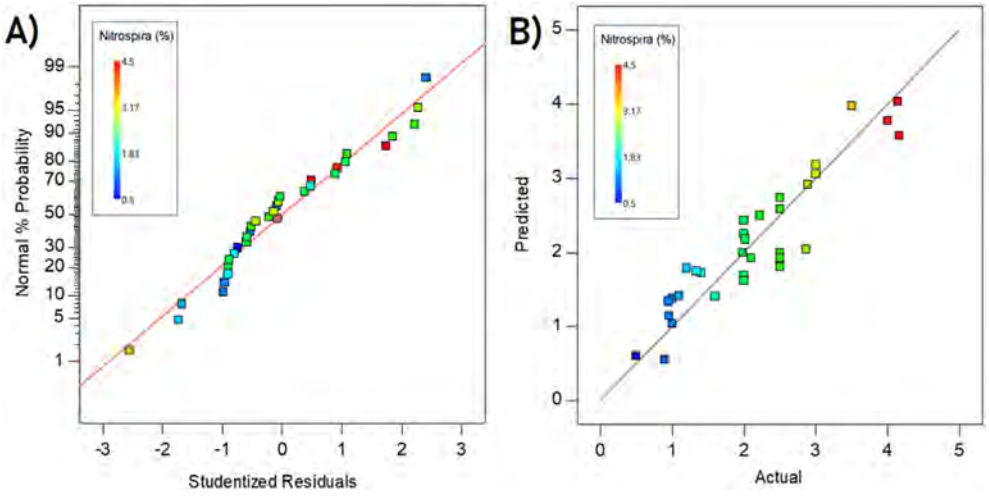

Fig. 5. A) Data normality, B) validation of the regression equation (predicted versus actual data).

Table 5
Validation of the regression equation results.

pH	Temp. (°C)	DO (mg/L)	NH_4-N (mg/L)	*Nitrospira* abundance (%)		References
				Predicted	Actual	
7.5*	22.2*	0.5	4.06	1.26	1.0	Gao et al., 2018
7.5*	25	2.07*	13	2.24	2.0	
7.2	22*	3.6	19	2.13	2.6	Courtens et al., 2016a
7	30	0.6	23	2.59	2.0	Yang et al., 2018
8.2	30	2	4.1	3.16	3.0	Dong et al., 2017

The authors observed that at high HRTs (> 3 days), *Nitrospira* outcompeted *Nitrobacter* instantaneously, while at the HRT higher than 0.64 day, *Nitrospira* was washed out of the reactor. According to Li et al. (2013), in the HRT from 15 to 30 h, *Nitrospira* was a dominant NOB in the conventional activated sludge system, and its abundance increased from 2.6% to 10.3%. Along with a decreasing HRT from 15 to 5 h, *Nitrobacter* began to dominate over *Nitrospira*.

7.6. Others factors

Roots et al. (2018), Park et al. (2017), Ouyang et al. (2017), Courtens et al. (2016a), Regmi et al. (2014) and Huang et al. (2010) observed a positive correlation between abundance of *Nitrospira* and long operational time. In their studies, the operational times were 407, 220, 200, 200, 560, 340 and 370 days, respectively. A similar observation, however, for much shorter operation time was made by Zhang et al. (2018). The authors observed that during 62 days of continuous-flow operation, HRT of 6.3 h, temperature of 25 °C and DO of about 0.15 mg/L, the *Nitrospira* abundances improved up to ratios of 2.1% and 12.1%.

Liu et al. (2018) and Zheng et al. (2016b) analyzed the impact of tetracycline (typical antibiotic, frequently detected in municipal wastewater) on the *Nitrospira* in the N-DN process. Liu et al. (2018) observed the positive impact of trace concentrations of tetracycline on the *Nitrospira* growth. The addition of 20 and 50 μg/L of tetracycline, caused in *Nitrospira* increase from 5–7% to 15–16% of the overall microbial community. Yim et al. (2006) found a positive effect of dosing trace-level tetracycline on the enrichment of *Nitrospira*. The authors related that effect to the fact that trace antibiotics could play a role of the surrogate auto-inducer and activate the transcription from quorum-sensing promoters. However, in both cases, a negative impact of higher concentration of tetracycline on the *Nitrospira* growth rate was observed. The *Nitrospira* abundance dropped from 1.6 to 1.2% with the growth of chlortetracycline concentration from 10 to 35 mg/L in a low DO (0.5 mg/L) lab-sale SBR (Zheng et al., 2016a).

Many former observations indicate that salt is an important factor influencing growth of *Nitrospira* in nitrifying and anammox based reactors (Quartaroli et al., 2017; Wang et al., 2017; Moussa et al., 2006; Dionisi et al., 2002; Daims et al., 2001; Gieseke et al., 2001). The salinity effect on *Nitrospira* can be twofold – in nitrifying reactors is negative, whereas in anammox reactors could be positive. Quartaroli et al. (2017) noticed a significant decrease, from 10 to 0%, of the *Nitrospira* abundance in a nitrifying reactor. The decrease was caused by a small addition of sodium chloride to the reactor (125 mg NaCl/L). The higher salt concentration (10 g NaCl/L) was obtained by Moussa et al. (2006) after one year of adaptation of nitrifiers to higher salinity. *Nitrospira* was a dominant NOB at the salt concentration lower than 10 g NaCl/L. Wang et al. (2017) showed that salinity influenced the microbial population dynamics of the functional bacteria in a CANON system. The authors observed an increasing trend of *Nitrospira* abundance from 2% to 10.5%, when the salinity was increased from 5 to 15 g NaCl/L. The overgrowth of *Nitrospira*, despite an extreme sensitivity of the nitrate oxidation rate (NOR) to elevated salinity, should be an operational concern at salt levels up to 20 g NaCl/L, especially in substrate-limited (low DO and nitrite) environments.

A negative effect of high light intensity on *Nitrospira* was shown in algal-bacterial reactors (Merbt et al., 2012; Zhang et al. 2019). Merbt et al. (2012) showed that the irradiance level of 500 μmol $m^{-2}s^{-1}$ caused the complete inhibition of *Nitrospira multiformis*. Zhang et al. (2019) studied three systems with different light intensities, including no light (0 μmol/(m^2 s)), low intensity (142 ± 10 μmol/(m^2 s)), and high intensity (316 ± 12 μmol/(m^2 s)). The highest relative abundance of *Nitrospira* , which reached 3.2% of the total microbial community, was found at the low light intensity. In contrast, the lowest abundance (0.85%) was observed at the high light intensity. The beneficial effect of the lack of light was also shown by Marks et al. (2012). The authors observed that *Nitrospira* was a dominant member of a geothermal ecosystem isolated from light.

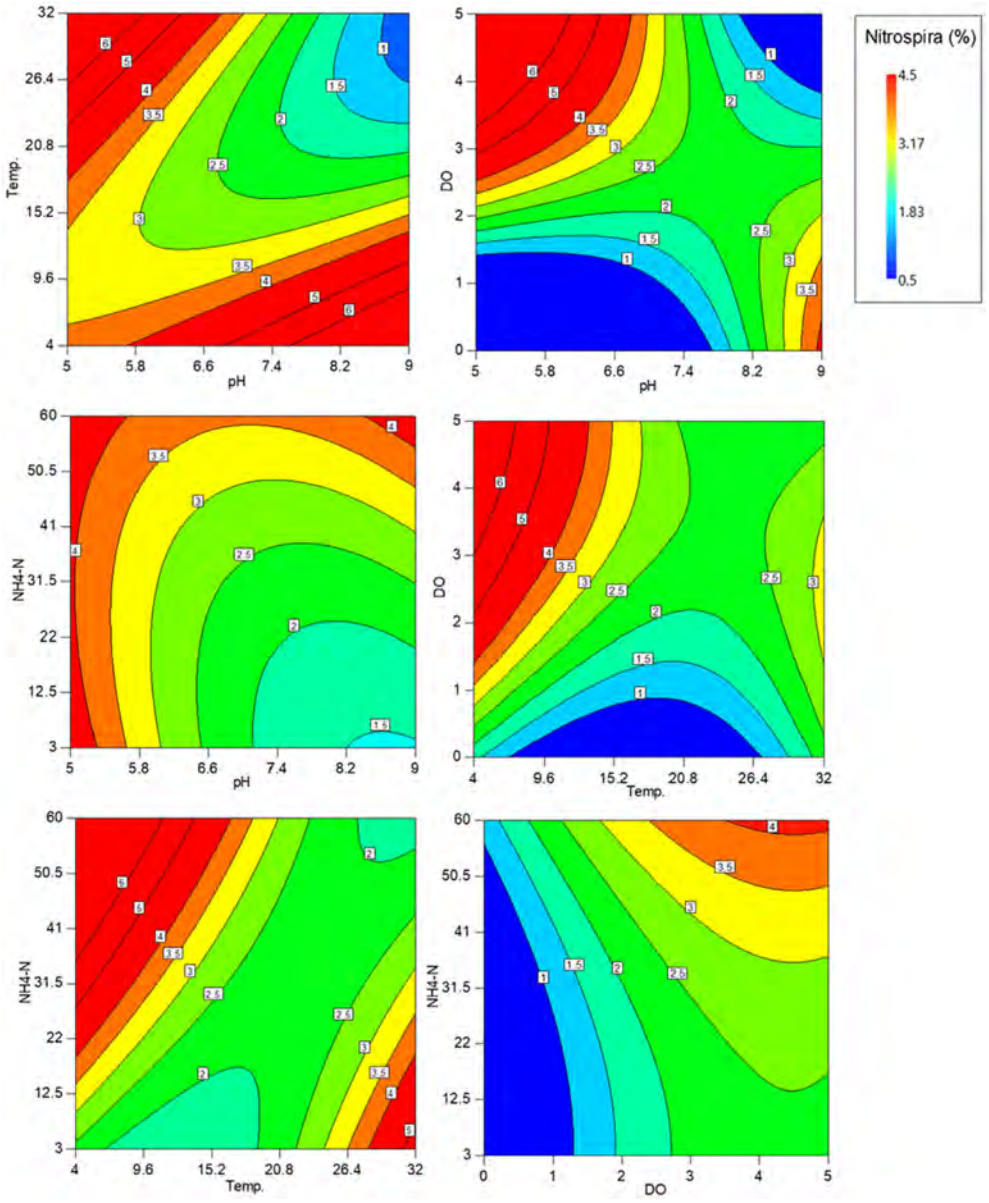

Fig. 6. Contour plot of the effect of the four factors on the response (*Nitrospira* abundance).

The factors that have a negative effect on the growth of *Nitrospira* also comprise high organic loads (Song et al., 2017), addition of sludge fermentation products (Yuan et al., 2016) and hydraulic loading rates (HLR) (Liang et al., 2017)). Along with an increase of COD concentration in the influent for membrane bioreactors (MBRs), from 200 to 600 mg COD/L, the *Nitrospira* abundance decreased from 9 to 4%. The C/N ratios were 10:1 and 30:1, respectively (Song et al., 2017). Yuan et al. (2016) observed that after addition of the sludge fermentation products, *Nitrospira* depicted a higher diversity (3.3%) in a SBR without sludge fermentation products than in a SBR with sludge fermentation products as (0.11%) operated at the same operational conditions. The negative effect of high HLR on *Nitrospira* has been reported in both activated sludge and constructed wetland systems. Liang et al. (2017) observed that the maximum number of *Nitrospira* genera sequences was significantly higher in a wetland with the HLR of 125 mm/d (92) in comparison with the HLR of 375 mm/d (34). The suppression of *Nitrospira* was obtained also by adding sodium azide (Pedrouso et al., 2017) or using ultrasound (Zheng et al., 2016a). In a lab-scale SBR with the PN-A process, by adding 5 mg/L of sodium azide, the *Nitrospira* abundance decreased sharply from 27.9 to 3.5%. Zheng et al. (2016a) obtained *Nitrospira* suppressing (from 3% to nearly zero) using ultrasonic treatment (frequency > 20 kHz).

8. Meta-analysis of the literature data

The Response Surface Methodology (RSM) is a method to investigate a relationship between one or more responses with multiple variables (factors). The RSM is useful where statistical data play a key role, and the effect of specific individual variables and their combined interaction on each response can be determined (Anwar et al., 2015). In this study, a standard RSM model, implemented in Minitab (19.1) and DX (10.1) software (Stat-Ease, USA), was applied to determine the effects and interactions of four process variables (factors) influencing the *Nitrospira* abundance (response) in nitrogen removal systems. Based on the results of previous studies, four process parameters were used as input independent variables, including DO concentration, influent NH_4-N concentration, pH, and temperature. The mean values of those variables were determined based on the reported range in literature.

Actual values are the response data and the model predictions are generated by using the approximation functions. Fig. 4 presents

scattered data on the matrix plot of distribution of the four factors vs. *Nitrospira* abundance. The majority of evaluated data varied in the range 7–8 for pH, 20–25 °C for temperature, 0.2–4.0 mg O_2/L for DO concentration, and 5–60 mg N/L for influent NH_4-N concentration. The independent variables were coded according to Eq. (2) for factor appraisals:

$$x_i = \frac{X_i - X_{cp}}{\Delta X_i} i = 1.2.\ 3 \cdots k \quad (2)$$

where, x_i is a dimensionless variable; Xi is the actual value of each independent variable; Xcp is the actual value of each independent variable at the focal point, and ΔX_i is the step change of the actual value of variable i.

A mathematical relationship between the predicted response, i.e. percentage of *Nitrospira* abundance (Y) and the four independent variables, i.e. pH (X1), temperature (X2), DO concentration (X3) and influent NH_4-N concentration (X4) can be described by the following empirical polynomial (second-order) model (Eq. (3)):

$$Y = \beta_0 + \sum_{i=1}^{n} \beta_i X_i + \sum_{i=1}^{n} \beta_{ii} X_i^2 + \sum \sum_{i<j} \beta_{ij} X_i X_j + \epsilon \quad (3)$$

where $\beta_0$is a constant coefficient, β_i are the linear coefficients, β_{ii} are the quadratic coefficients, β_{ij} are the interplay coefficients, X_i and X_j are each independent process variable (coded values), and ε is the residual error.

The data were normalized and fitted to the quadratic model. The overall prediction equation, resulted from the regression analysis, can be written in the following form:

$$\begin{aligned} &\text{Nitrospira abundance}\,(\%) \\ &= -20.\ 1 - 0.\ 52\ \text{pH} + 1.\ 216\ \text{Temp.} + 8.\ 88\ \text{DO} - 0.002 \\ &\quad \text{NH}_4 - \text{N} + 0.\ 450\ \text{pH}^2 + 0.01215\ \text{Temp}^2 - 0.\ 1620\ \text{DO}^2 + \\ &\quad 0.000544\ \text{NH}_4 - \text{N}^2 - 0.\ 200\ \text{pH} \times \text{Temp.} - 1.\ 027\ \text{pH} \times \text{DO} + \\ &\quad 0.0167\ \text{pH} \times \text{NH}_4 - \text{N} - 0.0159\ \text{Temp.} \times \text{DO} - 0.00690 \\ &\quad \text{Temp.} \times \text{NH}_4 - \text{N} + 0.00217\ \text{DO} \times \text{NH}_4 - \text{N} \end{aligned} \quad (4)$$

The residual versus normal probability plot (Fig. 5a) verified the assumption of the normality of residuals, whereas Fig. 5b illustrates the high accuracy of model predictions. A low value of the standard deviation ($\sigma = 0.5$) and a high value of the determination coefficient ($R^2 = 0.86$) confirm the acceptable goodness-of-fit. Specifically, the factors explain 86% of the variation in the response, while the standard deviation between the data points and the model predictions is approximately 0.5 unit. The ANOVA results with low p-values indicate suitable evidence against the null hypothesis. The level of importance (sensitive analysis) of each input factor and interaction between them were evaluated using the Pareto analysis. In addition, the regression equation was accurately validated with other data, which had not been used for the statistical analysis (Table 5).

The combined effect of each pair of the independent variables on the response (*Nitrospira* abundance) are shown in Fig. 6 (contour plots). From the figures, it can be seen that the highest *Nitrospira* abundances (red areas) can be expected under the following conditions (occurring simultaneously): high DO (> 3.0 mg O_2/L) and influent NH_4-N (> 20 mg N/L) as well as low temperature (< 15 °C) and pH (< 7). On the contrary, the simultaneous conditions for the lowest *Nitrospira* abundances cannot be specified unambiguously.

9. Conclusions

The latest genetic and experimental surveys revealed extraordinary versatility, adaptive capabilities and significant role of *Nitrospira* in catalyzing metabolic pathways during nitrification. Despite the canonical role in nitritation, the discovery of comammox, performed by selected *Nitrospira* representatives, reconsiders the current understanding of nitrification as a strict interaction between AOB and NOB. However, the actual role and significance of *Nitrospira* in nitrogen removal process still needs to be validated by application of the latest approaches, such as a combination of genomic and transcriptomic data. The meta-analysis of literature data identified specific individual variables and their combined interactions on the *Nitrospira* abundance.

Declaration of Competing Interest

The authors declare that they have no known competing financial interests or personal relationships that could have appeared to influence the work reported in this paper.

Acknowledgments

The study was supported by the Polish National Science Center under the project no. UMO-2017/27/B/NZ9/01039.

Appendix A. Supplementary data

Supplementary data to this article can be found online at https://doi.org/10.1016/j.biortech.2020.122936.

References

Akaboci, T.R., Gich, F., Ruscalleda, M., Balaguer, M.D., Colprim, J., 2018. Assessment of operational conditions towards mainstream partial nitritation-anammox stability at moderate to low temperature: reactor performance and bacterial community. Chem. Eng. J. 350, 192–200.
Alawi, M., Off, S., Kaya, M., Spieck, E., 2009. Temperature influences the population structure of nitrite-oxidizing bacteria in activated sludge. Environ. Microbiol. Rep. 3, 184–190.
Andrews, J.H., Harris, R.F., 1986. r- and K-Selection and Microbial Ecology. in: Advances in Microbial Ecology. Springer, US. Boston, MA.
Annavajhala, M.K., Kapoor, V., Santo-Domingo, J., Chandran, K., 2018. Comammox functionality identified in diverse engineered biological wastewater treatment systems. Environ. Sci. Technol. Lett. 5, 110–116.
Anwar, K., Mohamad Said, K.A., Afizal, M., Amin, M., 2015. Overview on the Response Surface Methodology (RSM) in extraction processes. Appl. Sci. Proc. Eng. 2, 8–17.
Bao, T., Chen, T., Tan, J., Wille, M.L., Zhu, D., Chen, D., Xi, Y., 2016. Synthesis and performance of iron oxide-based porous ceramsite in a biological aerated filter for the simultaneous removal of nitrogen and phosphorus from domestic wastewater. Sep. Purif. Technol. 167, 154–162.
Bartosch, S., Hartwig, C., Spieck, E., Bock, E., 2002. Immunological detection of nitrospira-like bacteria in various soils. Microb. Ecol. 43, 26–33.
Bhatia, A., Singh, N.K., Bhando, T., Pathania, R., Kazmi, A.A., 2017. Effect of intermittent aeration on microbial diversity in an intermittently aerated IFAS reactor treating municipal wastewater: a field study. J. Environ. Sci. Heal. A. 52, 440–448.
Blackburne, R., Vadivelu, V.M., Yuan, Z., Keller, J., 2007. Kinetic characterisation of an enriched Nitrospira culture with comparison to Nitrobacter. Water Res. 41, 3033–3042.
Blackburne, R., Yuan, Z., Keller, J., 2008. Partial nitrification to nitrite using low dissolved oxygen concentration as the main selection factor. Biodegradation 19, 303–312.
Camejo, P.Y., Santo Domingo, J., McMahon, K.D., Noguera, D.R., 2017. Genome-Enabled Insights into the Ecophysiology of the Comammox Bacterium "*Candidatus* Nitrospira nitrosa". mSystems 2, 1–16.
Cao, Y., Kwok, B.H., van Loosdrecht, M., Daigger, G., Png, H.Y., Long, W.Y., Eng, O.K., 2018. The influence of dissolved oxygen on partial nitritation/anammox performance and microbial community of the 200,000 m3/d activated sludge process at the Changi water reclamation plant (2011 to 2016). Water Sci. Technol. 78, 634–643.
Cao, Y., van Loosdrecht, M.C.M., Daigger, G.T., 2017. Mainstream partial nitritation–anammox in municipal wastewater treatment: status, bottlenecks, and further studies. Appl. Microbiol. Biot. 101, 1365–1383.
Chang, M., Wang, Y., Pan, Y., Zhang, K., Lyu, L., Wang, M., Zhu, T., 2019. Nitrogen removal from wastewater via simultaneous nitrification and denitrification using a biological folded non-aerated filter. Bioresour. Technol. 289, 121696.
Chao, Y., Mao, Y., Yu, K., Zhang, T., 2016. Novel nitrifiers and comammox in a full-scale hybrid biofilm and activated sludge reactor revealed by metagenomic approach. Appl. Microbiol. Biot. 100, 8225–8237.
Chen, M., Chen, Y., Dong, S., Lan, S., Zhou, H., Tan, Z., Li, X., 2018. Mixed nitrifying bacteria culture under different temperature dropping strategies: Nitrification performance, activity, and community. Chemosphere 195, 800–809.
Costa, E., Pérez, J., Kreft, J.-U., 2006. Why is metabolic labour divided in nitrification? Trends Microbiol. 14, 213–219.
Courtens, E.N.P., Spieck, E., Vilchez-Vargas, R., Bodé, S., Boeckx, P., Schouten, S., Jauregui, R., Pieper, D.H., Vlaeminck, S.E., Boon, N., 2016a. A robust nitrifying community in a bioreactor at 50 °C opens up the path for thermophilic nitrogen

removal. ISME J. 10, 2293.
Courtens, E.N.P., Vandekerckhove, T., Prat, D., Vilchez-Vargas, R., Vital, M., Pieper, D.H., Meerbergen, K., Lievens, B., Boon, N., Vlaeminck, S.E., 2016b. Empowering a mesophilic inoculum for thermophilic nitrification: Growth mode and temperature pattern as critical proliferation factors for archaeal ammonia oxidizers. Water Res. 92, 94–103.
Crovadore, J., Soljan, V., Calmin, G., Chablais, R., Cochard, B., Lefort, F., 2018. Metagenomes and metatranscriptomes of activated sludge from a sewage plant, with or without aerobic granule enrichment. Genome Announc. 5, e00372–17.
Daims, H., Lebedeva, E.V., Pjevac, P., Han, P., Herbold, C., Albertsen, M., Jehmlich, N., Palatinszky, M., Vierheilig, J., Bulaev, A., Kirkegaard, R.H., von Bergen, M., Rattei, T., Bendinger, B., Nielsen, P.H., Wagner, M., 2015. Complete nitrification by Nitrospira bacteria. Nature 528, 504–509.
Daims, H., Lücker, S., Wagner, M., 2016. A New perspective on microbes formerly known as nitrite-oxidizing bacteria. Trends Microbiol. 24, 699–712.
Daims, H., Nielsen, J.L., Nielsen, P.H., Schleifer, K.H., Wagner, M., 2001. In situ characterization of nitrospira-like nitrite-oxidizing bacteria active in wastewater treatment plants. Appl. Environ. Microbiol. 67, 5273–5284.
Daims, H., Wagner, M., 2011. Situ techniques and digital image analysis methods for quantifying spatial localization patterns of nitrifiers and other microorganisms in biofilm and flocs. In: In: Klotz, M.G., Stein, L.Y. (Eds.), Methods in Enzymology, vol. 496. Academic Press, pp. 185–215.
Daims, H., Wagner, M., 2018. Nitrospira. Trends Microbiol. 26, 462–463.
De Clippeleir, H., Vlaeminck, S.E., De Wilde, F., Daeninck, K., Mosquera, M., Boeckx, P., Boon, N., 2013. One-stage partial nitritation/anammox at 15 C on pretreated sewage: feasibility demonstration at lab-scale. Appl. Microbial. Biot. 97, 10199–10210.
De Clippeleir, H., Yan, X., Verstraete, W., Vlaeminck, S.E., 2011. OLAND is feasible to treat sewage-like nitrogen concentrations at low hydraulic residence times. Appl. Microbial. Biot. 90, 1537–1545.
Dionisi, H.M., Layton, A.C., Harms, G., Gregory, I.R., Robinson, K.G., Sayler, G.S., 2002. Quantification of Nitrosomonas oligotropha-like ammonia-oxidizing bacteria and Nitrospira spp. from full-scale wastewater treatment plants by competitive PCR. Appl. Environ. Microbiol. 6, 245–253.
Dong, H., Wang, W., Song, Z., Dong, H., Wang, J., Sun, S., Zhang, Z., Ke, M., Zhang, Z., Wu, W.M., Zhang, G., Ma, J., 2017. A high-efficiency denitrification bioreactor for the treatment of acrylonitrile wastewater using waterborne polyurethane immobilized activated sludge. Bioresour. Technol. 239, 472–481.
Du, S., Yu, D., Zhao, J., Wang, X., Bi, C., Zhen, J., Yuan, M., 2019. Achieving deep-level nutrient removal via combined denitrifying phosphorus removal and simultaneous partial nitrification-endogenous denitrification process in a single-sludge sequencing batch reactor. Bioresour. Technol. 289, 121690.
Dworkin, M., Gutnick, D., 2012. Sergei Winogradsky: a founder of modern microbiology and the first microbial ecologist. FEMS Microbiol. Rev. 36, 364–379.
Edwards, T.A., Calica, N.A., Huang, D.A., Manoharan, N., Hou, W., Huang, L., Panosyan, H., Dong, H., Hedlund, B.P., 2013. Cultivation and characterization of thermophilic Nitrospira species from geothermal springs in the US Great Basin, China, and Armenia. FEMS Microbiol. Ecol. 85, 283–292.
Ehrich, S., Behrens, D., Lebedeva, E., Ludwig, W., Bock, E., 1995. A new obligately hemolithoautotrophic, nitrite-oxidizing bacterium, Nitrospira moscoviensis sp. nov. and its phylogenetic relationship. Arch. Microbiol. 164, 16–23.
Feng, Y., Lu, X., Al-Hazmi, H., Makinia, J., 2017. An overview of the strategies for the deammonification process start-up and recovery after accidental operational failures. Rev. Environ. Sci. Biotechnol. 16, 541–568.
Fitzgerald, C.M., Camejo, P., Oshlag, J.Z., Noguera, D.R., 2015. Ammonia-oxidizing microbial communities in reactors with efficient nitrification at low-dissolved oxygen. Water Res. 70, 38–51.
Gao, F., Li, Z., Chang, Q., Gao, M., She, Z., Wu, J., Jin, C., Zheng, D., Guo, L., Zhao, Y., Wang, S., 2018. Effect of florfenicol on performance and microbial community of a sequencing batch biofilm reactor treating mariculture wastewater. Environ. Technol. 39, 363–372.
Gao, L., Zhou, W., Huang, J., He, S., Yan, Y., Zhu, W., Wu, S., Zhang, X., 2017. Nitrogen removal by the enhanced floating treatment wetlands from the secondary effluent. Bioresour. Technol. 234, 243–252.
Gieseke, A., Purkhold, U., Wagner, M., Amann, R., Schramm, A., 2001. Community structure and activity dynamics of nitrifying bacteria in a phosphate-removing biofilm. Appl. Environ. Microbiol. 67, 1351–1362.
Gilbert, E.M., Agrawal, S., Schwartz, T., Horn, H., Lackner, S., 2015. Comparing different reactor configurations for partial nitritation/anammox at low temperatures. Water Res. 81, 92–100.
Gilbride, K., 2014. Molecular Methods for the Detection of Waterborne Pathogens in Waterborne Pathogens, Detection Methods and Applications. Elsevier B.V, London, UK.
Gómez-Silván, C., Vílchez-Vargas, R., Arévalo, J., Gómez, M.A., González-López, J., Pieper, D.H., Rodelas, B., 2014. Quantitative response of nitrifying and denitrifying communities to environmental variables in a full-scale membrane bioreactor. Bioresour. Technol. 169, 126–133.
Gruber-Dorninger, C., Pester, M., Kitzinger, K., Savio, D.F., Loy, A., Rattei, T., Wagner, M., Daims, H., 2014. Functionally relevant diversity of closely related Nitrospira in activated sludge. ISME J. 9, 643–655.
Grunditz, C., Dalhammar, G., 2001. Development of nitrification inhibition assays using pure cultures of nitrosomonas and nitrobacter. Water Res. 35, 433–440.
Harms, G., Layton, A.C., Dionisi, H.M., Gregory, I.R., Garrett, V.M., Hawkins, S.A., Robinson, K.G., Sayler, G.S., 2003. Real-time PCR quantification of nitrifying bacteria in a municipal wastewater treatment plant. Environ. Sci. Technol. 37, 343–351.
He, S., Ding, L., Li, K., Hu, H., Ye, L., Ren, H., 2018. Comparative study of activated sludge with different individual nitrogen sources at a low temperature: effluent dissolved organic nitrogen compositions, metagenomic and microbial community. Bioresour. Technol. 247, 915–923.
How, S.W., Lim, S.Y., Lim, P.B., Aris, A.M., Ngoh, G.C., Curtis, T.P., Chua, A.S.M., 2018. Low-dissolved-oxygen nitrification in tropical sewage: an investigation on potential, performance and functional microbial community. Water Sci. Technol. 77, 2274–2283.
Hu, H.W., He, J.Z., 2017. Comammox—a newly discovered nitrification process in the terrestrial nitrogen cycle. J. Soils. Sediments 17, 2709–2717.
Huang, H., Fan, X., Peng, C., Geng, J., Ding, L., Zhang, X., Ren, H., 2019. Linking microbial respiratory activity with phospholipid fatty acid of biofilm from full-scale bioreactors. Bioresour. Technol. 272, 599–605.
Huang, Z., Gedalanga, P.B., Asvapathanagul, P., Olson, B.H., 2010. Influence of physicochemical and operational parameters on Nitrobacter and Nitrospira communities in an aerobic activated sludge bioreactor. Water Res. 44, 4351–4358.
Isanta, E., Reino, C., Carrera, J., Pérez, J., 2015. Stable partial nitritation for low-strength wastewater at low temperature in an aerobic granular reactor. Water Res. 80, 149–158.
Jia, F., Lai, C., Chen, L., Zeng, G., Huang, D., Liu, F., Li, X., Luo, P., Wu, J., Qin, L., Zhang, C., Cheng, M., Xu, P., 2017. Spatiotemporal and species variations in prokaryotic communities associated with sediments from surface-flow constructed wetlands for treating swine wastewater. Chemosphere 185, 1–10.
Joss, A., Salzgeber, D., Eugster, J., König, R., Rottermann, K., Burger, S., Siegrist, H., 2009. Full-scale nitrogen removal from digester liquid with partial nitritation and anammox in one SBR. Environ. Sci. Technol. 43, 5301–5306.
Katsogiannis, A.N., Kornaros, M., Lyberatos, G., 2003. Enhanced nitrogen removal in SBRs bypassing nitrate generation accomplished by multiple aerobic/anoxic phase pairs. Water Sci. Technol. 47, 53–59.
Kim, D.J., Kim, S.H., 2006. Effect of nitrite concentration on the distribution and competition of nitrite-oxidizing bacteria in nitratation reactor systems and their kinetic characteristics. Water Res. 40, 887–894.
Kindaichi, T., Tsushima, I., Ogasawara, Y., Shimokawa, M., Ozaki, N., Satoh, H., Okabe, S., 2007. In situ activity and spatial organization of anaerobic ammonium-oxidizing (anammox) bacteria in biofilms. Appl. Environ. Microbiol. 73, 4931–4939.
Kinnunen, M., Gülay, A., Albrechtsen, H.J., Dechesne, A., Smets, B.F., 2017. Nitrotoga is selected over Nitrospira in newly assembled biofilm communities from a tap water source community at increased nitrite loading. Environ. Microbiol. 19, 2785–2793.
Koch, H., van Kessel, M.A.H.J., Lücker, S., 2019. Complete nitrification: insights into the ecophysiology of comammox Nitrospira. Appl. Microbiol. Biotechnol. 103, 177–189.
Kouba, V., Vejmelkova, D., Proksova, E., Wiesinger, H., Concha, M., Dolejs, P., Hejnic, J., Jenicek, P., Bartacek, J., 2017. High-rate partial nitritation of municipal wastewater after psychrophilic anaerobic pretreatment. Environ. Sci. Technol. 51, 11029–11038.
Kowalchuk, G.A., Stephen, J.R., 2001. Ammonia-oxidizing bacteria: a model for molecular microbial ecology. Annu. Rev. Microbiol. 55, 485–529.
Law, Y., Matysik, A., Chen, X., Swa Thi, S., Ngoc Nguyen, T.Q., Qiu, G., Natarajan, G., Williams, R.B.H., Ni, B.J., Seviour, T.W., Wuertz, S., 2019. High dissolved oxygen selection against nitrospira sublineage I in full-scale activated sludge. Environ. Sci. Technol. 53, 8157–8166.
Lawson, C.E., Lücker, S., 2018. Complete ammonia oxidation: an important control on nitrification in engineered ecosystems? Curr. Opin. Biotechnol. 50, 158–165.
Lebedeva, E.V., Alawi, M., Maixner, F., Jozsa, P.-G., Daims, H., Spieck, E., 2008. Physiological and phylogenetic characterization of a novel lithoautotrophic nitrite-oxidizing bacterium, 'Candidatus Nitrospira bockiana'. Int. J. Syst. Evol. Microbiol. 58, 242–250.
Lebedeva, E.V., Off, S., Zumbrägel, S., Kruse, M., Shagzhina, A., Lücker, S., Maixner, F., Lipski, A., Daims, H., Spieck, E., 2011. Isolation and characterization of a moderately thermophilic nitrite-oxidizing bacterium from a geothermal spring. FEMS Microbiol. Ecol. 75, 195–204.
Lenaerts, J., Lappin-Scott, H.M., Porter, J., 2007. Improved fluorescent in-situ hybridization method for detection of bacteria from activated sludge and river water by using DNA molecular beacons and flow cytometry. Appl. Environ. Microbiol. 73, 2020–2023.
Li, H., Zhang, Y., Yang, M., Kamagata, Y., 2013. Effects of hydraulic retention time on nitrification activities and population dynamics of a conventional activated sludge system. Front. Environ. Sci. Eng. 7, 43–48.
Li, J., Elliott, D., Nielsen, M., Healy, M.G., Zhan, X., 2011. Long-term partial nitrification in an intermittently aerated sequencing batch reactor (SBR) treating ammonium-rich wastewater under controlled oxygen-limited conditions. Biochem. Eng. J. 55, 215–222.
Liang, K., Dai, Y., Wang, F., Liang, W., 2017. Seasonal variation of microbial community for the treatment of tail water in constructed wetland. Water Sci. Technol. 75, 2434–2442.
Liang, Y., Li, D., Zhang, X., Zeng, H., Yang, Z., Cui, S., Zhang, J., 2014. Nitrogen removal and microbial characteristics in CANON biofilters fed with different ammonia levels. Bioresour. Technol. 171, 168–174.
Liang, Y., Li, D., Zhang, X., Zeng, H., Yang, Z., Cui, S., Zhang, J., 2015. Stability and nitrite-oxidizing bacteria community structure in different high-rate CANON reactors. Bioresour. Technol. 175, 189–194.
Lipski, A., Spieck, E., Makolla, A., Altendorf, K., 2001. Fatty acid profiles of nitrite-oxidizing bacteria reflect theirphylogenetic heterogeneity. Syst. Appl. Microbiol. 24, 377–384.
Liu, G., Wang, J., 2013. Long-term low DO enriches and shifts nitrifier community in activated sludge. Environ. Sci. Technol. 47, 5109–5117.
Liu, H., Yang, Y., Sun, H., Zhao, L., Liu, Y., 2018. Effect of tetracycline on microbial community structure associated with enhanced biological NandP removal in sequencing batch reactor. Bioresour. Technol. 256, 414–420.
Liu, J., Yi, N.K., Wang, S., Lu, L.J., Huang, X.F., 2016. Impact of plant species on spatial

distribution of metabolic potential and functional diversity of microbial communities in a constructed wetland treating aquaculture wastewater. Ecol. Eng. 94, 564–573.
Liu, W., Yang, D., Chen, W., Gu, X., 2017. High-throughput sequencing-based microbial characterization of size fractionated biomass in an anoxic anammox reactor for low-strength wastewater at low temperatures. Bioresour. Technol. 231, 45–52.
Lopez-Vazquez, C.M., Kubare, M., Saroj, D.P., Chikamba, C., Schwarz, J., Daims, H., Brdjanovic, D., 2014. Thermophilic biological nitrogen removal in industrial wastewater treatment. Appl. Microbiol. Biotechnol. 98, 945–956.
Luo, H., Song, Y., Zhou, Y., Yang, L., Zhao, Y., 2017. Effects of rapid temperature rising on nitrogen removal and microbial community variation of anoxic/aerobic process for ABS resin wastewater treatment. Environ. Sci. Pollut. Res. 24, 5509–5520.
Ma, B., Wang, S., Li, Z., Gao, M., Li, S., Guo, L., She, Z., Zhao, Y., Zheng, D., Jin, C., Wang, X., Gao, F., 2017. Magnetic Fe3O4 nanoparticles induced effects on performance and microbial community of activated sludge from a sequencing batch reactor under long-term exposure. Bioresour. Technol. 225, 377–385.
Ma, F., Li, P., Zhang, X.Q., Sun, J.W., Wang, H.Y., Zhang, J., 2011. The influencing factors and the characteristics of simultaneous nitrification-denitrification in SBR. J. Harbin Inst. Tech. 43, 55–60.
Ma, T., Zhao, C., Peng, Y., Liu, X., Zhou, L., 2009. Applying real-time control for realization and stabilization of shortcut nitrification-denitrification in domestic water treatment. Water Sci. Technol. 59, 787–796.
Malovanyy, A., Yang, J., Trela, J., Plaza, E., 2015. Combination of upflow anaerobic sludge blanket (UASB) reactor and partial nitritation/anammox moving bed biofilm reactor (MBBR) for municipal wastewater treatment. Bioresour. Technol. 180, 144–153.
Manser, R., Gujer, W., Siegrist, H., 2005. Consequences of mass transfer effects on the kinetics of nitrifiers. Water Res. 39, 4633–4642.
Mardanov, A.V., Beletskii, A.V., Kallistova, A.Y., Kotlyarov, R.Y., Nikolaev, Y.A., Kevbrina, M.V., Agarev, A.M., Ravin, N.V., Pimenov, N.V., 2016. Dynamics of the composition of a microbial consortium during start-up of a single-stage constant flow laboratory nitritation/anammox setup. Microbiology 85, 681–692.
Marks, C.R., Stevenson, B.S., Rudd, S., Lawson, P.A., 2012. Nitrospira-dominated biofilm within a thermal artesian spring: a case for nitrification-driven primary production in a geothermal setting. Geobiology 10, 457–466.
Merbt, S.N., Stahl, D.A., Casamayor, E.O., Martí, E., Nicol, G.W., Prosser, J.I., 2012. Differential photoinhibition of bacterial and archaeal ammonia oxidation. FEMS. Microbiol. Lett. 327, 41–46.
Miao, Y., Peng, Y., Zhang, L., Li, B., Li, X., Wu, L., Wang, S., 2018. Partial nitrification-anammox (PNA) treating sewage with intermittent aeration mode: effect of influent C/N ratios. Chem. Eng. J. 334, 664–672.
Miao, Y., Zhang, L., Yang, Y., Peng, Y., Li, B., Wang, S., Zhang, Q., 2016. Start-up of single-stage partial nitrification-anammox process treating low-strength swage and its restoration from nitrate accumulation. Bioresour. Technol. 218, 771–779.
Mota, C., Head, M.A., Ridenoure, J.A., Cheng, J.J., de los Reyes, F.L., 2005. Effects of aeration cycles on nitrifying bacterial populations and nitrogen removal in intermittently aerated reactors. Appl. Environ. Microbiol. 71, 8565.
Moussa, M.S., Sumanasekera, D.U., Ibrahim, S.H., Lubberding, H.J., Hooijmans, C.M., Gijzen, H.J., van Loosdrecht, M.C.M., 2006. Long term effects of salt on activity, population structure and floc characteristics in enriched bacterial cultures of nitrifiers. Water Res. 40, 1377–1388.
Nemati, M., Hamidi, A., Maleki, Dizaj S., Javaherzadeh, V., Lotfipour, F., 2016. An overview on novel microbial determination methods in pharmaceutical and food quality control. Adv. Pharm. Bull. 6, 301–308.
Nielsen, P.H., McMahon, K.D., 2014. Microbiology and microbial ecology of the activated sludge process. In: Jenkins, D., Wanner, J. (Eds.), Activated Sludge – 100 Years and Counting. IWA Publishing, London, pp. 53–75.
Nogueira, R., Melo, L.F., 2006. Competition between Nitrospira spp. and Nitrobacter spp. in nitrite-oxidizing bioreactors. Biotechnol. Bioeng. 95, 169–175.
Nowka, B., Daims, H., Spieck, E., 2015. Comparison of oxidation kinetics of nitrite-oxidizing bacteria: nitrite availability as a key factor in niche differentiation. Appl. Environ. Microbiol. 81, 745–753.
Okabe, S., Satoh, H., Watanabe, Y., 1999. In situ analysis of nitrifying biofilms as determined by in situ hybridization and the use of microelectrodes. Appl. Environ. Microbiol. 65, 3182–3191.
Ouyang, E., Lu, Y., Ouyang, J., Wang, L., Wang, X., 2017. Bacterial community analysis of anoxic/aeration (A/O) system in a combined process for gibberellin wastewater treatment. PloS One 12, e0186743.
Palomo, A., Pedersen, A.G., Fowler, S.J., Dechesne, A., Sicheritz-Pontén, T., Smets, B.F., 2018. Comparative genomics sheds light on niche differentiation and the evolutionary history of comammox Nitrospira. ISME J. 12, 1779–1793.
Park, N.D., 2008. Nitrospira community composition in nitrifying reactors operated with two different dissolved oxygen levels. J. Microbiol. Biotechnol. 18, 1470–1474.
Park, M.-R., Park, H., Chandran, K., 2017. Molecular and kinetic characterization of planktonic Nitrospira spp. selectively enriched from activated sludge. Environ. Sci. Technol. 51, 2720–2728.
Pedrouso, A., Val del Río, Á., Morales, N., Vázquez-Padín, J.R., Campos, J.L., Méndez, R., Mosquera-Corral, A., 2017. Nitrite oxidizing bacteria suppression based on in-situ free nitrous acid production at mainstream conditions. Sep. Purif. Technol. 186, 55–62.
Peng, Y., Zhu, G., 2006. Biological nitrogen removal with nitrification and denitrification via nitrite pathway. Appl. Microbial. Biotechnol. 73, 15–26.
Persson, F., Sultana, R., Suarez, M., Hermansson, M., Plaza, E., Wilén, B.M., 2014. Structure and composition of biofilm communities in a moving bed biofilm reactor for nitritation–anammox at low temperatures. Bioresour. Technol. 154, 267–273.
Pester, M., Maixner, F., Berry, D., Rattei, T., Koch, H., Lücker, S., Nowka, B., Richter, A., Spieck, E., Lebedeva, E., Loy, A., Wagner, M., Daims, H., 2014. NxrB encoding the beta subunit of nitrite oxidoreductase as functional and phylogenetic marker for nitrite-oxidizing Nitrospira. Environ. Microbiol. 16, 3055–3071.
Pinto, A.J., Marcus, D.N., IjazBautista, U.Z., de lose Santos, Q.M., Dick, G.J., Raskin, L., 2016. Metagenomic evidence for the presence of comammox Nitrospira-like bacteria in a drinking water system. Msphere 1 e00054-15.
Pjevac, P., Schauberger, C., Poghosyan, L., Herbold, C.W., van Kessel, M.A.H.J., Daebeler, A., Steinberger, M., Jetten, M.S.M., Lücker, S., Wagner, M., Daims, H., 2017. AmoA-targeted polymerase chain reaction primers for the specific detection and quantification of comammox nitrospira in the environment. Front. Microbiol. 8, 1508.
Pongsak, N., Supaporn, P., Tamao, K., Junko, M.M., Linda, A.F., 2017. Comparison of nitrogen removal and full-scale wastewater treatment plant characteristics in Thailand and Japan. Environ. Asia 10, 92–98.
Poot, V., Hoekstra, M., Geleijnse, M.A., van Loosdrecht, M.C., Pérez, J., 2016. Effects of the residual ammonium concentration on NOB repression during partial nitritation with granular sludge. Water Res. 106, 518–530.
Qian, F., Wang, J., Shen, Y., Wang, Y., Wang, S., Chen, X., 2017. Achieving high performance completely autotrophic nitrogen removal in a continuous granular sludge reactor. Biochem. Eng. J. 118, 97–104.
Quartaroli, L., Silva, L.C.F., Silva, C.M., Lima, H.S., de Paula, S.O., de Oliveira, V.M., de Cássia, S., da Silva, M., Kasuya, M.C.M., de Sousa, M.P., Torres, A.P.R., Souza, R.S., Bassin, J.P., da Silva, C.C., 2017. Ammonium removal from high-salinity oilfield-produced water: assessing the microbial community dynamics at increasing salt concentrations. Appl. Microbiol. Biotechnol. 101, 859–870.
Ramdhani, N., Kumari, S., Bux, F., 2013. Distribution of nitrosomonas-related ammonia-oxidizing bacteria and nitrobacter-related nitrite-oxidizing bacteria in two full-scale biological nutrient removal plants. Water Environ. Res. 85, 374–381.
Ratkowsky, D.A., Lowry, R.K., McMeekin, T.A., Stokes, A.N., Chandler, R., 1983. Model for bacterial culture growth rate throughout the entire biokinetic temperature range. J. Bacteriol. 154, 1222–1226.
Regmi, P., Miller, M.W., Holgate, B., Bunce, R., Park, H., Chandran, K., Wett, B., Murthy, S., Bott, C.B., 2014. Control of aeration, aerobic SRT and COD input for mainstream nitritation/denitritation. Water Res. 57, 162–171.
Rodrigues, V.A.J., Mac Conell, E.F.A., Dias, D.F.C., von Sperling, M., de Araújo, J.C., Vasel, J.L., 2017. Nitrogen removal in a shallow maturation pond with sludge accumulated during 10 years of operation in Brazil. Water Sci. Technol. 76, 268–278.
Roots, P., Wang, Y., Rosenthal, A., Griffin, J., Sabba, F., Petrovich, M., Yang, F., Kozak, J., Zhang, H., Wells, G., 2018. Comammox Nitrospira are the dominant ammonia oxidizers in a mainstream low dissolved oxygen nitrification reactor. Water Res. 157, 396–405.
Salmonová, H., Bunešová, V., 2017. Methods of studying diversity of bacterial comunities: a review. Sci. Agric. Bohem. 48, 154–165.
Santoro, A.E., 2016. The do-it-all nitrifier. Science 351, 342–343.
Schramm, A., de Beer, D., van den Heuvel, J.C., Ottengraf, S., Amann, R., 1999. Microscale distribution of populations and activities of Nitrosospira and Nitrospira spp. along a macroscale gradient in a nitrifying bioreactor: quantification by in situ hybridization and the use of microsensors. Appl. Environ. Microbial. 65, 3690–3696.
Silva, A.F., Antunes, S., Saunders, A., Freitas, F., Vieira, A., Galinha, C.F., Nielsen, P.H., Barreto Crespo, M.T., Carvalho, G., 2016. Impact of sludge retention time on the fine composition of the microbial community and extracellular polymeric substances in a membrane bioreactor. Appl. Microbiol. Biotechnol 100, 8507–8521.
Simm, R.A., Mavinic, D.S., Ramey, W.D., 2006. A targeted study on possible free ammonia inhibition of Nitrospira. J. Environ. Eng. Sci. 5, 365–376.
Soliman, M., Eldyasti, A., 2016. Development of partial nitrification as a first step of nitrite shunt process in a Sequential Batch Reactor (SBR) using Ammonium Oxidizing Bacteria (AOB) controlled by mixing regime. Bioresour. Technol. 221, 85–95.
Song, H.L., Yang, X.L., Xia, M.Q., Chen, M., 2017. Co-metabolic degradation of steroid estrogens by heterotrophic bacteria and nitrifying bacteria in MBRs. J. Environ. Sci. Health A 52, 778–784.
Sun, Z., Liu, C., Cao, Z., Chen, W., 2018. Study on regeneration effect and mechanism of high-frequency ultrasound on biological activated carbon. Ultrason. Sonochem. 44, 86–96.
Tsukuda, M., Kitahara, K., Miyazaki, K., 2017. Comparative RNA function analysis reveals high functional similarity between distantly related bacterial 16 S rRNAs. Sci. Rep. 7, 9993.
Tian, Q., Zhuang, L., Ong, S.K., Wang, Q., Wang, K., Xie, X., Zhu, Y., Li, F., 2017. Phosphorus (P) recovery coupled with increasing influent ammonium facilitated intracellular carbon source storage and simultaneous aerobic phosphorus and nitrogen removal. Water Res. 119, 267–275.
Ushiki, N., Jinno, M., Fujitani, H., Suenaga, T., Terada, A., Tsuneda, S., 2017. Nitrite oxidation kinetics of two Nitrospira strains: the quest for competition and ecological niche differentiation. J. Biosci. Bioeng. 123, 581–589.
van Kessel, M.A.H.J., Speth, D.R., Albertsen, M., Nielsen, P.H., Op den Camp, H.J.M., Kartal, B., Jetten, M.S.M., Lücker, S., 2015. Complete nitrification by a single microorganism. Nature 528, 555.
Varas, R., Guzmán-Fierro, V., Giustinianovich, E., Behar, J., Fernández, K., Roeckel, M., 2015. Startup and oxygen concentration effects in a continuous granular mixed flow autotrophic nitrogen removal reactor. Bioresour. Technol. 190, 345–351.
Wagner, M., Loy, A., Nogueira, R., Purkhold, U., Lee, N., Daims, H., 2002. Microbial community composition and function in wastewater treatment plants. Antonie van Leeuwenhoek 81, 665–680.
Wang, D., Wang, Q., Laloo, A., Xu, Y., Bond, P.L., Yuan, Z., 2016. Achieving stable nitritation for mainstream deammonification by combining free nitrous acid-based sludge treatment and oxygen limitation. Sci. Rep. 6, 25547.
Wang, H., Einola, J., Heinonen, M., Kulomaa, M., Rintala, J., 2008. Group-specific quantification of methanotrophs in landfill gas-purged laboratory biofilters by tyramide signal amplification-fluorescence in situ hybridization. Bioresour. Technol. 99,

6426–6433.
Wang, L., Li, T., 2015. Effects of seasonal temperature variation on nitrification, anammox process, and bacteria involved in a pilot-scale constructed wetland. Environ. Sci. Pollut. Res. Int. 22, 3774–3783.
Wang, M., Huang, G., Zhao, Z., Dang, C., Liu, W., Zheng, M., 2018. Newly designed primer pair revealed dominant and diverse comammox amoA gene in full-scale wastewater treatment plants. Bioresour. Technol. 270, 580–587.
Wang, X., Gao, D., 2016. In-situ restoration of one-stage partial nitritation-anammox process deteriorated by nitrate build-up via elevated substrate levels. Sci. Rep. 6, 37500.
Wang, X., Gao, D., 2018. The transformation from anammox granules to deammonification granules in micro-aerobic system by facilitating indigenous ammonia oxidizing bacteria. Bioresour. Technol. 250, 439–448.
Wang, Y., Chen, J., Zhou, S., Wang, X., Chen, Y., Lin, X., Yan, Y., Ma, X., Wu, M., Han, H., 2017. 16S rRNA gene high-throughput sequencing reveals shift in nitrogen conversion related microorganisms in a CANON system in response to salt stress. Chem. Eng. J. 317, 512–521.
Watari, T., Cuong Mai, T., Tanikawa, D., Hirakata, Y., Hatamoto, M., Syutsubo, K., Fukuda, M., Nguyen, N.B., Yamaguchi, T., 2016. Development of downflow hanging sponge (DHS) reactor as post treatment of existing combined anaerobic tank treating natural rubber processing wastewater. Water Sci. Technol. 75, 57–68.
Watson, S.W., Bock, E., Valois, F.W., Waterbury, J.B., Schlosser, U., 1986. Nitrospira marina gen. nov. sp. nov.: a chemolithotrophic nitrite-oxidizing bacterium. Arch. Microbiol. 144, 1–7.
Wegen, S., Nowka, B., Spieck, E., 2019. Low Temperature and neutral pH define "*Candidatus* Nitrotoga sp". as a competitive nitrite oxidizer in coculture with Nitrospira defluvii. Appl. Environ. Microbiol. 85, e02569–18.
Winkler, M.K., Bassin, J.P., Kleerebezem, R., Sorokin, D.Y., van Loosdrecht, M.C., 2012. Unravelling the reasons for disproportion in the ratio of AOB and NOB in aerobic granular sludge. Appl. Microbiol. Biotechnol. 94, 1657–1666.
Winkler, M.K.H., Boets, P., Hahne, B., Goethals, P., Volcke, E.I.P., 2017. Effect of the dilution rate on microbial competition: r-strategist can win over k-strategist at low substrate concentration. Plos One 12, e0172785.
Yang, B., Wang, J., Wang, J., Xu, H., Song, X., Wang, Y., Li, F., Liu, Y., Bai, J., 2018. Correlating microbial community structure with operational conditions in biological aerated filter reactor for efficient nitrogen removal of municipal wastewater. Bioresour. Technol. 250, 374–381.
Yao, Q., Peng, D.C., 2017. Nitrite oxidizing bacteria (NOB) dominating in nitrifying community in full-scale biological nutrient removal wastewater treatment plants. AMB Express 7, 25.
Yim, G., Huimi Wang, H., Davies, J., 2006. The truth about antibiotics. Int. J. Med. Microbiol. 296, 163–170.
Yu, C., Hou, L., Zheng, Y., Liu, M., Yin, G., Gao, J., Liu, C., Chang, Y., Han, P., 2018. Evidence for complete nitrification in enrichment culture of tidal sediments and diversity analysis of clade a comammox Nitrospira in natural environments. Appl. Microbiol. Biotechnol. 102, 9363–9377.
Yuan, Y., Liu, J., Ma, B., Liu, Y., Wang, B., Peng, Y., 2016. Improving municipal wastewater nitrogen and phosphorous removal by feeding sludge fermentation products to sequencing batch reactor (SBR). Bioresour. Technol. 222, 326–334.
Zekker, I., Rikmann, E., Kroon, K., Mandel, A., Mihkelson, J., Tenno, T., Tenno, T., 2017. Ameliorating nitrite inhibition in a low-temperature nitritation– anammox MBBR using bacterial intermediate nitric oxide. Int. J. Environ. Sci. Technol. 14, 2343–2356.
Zhang, Q., De Clippeleir, H., Su, C., Al-Omari, A., Wett, B., Vlaeminck, S.E., Murthy, S., 2016. Deammonification for digester supernatant pretreated with thermal hydrolysis: overcoming inhibition through process optimization. Appl. Microbial. Biotechnol. 100, 5595–5606.
Zhang, X., Zhou, Y., Ma, Y., Zhang, N., Zhao, S., Zhang, R., Zhang, J., Zhang, H., 2018. Effect of inorganic carbon concentration on the stability and nitrite-oxidizing bacteria community structure of the CANON process in a membrane bioreactor. Environ. Technol. 39, 457–463.
Zhang, B., Guo, Y., Lens, P.N.L., Zhang, Z., Shi, W., Cui, F., Tay, J.H., 2019. Effect of light intensity on the characteristics of algal-bacterial granular sludge and the role of N-acyl-homoserine lactone in the granulation. Sci. Total Environ. 659, 372–383.
Zheng, D., Chang, Q., Gao, M., She, Z., Jin, C., Guo, L., Zhao, Y., Wang, S., Wang, X., 2016a. Performance evaluation and microbial community of a sequencing batch biofilm reactor (SBBR) treating mariculture wastewater at different chlortetracycline concentrations. J. Environ. Manage. 182, 496–504.
Zheng, M., Liu, Y.C., Xin, J., Zuo, H., Wang, C.W., Wu, W.M., 2016b. Ultrasonic treatment enhanced ammonia-oxidizing bacterial (AOB) activity for nitritation process. Environ. Sci. Technol. 50, 864–871.
Zhou, X., Liu, X., Huang, S., Cui, B., Liu, Z., Yang, Q., 2018. Total inorganic nitrogen removal during the partial/complete nitrification for treating domestic wastewater: removal pathways and main influencing factors. Bioresour. Technol. 256, 285–294.
Zubrowska-Sudol, M., Yang, J., Trela, J., Plaza, E., 2011. Evaluation of deammonification process performance at different aeration strategies. Water Sci. Technol. 63, 1168–1176.

Paper II

M-J Mehrani, X Lu, P Kowal, D Sobotka, J Mąkinia. 2021. Incorporation of the complete ammonia oxidation (comammox) process for modeling nitrification in suspended growth wastewater treatment systems. **Journal of Environmental Management,** 297, 113223.

https://doi.org/10.1016/j.jenvman.2021.113223

Journal of Environmental Management 297 (2021) 113223

Contents lists available at ScienceDirect

Journal of Environmental Management

journal homepage: www.elsevier.com/locate/jenvman

Incorporation of the complete ammonia oxidation (comammox) process for modeling nitrification in suspended growth wastewater treatment systems

Mohamad-Javad Mehrani, Xi Lu, Przemyslaw Kowal, Dominika Sobotka, Jacek Mąkinia *

Faculty of Civil and Environmental Engineering, Gdansk University of Technology, Ul. Narutowicza 11/12, 80-233, Gdansk, Poland

ARTICLE INFO

Keywords:
Activated sludge
Kinetic model development
Nitrification
Nitrogen removal
Wastewater treatment systems

ABSTRACT

The newly discovered process complete ammonia oxidation (comammox) has changed the traditional understanding of nitrification. In this study, three possible concepts of comammox were developed and incorporated as part of an extended two-step nitrification model. For model calibration and validation, two series of long-term biomass washout experiments were carried out at 12 °C and 20 °C in a laboratory sequencing batch reactor. The inoculum biomass was withdrawn from a large biological nutrient removal wastewater treatment plant. The efficiency of the examined models was compared based on the behaviors of ammonia, nitrite, and nitrate in the studied reactor. Predictions of the conventional approach to comammox, assuming the direct oxidation of ammonia to nitrate, were slightly better than the two other approaches. Simulation results revealed that comammox could be responsible for the conversion of >20% of the influent ammonia load. Therefore, the role of commamox in the nitrogen mass balance in activated sludge systems should not be neglected and requires further investigation. Furthermore, sensitivity and correlation analysis revealed that the maximum growth rates (μ), oxygen half-saturation (K_O), and decay rates (b) of the canonical nitrifiers and comammox were the most sensitive factors, and the highest correlation was found between μ and b among all considered kinetic parameters. The estimated μ values by the best model were 0.57, 0.11, and 0.15 d^{-1} for AOB, NOB, and comammox bacteria, respectively.

1. Introduction

Nitrification is a vital process for effective nitrogen (N) removal in wastewater treatment plants (WWTPs). Traditionally, that process has been assumed to consist of two consecutive steps, including ammonia oxidation to nitrite by ammonia oxidizing bacteria (AOB), followed by nitrite oxidation to nitrate by nitrite oxidizing bacteria (NOB) (Jaramillo et al., 2018; Noriega-Hevia et al., 2020). However, the recently discovered complete ammonia oxidation (comammox) process has changed the dogma of the strict two-step nitrification (Daims et al., 2015; van Kessel et al., 2015).

Comammox is a process of converting ammonia directly to nitrate by a single microorganism belonging to *Nitrospira*, further referred to as comammox *Nitrospira*. In comparison with canonical NOB, comammox *Nitrospira* possesses genes related to both ammonia oxidation and nitrite oxidation (Lawson and Lücker, 2018). This unique metabolic pathway makes comammox bacteria different from other canonical nitrifiers (Palomo et al., 2018; Annavajhala et al., 2018).

There has been some evidence that comammox bacteria are not able to compete with other nitrifiers (AOB, NOB) in wastewater treatment systems (Annavajhala et al., 2018; Gonzalez-Martinez et al., 2016). In contrast, comammox *Nitrospira* were found to be dominant in comparison with either AOB (Roots et al., 2019) or NOB (Sun et al., 2018; Zhou et al., 2018) in nitrifying activated sludge systems. The potentially favorable conditions for the growth of comammox *Nitrospira* comprise either low dissolved oxygen (DO) and ammonia concentrations (Palomo et al., 2018; Roots et al., 2019) or a nitrite-limited environment (Park et al., 2017) with long solids retention times (SRTs) (Qian et al., 2017). The competition for ammonia (NH_4–N) between canonical AOB and comammox microorganisms could play a vital role in achieving partial nitrification (nitritation), which is required in shortcut N removal processes, such as “nitrite shunt” or deammonification (Izadi et al., 2021).

Simulation models are an important management tool in the operation of WWTPs and help in understanding the complex microbial interactions in biological wastewater treatment systems (Metcalf and Eddy, 2014). Nitrification is an inherent part of activated sludge models (ASMs). For simplicity, the full nitrification pathway, i.e., oxidation of ammonia to nitrate, has traditionally been modeled as a single-step

* Corresponding author. Gdansk University of Technology, Ul. Narutowicza 11/12, 80-233, Gdansk, Poland.
E-mail address: jmakinia@pg.edu.pl (J. Mąkinia).

https://doi.org/10.1016/j.jenvman.2021.113223
Received 6 March 2021; Received in revised form 1 July 2021; Accepted 2 July 2021
Available online 15 July 2021

process assuming that the first step (ammonia oxidation to nitrite) is typically the rate-limiting conversion in the entire oxidation pathway. This approach has been adopted in all the most common complex activated sludge models (ASMs), including the IWA ASM series (Henze, 2000). Two-step nitrification models have been known and continuously developed for almost 60 years as summarized by (Makinia and Zaborowska, 2020). However, those models became particularly important when nitrite received growing attention as the central component in the shortcut N removal processes.

Cao et al. (2017) noted that the nitrification models should appropriately accommodate the competition between AOB and NOB to understand factors influencing the competition between autotrophic N-converting organisms. Multistep nitrification models also incorporate AOB-mediated pathways of N_2O production pathways via hydroxylamine production or/and autotrophic denitrification (Domingo-Félez and Smets, 2016). An ASM3 model was applied for optimization and simulation of chemical oxygen demand (COD) and ammonia removal from coking wastewater treatment plants (WWTPs) by (Wu et al., 2016), and very recently, Karlikanovaite-Balikci and Yagci (2019) determined the characteristics of a sludge reduction process by calibration of kinetic parameters using modified ASM1. Additionally (Yu et al., 2020), expanded the traditional two-step nitrification model and incorporated different species of AOB (*Nitrosomonas* vs. *Nitrosospira*) and NOB (*Nitrobacter* vs. *Nitrospira*) based on the r/K theory assumptions.

Despite the fast-growing number of experimental studies on comammox, the process has not yet been considered for expansion of nitrification models. The present study aimed to (1) evaluate the capabilities and limits of three novel model concepts for the comammox process, (2) predict the coexistence of comammox and canonical AOB and NOB under highly dynamic conditions during biomass washout experiments, and (3) evaluate the role of comammox in ammonia conversion to nitrate. The models were calibrated and validated with experimental data from a laboratory-scale sequencing batch reactor (SBR) with inoculum biomass from a full-scale WWTP. Sensitivity analysis and correlation matrix analysis were performed to identify kinetic parameters that were most influential for predictions of the expanded models. It was hypothesized that the newly developed mechanistic models could reveal the potential role of comammox in nitrifying systems and enhance the current understanding of N conversions in those systems.

2. Materials and methods

2.1. Conceptual and mathematical model description

Even though it is well established that comammox is a two-step process and comammox Nitrospira possesses key enzymes for both NH_4–N and NO_2–N oxidation. However, there is no consensus in the literature if NO_2–N is released outside of the cells during the process. Daims et al. (2016) hypothesized and Wu et al. (2019) experimentally demonstrated that NO_2–N could be an intracellular transit product of comammox. On the other hand, transient NO_2–N accumulation produced by comammox Nitrospira during NH_4–N oxidation has also been reported (Kits et al., 2017; Ren et al., 2020). Furthermore, Koch et al. (2019) noted that in contrast to canonical NOB, currently cultivable comammox Nitrospira species cannot grow under NO_2–N only conditions. Other authors did not exclude that comammox bacteria could use NO_2–N as electron donors when NH_4–N is temporarily unavailable (Kits et al., 2017; Palomo et al., 2018; Roots et al., 2019). In a very recent study, Sun et al. (2018) have noted that the comammox species reveal variable nitrite affinities.

The current study attempted to differentiate between the potential mechanisms of the comammox process in converting NH_4–N to NO_3–N. Three different nitrification model concepts, including comammox, are presented in Fig. 1. A mathematical notation of those models, including their stoichiometric matrices and vectors of kinetic expressions, is presented in Table S1 in the Supplementary Information (SI).

In Model I, the complete NH_4–N oxidation is assumed to be a one-step process (NH_4–N→NO_3–N) without release of extracellular NO_2–N, and comammox bacteria are not able to utilize extracellular NO_2–N as electron donors. In Model II and Model III, comammox bacteria are assumed to be able to utilize extracellular NO_2–N as the electron donors. The difference between those two models is that NH_4–N and NO_2–N oxidation is modeled as either a sequential two-step process (NH_4–N→NO_2–N→NO_3–N) in Model II or a hybrid process in Model III, e.g., NH_4–N→NO_3–N (similar to Model I) and NO_2–N→NO_3–N (similar to Model II). However, the latter process is activated by a switching function, when the availability of NH_4–N becomes limited.

2.2. Stoichiometric and kinetic parameters

An overview of recent literature data on stoichiometric and kinetic parameters for canonical AOB, canonical NOB, and comammox bacteria is presented in Table S2 in the SI. In terms of r/K selection theory, canonical nitrifiers can be categorized into the fast-growing (r-strategists) and the slow-growing (K-strategists) bacteria. These differences result from the operational conditions, sludge floc morphology, and cultivation environment (Yu et al., 2020). Comammox *Nitrospira* may have a higher growth yield compared to other canonical AOB and NOB in addition to the key characteristics of canonical AOB, including a high ammonia affinity and a low maximum specific growth rate (Kits et al., 2017). Moreover, Koch et al. (2019) reported that two distinct clades (A and B) were found within comammox *Nitrospira*, showing similar ammonium affinities to either AOB or canonical *Nitrospira*.

2.3. Modeling and simulation platform

The GPS-X (Hydromantis, Canada) (www.hydromantis.com) is an

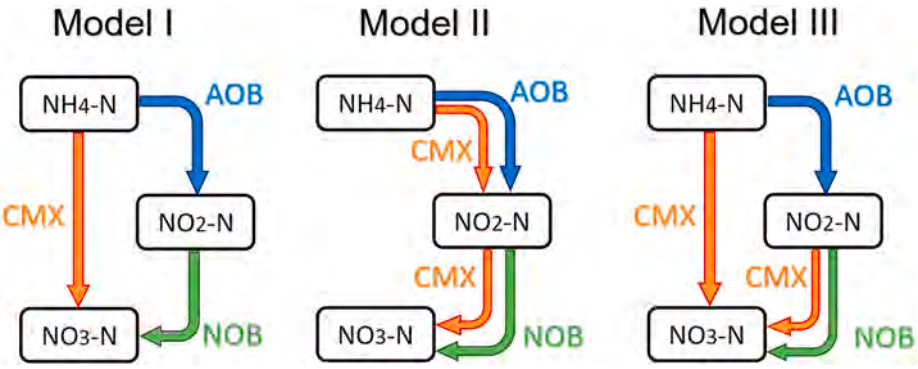

Fig. 1. Three conceptual models of comammox as an extension of the two-step nitrification pathways (microorganisms responsible for the specific processes are AOB (nitritation), NOB (nitratation), and CMX (comammox).

open modeling and simulation platform for various wastewater treatment processes. Some of the useful features were used in the present study, including the following:

- ***Model Developer (MD)***, which allows for the writing of new models and modification of existing models (stoichiometric matrix and vector of kinetic rate expressions).
- ***Sensitivity Analyzer***, which performs steady-state, phase dynamic, or time dynamic simulations for selected intervals of any independent variable.
- ***Parameter Optimizer***, which uses the Nelder-Mead simplex method with one of five different objective functions to search for the parameter values with the minimum variance between measured data and model predictions.

2.4. Experimental data for model calibration and validation

2.4.1. Biomass washout experiments in a sequencing batch reactor

Washout experiments aim at washing out specific groups of microorganisms (most often NOB) from a system by applying specific operational conditions. In this study, long-term biomass cultivations were conducted at decreasing SRTs. The inoculum biomass for two experiments was withdrawn in the winter and summer seasons from the "Czajka" WWTP in Warsaw. These experiments were carried out in an SBR with a working volume of 10 L. In both cases, the reactor was operated for 30 days at 12 °C (experiment 1) and 20 °C (experiment 2). Air was supplied in a continuous aeration mode, the DO set point was 0.6 ± 0.1 mg O_2/L, and the pH was kept at 7.5 for both experiments.

A single operational cycle lasted 480 min and consisted of three phases: feeding (15 min), reaction (450 min), and decanting (15 min). The SRT gradually decreased from 4 d to approximately 1 d. The reduced SRT and low DO concentration were combined factors to evaluate the suppression of NOB in the SBR. The initial mixed liquor suspended solids (MLSS) concentration and its volatile fraction (MLVSS) were approximately 2000 mg/L and 1300 mg/L at 12 °C, and 2500 mg/L, 1500 mg/L for 20 °C, respectively. The SBR was fed ammonium-rich synthetic medium with tracer elements. The volumetric nitrogen loading rates (NLRs) were generally kept at approximately 0.02 ± 0.01 g N/(L·d) and 0.05 ± 0.01 g N/(L·d) during the 12 °C and 20 °C experiments, respectively.

2.4.2. Short-term batch experiments

Before the long-term washout experiments in the SBR, two series of short-term batch experiments were carried out with mixed liquor from the Czajka WWTP. These experiments aimed to estimate kinetic parameters (half-saturation constants – $K_{O,AOB}$, $K_{O,NOB}$, $K_{NO2,NOB}$) for the two-step nitrification model. The kinetic parameters were estimated after linearization of the Monod equation as described in detail in the SI. The tests were carried out at seven DO concentrations (0.2, 0.5, 0.7, 1.0, 1.5, 2.0, 2.5 mg O_2/L) under winter (12 °C) and summer (20 °C) conditions. The substrate was a synthetic medium containing either ammonium (NH_4Cl) or nitrite ($NaNO_2$) with supplemental sodium bicarbonate ($NaHCO_3$) as an inorganic carbon source. In both cases, the initial concentration of the substrate was approximately 20 mg N/L. The pH was kept at 7.5 by dosing NaOH (2 M solution).

2.5. Initial biomass concentration and composition

The initial shares of AOB, NOB and coammox bacteria for modeling were determined in two steps. First, since the exact operating data were not available at the studied plant, the overall nitrifier concentration was assumed based on the previous results of stead-state and dynamic simulations of two similar large WWTPs in Poland (Makinia et al., 2006). The predicted concentrations ranged from 38 to 62 mg COD/L which was on average approximately 2% of the particulate COD in the studied WWTPs. In the second step, the relative distributions of AOB, canonical NOB, and comammox bacteria were estimated from microbial analysis using a combined approach of 16 S rRNA gene high-throughput sequencing technique and quantitative PCR (qPCR), which were described in detail elsewhere (Kowal et al., 2021). For simulations, the average initial ratios of AOB:NOB:comammox bacteria were set at 3:9:1 for both experiments. This assumption was made based on the observation of similar trends of NH_4–N, NO_2–N and NO_3–N during both washout experiments. It should be emphasized that the total nitrifier abundance and AOB:NOB proportions were within the ranges reported by (Griffin and Wells, 2017) for six full-scale bioreactors.

2.6. Model implementation, calibration, validation, and comparison

The three mathematical models, described in section 2.1, were implemented in GPS-X using the MD utility and the ASM1 (Henze et al., 2000) as the core model. The nitrification process was expanded from one stage into two separate stages (AOB and NOB) and the comammox kinetics and stoichiometry were defined. Sensitivity analysis was performed to select the most sensitive parameters related to the nitrification process. Pairs of the highly correlated parameters were identified based on the correlation matrix results.

Calibration and validation are critical steps in the modeling process that address the model prediction capability and its reliability of use under different conditions. Therefore, in the present study, each examined model was calibrated with the same measurement data (NH_4–N, NO_2–N, NO_3–N) from the experiment carried out at 12 °C. The influential and noncorrelated parameters were estimated using the GPS-X "optimizer" utility. The estimation process was conducted until the maximum sizes for all of the parameter dimensions decreased below the parameter tolerance (Lu et al., 2018). Moreover, the 95% confidence limits for each parameter estimate were calculated from the variance-covariance matrix.

Subsequently, the models were validated with another set of experimental data from the experiment carried out at 20 °C. In addition, the comammox influence on the model predictions was evaluated by setting the values of μ_{CMX} and b_{CMX} to 0. The entire modeling/simulation procedure is presented in Fig. 2 and the most important steps are described in the following sections.

Although the operational conditions were unfavorable for denitrification (there was no organic carbon in the feed and reactor aeration), that process was still considered in modeling but without further adjustments of the model default parameters.

2.6.1. Local sensitivity analysis

Local sensitivity analysis (LSA) is a method in which one or more uncertain variables are selected to determine their influence on some results or quantities of importance in mathematical models (Hong et al., 2019; Razavi et al., 2021). In the present study, a local one-variable-at-a-time sensitivity analysis was carried out for 13 kinetic parameters targeting the N components, such as NH_4–N, NO_2–N, and NO_3–N concentrations. The initial values for the examined kinetic parameters are presented in Table 1. Simulations were run under dynamic conditions using a GPS-X "phase dynamic" sensitivity analyzer. Similar to (Lu et al., 2018), an uncertainty of 20% (±10% of the adjusted value) was allocated to each considered parameter. The normalized sensitivity coefficient ($S_{i,j}$) was defined as the ratio of the percentage change ($\Delta y_{i,j}/y_i$) in the *i-th* output variable (y_i) to the percentage change ($\Delta x_j/x_j$) in the *j-th* model parameter (x_j):

$$S_{i,j} = \left| \frac{\Delta y_{i,j}}{y_i} \cdot \frac{x_j}{\Delta x_j} \right| \quad (1)$$

The influence of each adjusted parameter on the specific model output was defined using the following classification (Lu et al., 2018): 1) insignificantly influential ($S_{i,j} < 0.25$), 2) influential ($0.25 \leq S_{i,j} < 1$), 3) very influential ($1 \leq S_{i,j} < 2$), and 4) extremely influential ($S_{i,j} \geq 2$).

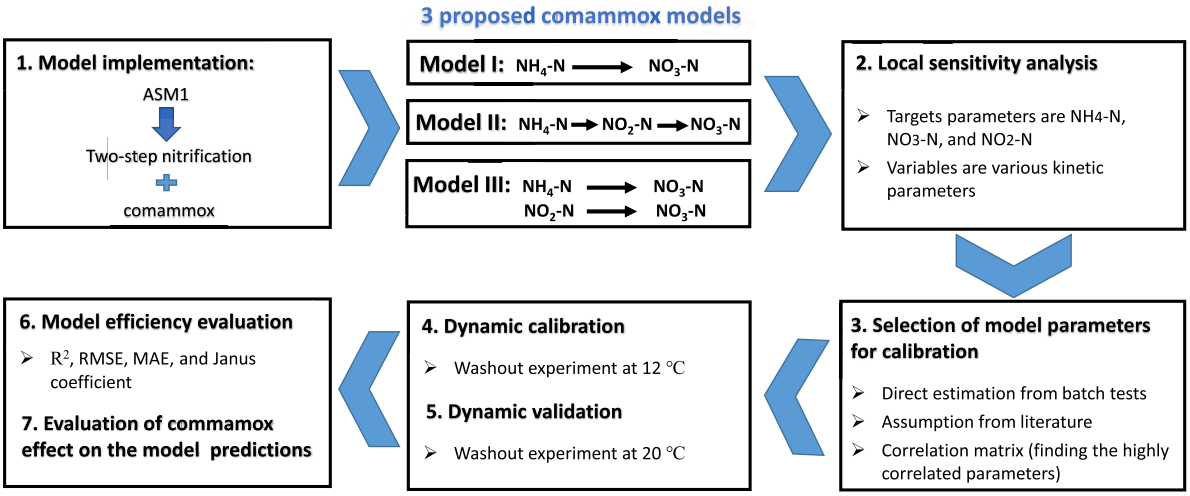

Fig. 2. The procedure of the implementation, calibration, validation, and comparison of the expanded nitrification models including comammox.

Table 1
Initial values of the kinetic parameters selected for sensitivity analysis of the models.

Bacteria	Kinetic parameter	Unit	Initial values	Reference
AOB	μ_{AOB}	d^{-1}	1.01	Yu et al. (2020)
	$K_{NH4,AOB}$	mg N/L	0.675	Yu et al. (2020)
	$K_{O,AOB}$	mg O_2/L	0.30	Batch test
	b_{AOB}	d^{-1}	0.15	Yu et al. (2020)
NOB	μ_{NOB}	d^{-1}	0.31	Yu et al. (2020)
	$K_{NO2,NOB}$	mg N/L	0.057	Batch test
	$K_{O,NOB}$	mg O_2/L	0.2	Batch test
	b_{NOB}	d^{-1}	0.05	Yu et al. (2020)
CMX	μ_{CMX}	d^{-1}	0.69	Park et al. (2017)
	$K_{NH4,CMX}$	mg N/L	0.01	Koch et al. (2019)
	$K_{NO2,CMX}$	mg N/L	6.29	Koch et al. (2019)
	$K_{O,CMX}$	mg O_2/L	0.33	Park et al. (2017)
	b_{CMX}[a]	d^{-1}	0.05	Yu et al. (2020)

[a] no reference available yet (the assumed value is the same as that for NOB).

2.6.2. Selection of the kinetic parameters for optimization in GPS-X

Two groups of kinetic parameters were excluded from the selection for optimization in GPS-X:

- Least influential parameters determined based on the LSA results.
- Three important kinetic parameters, including the oxygen half-saturation constants for AOB and NOB ($K_{O,AOB}$, $K_{O,NOB}$), and nitrite half-saturation constants for NOB ($K_{NO2,NOB}$) were determined directly based on the preliminary batch experiments (section 2.4.2). A detailed description of the calculations can be found in the SI.

Subsequently, the correlation matrix was developed to evaluate the linear relationship, its strength, and direction (positive vs. negative) for pairs of influential model parameters. If the obtained correlation coefficient is strong enough for any parameter pair, then the calibration process can be simplified by fixing one of the parameters (Zhu et al., 2015). Cao et al. (2020) defined the correlations as strong, moderate, and weak when the coefficients were >0.68, 0.36–0.68, and <0.36, respectively. This classification was adopted in the present study.

2.6.3. Comparison of model efficiencies

To examine the model efficiency (goodness-of-fit), diverse evaluation measures can be used (Hauduc et al., 2015). The most common ones, implemented in GPS-X, include the determination coefficient (R^2), root mean square error (RMSE), and mean absolute error (MAE). The RMSE quantifies the global error of the model while keeping the same unit as the target variable, whereas the MAE evaluates the quality of an estimated parameter in terms of its variation and unbiasedness (Hauduc et al., 2015). In addition, the Janus coefficient (J^2) was calculated in the present study. The J^2 coefficient does not evaluate the model efficiency, but it indicates a change in the model efficiency between the calibration and validation steps. When J^2 is close to 1, the model performance is similar in both steps (the model is valid), whereas high J^2 values could indicate a lack of model robustness.

3. Results and discussion

3.1. Local sensitivity analysis

Fig. 3 shows the sensitivity coefficients for all 13 kinetic parameters related to AOB, NOB, and comammox bacteria in the three examined model structures (Models I, II, and III). The extremely influential parameters (2 parameters with $S_{i,j} \geq 2$) occurred only in Model I, but the highest number of the influential parameters (6 parameters with $S_{i,j} \geq 1$) occurred in Model II.

For all three model structures, the maximum specific growth rate of AOB (μ_{AOB}) was the most influential parameter concerning the behavior of both nitritation substrate (NH_4–N) and product (NO_2^-N), with $S_{i,j}$ ranges of approximately 1.0–1.5 and 1.1–2.3, respectively. The oxygen half-saturation coefficient for AOB ($K_{O,AOB}$) and decay coefficient for AOB (b_{AOB}) were very influential on the behavior of NO_2^-N, with $S_{i,j}$ ranges of approximately 0.9–1.8 ($K_{O,AOB}$) and 1.3–1.6 (b_{AOB}). These two parameters were still very influential in Models I and III with respect to the behavior of NH_4–N. The parameters related to the NOB kinetics, i.e. the maximum specific growth rate (μ_{NOB}) and oxygen half-saturation constant ($K_{O,NOB}$), were at least influential ($S_{i,j} > 0.25$) on the behavior of both nitratation substrate (NO_2^-N) and product (NO_3–N).

The influence of the parameters related to the comammox kinetics varied among the examined models. For Model I, the maximum specific growth rate of comammox bacteria (μ_{CMX}) was extremely influential with respect only to NO_3^-N (comammox product), with the highest sensitivity coefficient among all the models ($S_{i,j} = 2.47$). The oxygen half-saturation coefficient ($K_{O,CMX}$) and decay coefficient (b_{CMX}) for comammox bacteria were very influential only on the behavior of NO_3^-N, with $S_{i,j}$ of approximately 1.4 for both parameters. For Models II and III, μ_{CMX} was very influential on the behavior of NO_2–N ($S_{i,j} \approx$ 1.3–1.4) and NO_3–N ($S_{i,j} \approx$ 0.8–1.6). Moreover, for Model III, b_{CMX} had the highest influence ($S_{i,j} = 0.87$) on NO_3–N among all the kinetic parameters.

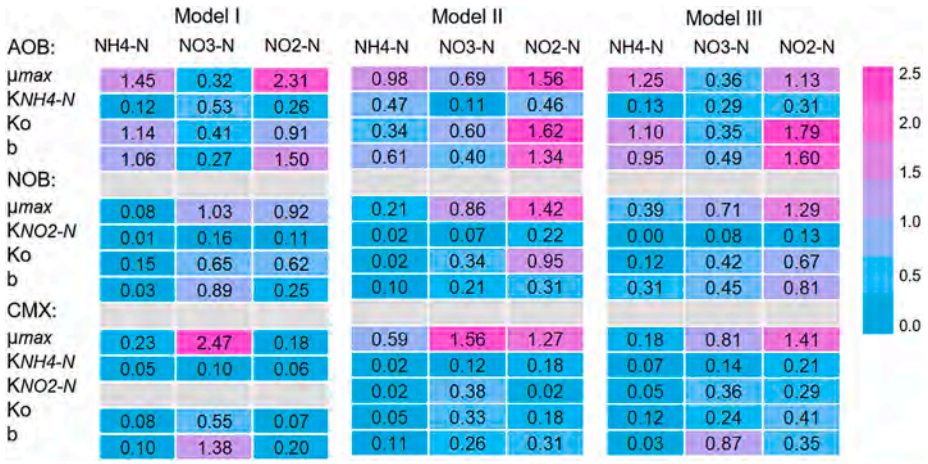

Fig. 3. Heatmap of the sensitivity coefficients for the three examined models.

3.2. Values of the kinetic parameters

For simulations, the kinetic parameter values were selected using three approaches: literature data, direct determination from the batch experiments, and mathematical optimization (estimation) (Table 2). Based on the sensitivity analysis results, values for the least influential parameters, including the half-saturation coefficients for AOB ($K_{NH4,AOB}$) and comammox bacteria ($K_{NH4,CMX}$, $K_{NO2,CMX}$), were adopted from the literature (Koch et al., 2019; Park et al., 2017; Yu et al., 2020) as shown in Table S2 in SI.

The values of DO half-saturation coefficients for AOB ($K_{O,AOB}$) and NOB ($K_{O,NOB}$) and the nitrite half-saturation coefficient for NOB ($K_{NO2,NOB}$) were determined from the batch experiments as described in the SI. Three different linearized forms of the Monod equation and the least-square method were used. In all cases, the highest determination coefficient ($R^2 > 0.9$) was obtained for the Hanes equation.

The values of $K_{O,AOB} = 0.3$ mg O_2/L and $K_{O,NOB} = 0.2$ mg O_2/L were within the literature ranges of 0.16–1.22 mg O_2/L (Zhang et al., 2019) and 0.17–4.32 mg O_2/L (Park et al., 2017), respectively. The value of $K_{NO2-N} = 0.057$ mg N/L was slightly below the ranges reported by (Park et al., 2017) and Koch et al. (2019) for canonical K–NOB (Table 2). Furthermore, a comparison of the process rates at 12 °C and 20 °C suggested that the temperature correction factors in the Arrhenius equation for AOB and NOB were approximately 1.11 (see: SI for details). This value has commonly been used in activated sludge modeling studies (Henze et al., 2000). The most influential parameters (μ_{AOB}, μ_{NOB}, μ_{CMX}, $K_{O,AOB}$, $K_{O,NOB}$, $K_{O,CMX}$, and b_{AOB}, b_{NOB}, b_{CMX}) were selected for evaluation in the correlation matrix before mathematical optimization using the GPS-X "Optimizer" utility.

3.3. Correlation matrix

Fig. 4 shows the overall correlation matrix developed for the most influential kinetic parameters. In the case of all the nitrifier groups, the DO half-saturation constants (Ko) revealed a strong correlation with the maximum specific growth rates (μ) in the three examined models. Therefore, the K_O coefficients were excluded from the optimization process and their values were either determined from the batch test results ($K_{O,AOB}$ and $K_{O,NOB}$) or adopted from the literature ($K_{O,CMX}$).

In general, the highest values of the correlation coefficient referred to the relationship of μ_{AOB}, μ_{NOB}, and μ_{CMX} with the corresponding decay coefficients (b_{AOB}, b_{NOB} and b_{CMX}) in all three models. At short SRTs, as in the present study, attention is normally directed towards growth rather than decay kinetics. Hence, only the maximum specific growth rates were selected for the further optimization process, while the default values of b coefficients were assumed for simulations. However, the accurate estimation of b coefficients becomes more important with increasing SRT (Dold et al., 2005).

The other pairs of highly correlated parameters comprised μ_{AOB} with μ_{NOB} (0.62–0.71), and $K_{O,AOB}$ with $K_{O,NOB}$ (0.66–0.74). High correlations (0.71–0.74) were also found in specific models between b_{AOB} and μ_{AOB} (Model III), μ_{AOB} and μ_{NOB} (Model III) as well as $K_{O,AOB}$ and $K_{O,NOB}$ (Model I).

Table 2
Methods of selection of kinetic parameters and their values in the three examined models.

Bacteria	Kinetic parameter	Unit	Initial value	Calibration results			Source		
				Model I	Model II	Model III	Literature	Batch tests	Calibration
AOB	μ_{AOB}	d^{-1}	1.01	0.57	0.55	0.60			×
	$K_{NH4,AOB}$	mg N/L	0.675	0.675	0.675	0.675	×		
	$K_{O,AOB}$	mg O_2/L	0.30	0.30	0.30	0.30		×	
	b_{AOB}	d^{-1}	0.15	0.15	0.15	0.15	×		
NOB	μ_{NOB}	d^{-1}	0.31	0.11	0.11	0.11			×
	$K_{NO2,NOB}$	mg N/L	0.057	0.057	0.057	0.057		×	
	$K_{O,NOB}$	mg O_2/L	0.2	0.2	0.2	0.2		×	
	b_{NOB}	d^{-1}	0.05	0.05	0.05	0.05	×		
CMX	μ_{CMX}	d^{-1}	0.69	0.15	0.20	0.22			×
	$K_{NH4,CMX}$	mg N/L	0.01	0.01	0.01	0.01	×		
	$K_{NO2,CMX}$	mg N/L	6.29	0.0[a]	6.29	6.29	×		
	$K_{O,CMX}$	mg O_2/L	0.33	0.33	0.33	0.33	×		
	b_{CMX}	d^{-1}	0.05	0.05	0.05	0.05	×		

μ: maximum specific grow rate, K: half-saturation coefficient, b: decay coefficient.
[a] Model I does not use nitrite as a substrate in comammox process.

Fig. 4. Correlation matrix of the adjusted kinetic parameters.

3.4. Model calibration (parameter estimation)

In the first step, the predicted biomass concentrations (MLSS and MLVSS) were checked against the measurements at 12 °C for each model as shown in Fig. 5a. The initial measured MLSS concentration was approximately 1950 mg/L and it decreased below 300 mg/L at the end of the experiment. The nitrifier population was subjected to great dynamics under specific operational conditions, resulting from aggressive SRT reduction. Fig. 5b shows the predicted biomass concentrations of the specific groups of nitrifiers. Their predicted ultimate washout was confirmed by microbiological analyses using a combination of 16 S rRNA high-throughput sequencing and qPCR techniques (Kowal et al., 2021).

The observed and predicted behaviors of NH_4–N, NO_3–N, and NO_2–N are shown in Fig. 6. The prediction accuracy of each model for the three N components was individually interpreted by plotting the model predictions vs. measured data, as shown in Fig. 7. Numerical values of all the model efficiency measures (R^2, RMSE, MAE) are listed in Table 3. From the comparative results of the calibrated models, it appears that the best goodness-of-fit was obtained for Model I. That model revealed the highest R^2 values of 0.96, 0.92, and 0.93 for NH_4–N, NO_3–N, and NO_2–N, respectively. Moreover, the RMSE and MAE were also lower than those of the other two models.

When comparing the values of model parameters adjusted during calibration (Table 2), it appears that there were only slight changes in μ_{AOB} and μ_{NOB} between the models. The optimized values of 0.55–0.60 d^{-1} (μ_{AOB}) and 0.11 d^{-1} (μ_{NOB}) are within the ranges reported in other studies (Park et al., 2017; Zhang et al., 2019) (Table S2). In addition, low variances were observed between the examined models for μ_{CMX} (0.15–0.22 d^{-1}), which resulted from the number of substrates for comammox bacteria. In the model (Model I) with a single substrate (NH_4–N), $\mu_{CMX} = 0.15\ d^{-1}$ was lower than $\mu_{CMX} = 0.2$–$0.22\ d^{-1}$ in the models with two substrates (Model II and Model III). In this way, the overall growth rates of comammox bacteria became comparable.

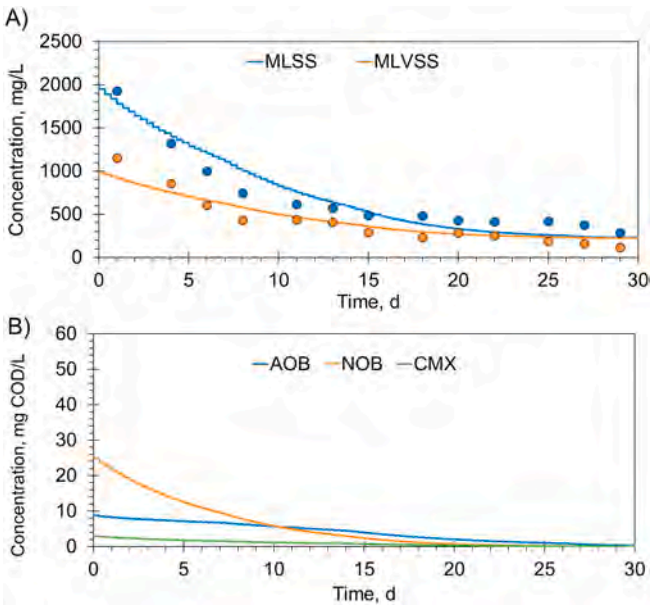

Fig. 5. Measured and predicted MLSS and MLVSS concentrations (A) and predicted active biomass concentrations of specific nitrifiers (AOB, NOB and CMX) (B) during the calibration phase.

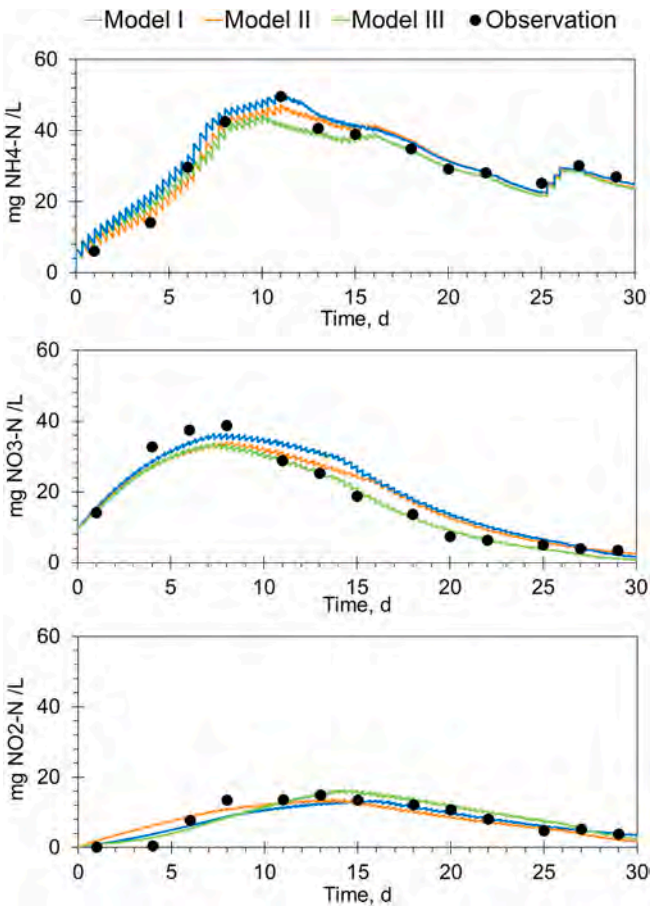

Fig. 6. Measured data vs. model predictions of NH_4–N, NO_2–N, and NO_3–N in Models I, II and III (calibration phase).

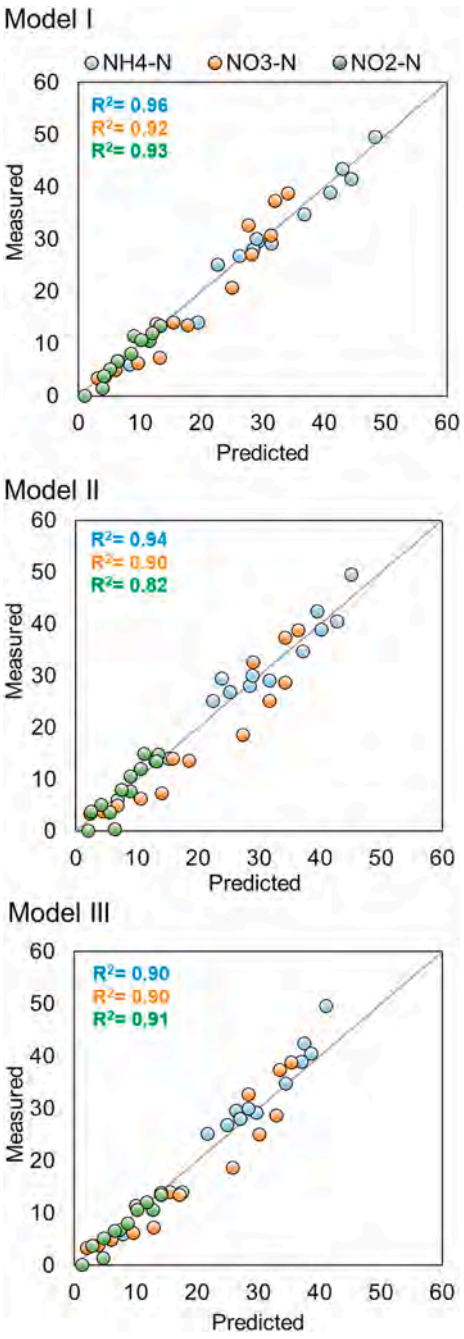

Fig. 7. Correlation between the observed data and model predictions of each examined model for the different N components.

3.5. Model validation

For model validation, predictions of the examined models were compared with the data from the washout experiment carried out at 20 °C. The observed and predicted behaviors of biomass (MLSS, MLVSS), NH_4–N, NO_3–N, and NO_2–N are shown in the SI (Figs. S5 and S6). The summarized information on the efficiency of the validated models is presented in Table 3. Overall, the validation results in terms of R^2, RMSE, and MAE confirm the reliability and robustness of the models despite different conceptual formulations of the commamox process. In addition, the Janus coefficient (J^2) was calculated to compare the goodness-of-fits in the calibration and validation phases. For Model III, the closest value to 1.0 was obtained, but the J^2 values for the other models were only slightly higher (Table 3). Therefore, all models are

Table 3
Summarized information on the model efficiency during the calibration and validation periods.

Model	State variables	Calibration phase			Validation phase			
		R^2	RMSE	MAE	R^2	RMSE	MAE	J^2
I	NH_4–N	0.96	1.84	1.91	0.76	2.90	4.75	2.48
	NO_3–N	0.92	2.08	2.13	0.88	3.10	4.18	2.22
	NO_2–N	0.93	2.13	2.28	0.64	4.23	5.24	3.76
II	NH_4–N	0.94	2.07	2.73	0.79	3.45	5.71	2.77
	NO_3–N	0.90	2.15	3.46	0.84	4.12	5.05	3.67
	NO_2–N	0.82	2.94	3.41	0.61	5.46	6.84	3.44
III	NH_4–N	0.90	2.13	3.72	0.80	3.30	5.50	2.40
	NO_3–N	0.90	2.89	4.31	0.86	3.10	4.25	1.15
	NO_2–N	0.91	2.25	3.01	0.79	3.140	4.30	1.94

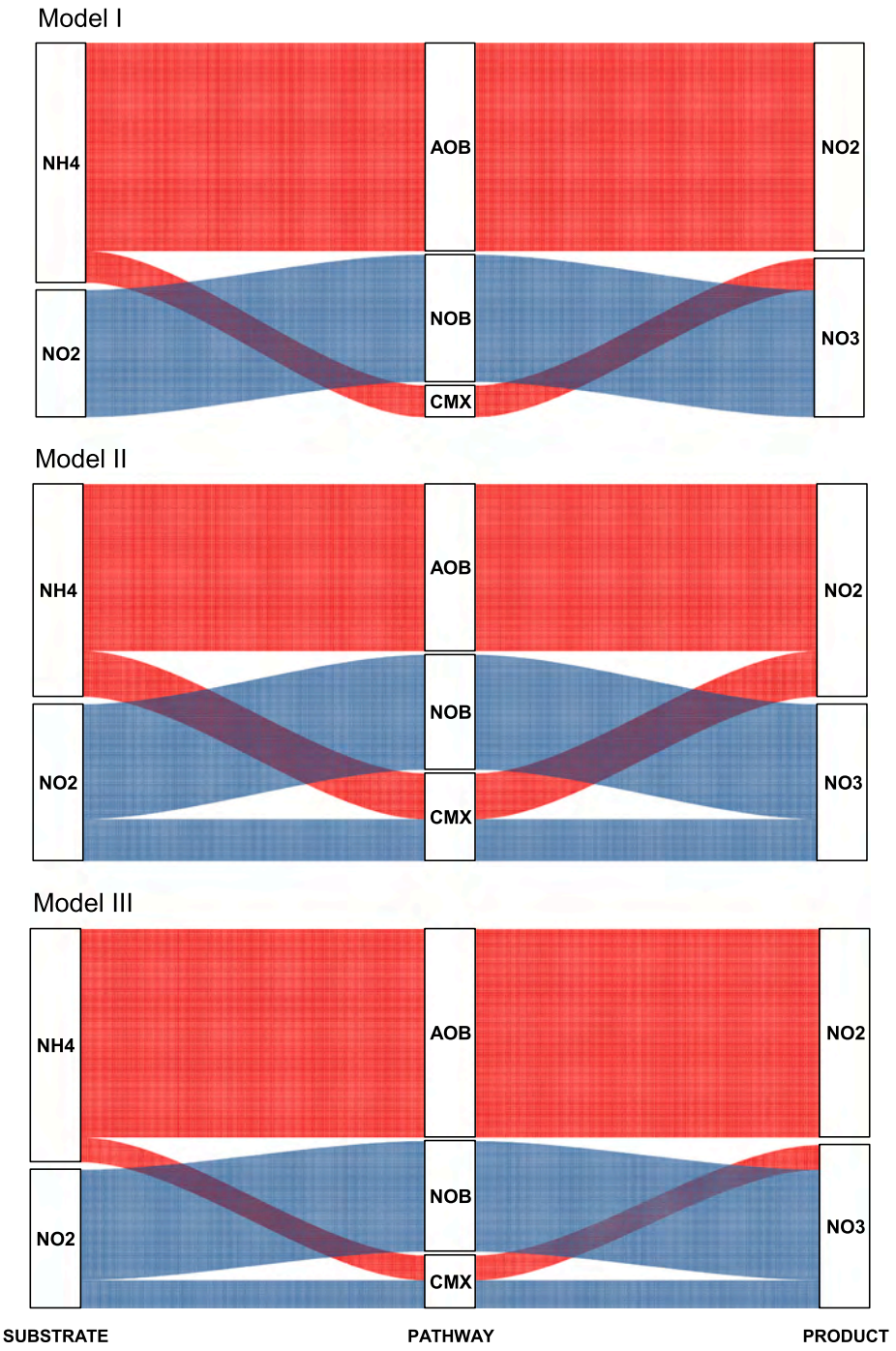

Fig. 8. Sankey graphs of the nitrogen conversions during the calibration phase (developed based on the average values during the entire calibration period).

valid in terms of Janus coefficient evaluation.

From the conceptual point of view, Model I was simplest among the examined models and its efficiency was only slightly better than the others under specific operational conditions (solely NH_4–N in the feed). However, Model I could be replaced with Model III when it was confirmed that NO_2–N is indeed a substrate for comammox bacteria.

3.6. Effect of commamox on the model predictions

To evaluate of comammox effect on the calibration process, two-step nitrification models were run without the comammox activity (μ_{CMX} and b_{CMX} set to 0) and the results are shown in the SI (Fig. S7).

The nitrogen conversion pathways in the examined models were also analyzed using Sankey graphs (Fig. 8) based on the average values for the entire calibration period (30 d). The predicted contribution of comammox bacteria was notable but less significant than that of canonical nitrifiers.

When the direct oxidation of NH_4–N to NO_3–N by comammox bacteria was considered (Models I and III), that pathway was responsible for the conversion of 14% (Model I) and 11% (Model III) of NH_4–N compared to 86% and 89%, respectively, oxidized to NO_2–N by AOB. In Model II considering the parallel oxidation of NH_4–N to NO_2–N by AOB and comammox bacteria, 21% of NH_4–N was oxidized by comammox bacteria and the remaining 79% was converted by AOB. When oxidation of NO_2–N to NO_3–N by comammox bacteria was considered (Models II and III), that pathway was also less significant than the oxidation by NOB. The contributions of commamox bacteria were 26% and 20% in Model II and Model III, respectively, with the remaining contributions of NOB.

4. Conclusions

Different comammox model concepts may be integrated with the existing two-step nitrification models while obtaining a similar predictive performance. The model efficiency measures (R^2, RMSE, MAE) for the approach assuming the direct oxidation of NH_4^+-N to NO_3^--N (without the use of NO_2^--N as an external substrate), were only slightly better than those of the other possible approaches. The model preference could be established after confirming the actual mechanism of NO_2^--N and determining the key model parameters for comammox.

Even though the maximum specific growth rate of comammox bacteria was variable between the examined models, its value remained in the same order as the *Nitrospira*-type NOB. The simulation results revealed that commamox could be responsible for the conversion of >10% and >20% of the influent ammonia load and nitrite respectively. Therefore, the role of commamox in the nitrogen mass balance in activated sludge systems should not be neglected and requires further investigation.

Declaration of competing interest

The authors declare that they have no known competing financial interests or personal relationships that could have appeared to influence the work reported in this paper.

Acknowledgments

The study was supported by the Polish National Science Center under project no. UMO-2017/27/B/NZ9/01039.

Appendix A. Supplementary data

Supplementary data to this article can be found online at https://doi.org/10.1016/j.jenvman.2021.113223.

Credit author statement

Mohamad-Javad Mehrani: Investigation, Software, Formal Analysis, Data Curation, Writing - Original Draft, Visualization; Xi Lu: Methodology, Software; Przemyslaw Kowal: Investigation, Formal Analysis; Dominika Sobotka: Methodology, Investigation, Formal Analysis; Jacek Makinia: Conceptualization, Methodology, Writing - Review & Editing, Supervision.

References

Annavajhala, M.K., Kapoor, V., Santo-Domingo, J., Chandran, K., 2018. Comammox functionality identified in diverse engineered biological wastewater treatment systems. Environ. Sci. Technol. Lett. 5, 110–116.
Cao, J., Zhang, T., Wu, Y., Sun, Y., Zhang, Y., Huang, B., Fu, B., Yang, E., Zhang, Q., Luo, J., 2020. Correlations of nitrogen removal and core functional genera in full-scale wastewater treatment plants: influences of different treatment processes and influent characteristics. Bioresour. Technol. 297, 122455.
Cao, Y., van Loosdrecht, M.C.M., Daigger, G.T., 2017. Mainstream partial nitritation–anammox in municipal wastewater treatment: status, bottlenecks, and further studies. Appl. Microbiol. Biotechnol. 101, 1365–1383.
Daims, H., Lebedeva, E.V., Pjevac, P., Han, P., Herbold, C., Albertsen, M., Jehmlich, N., Palatinszky, M., Vierheilig, J., Bulaev, A., Kirkegaard, R.H., von Bergen, M., Rattei, T., Bendinger, B., Nielsen, P.H., Wagner, M., 2015. Complete nitrification by Nitrospira bacteria. Nature 528, 504.
Daims, H., Lücker, S., Wagner, M., 2016. A new perspective on microbes formerly known as nitrite-oxidizing bacteria. Trends Microbiol. 24, 699–712.
Dold, P.L., Jones, R.M., Bye, C.M., 2005. Importance and measurement of decay rate when assessing nitrification kinetics. Water Sci. Technol. 52, 469–477.
Domingo-Félez, C., Smets, B.F., 2016. A consilience model to describe N2O production during biological N removal. Environ. Sci.: Water Research & Technology 2, 923–930.
Gonzalez-Martinez, A., Rodriguez-Sanchez, A., van Loosdrecht, M.C.M., Gonzalez-Lopez, J., Vahala, R., 2016. Detection of comammox bacteria in full-scale wastewater treatment bioreactors using tag-454-pyrosequencing. Environ. Sci. Pollut. Control Ser. 23, 25501–25511.
Griffin, J.S., Wells, G.F., 2017. Regional synchrony in full-scale activated sludge bioreactors due to deterministic microbial community assembly. ISME J. 11, 500–511.
Hauduc, H., Neumann, M.B., Muschalla, D., Gamerith, V., Gillot, S., Vanrolleghem, P.A., 2015. Efficiency criteria for environmental model quality assessment: a review and its application to wastewater treatment. Environ. Model. Software 68, 196–204.
Henze, M.G.W., Mino, T., van Loosdrecht, M.C.M., 2000. Activated Sludge Models ASM1, ASM2, ASM2d and ASM3. IWA Publishing, London, UK.
Hong, Y., Liao, Q., Bonhomme, C., Chebbo, G., 2019. Physically-based urban stormwater quality modelling: an efficient approach for calibration and sensitivity analysis. J. Environ. Manag. 246, 462–471.
Izadi, P., Izadi, P., Eldyasti, A., 2021. Towards mainstream deammonification: comprehensive review on potential mainstream applications and developed sidestream technologies. J. Environ. Manag. 279, 111615.
Jaramillo, F., Orchard, M., Muñoz, C., Zamorano, M., Antileo, C., 2018. Advanced strategies to improve nitrification process in sequencing batch reactors - a review. J. Environ. Manag. 218, 154–164.
Karlikanovaite-Balikci, A., Yagci, N., 2019. Determination and evaluation of kinetic parameters of activated sludge biomass from a sludge reduction system treating real sewage by respirometry testing. J. Environ. Manag. 240, 303–310.
Kits, K.D., Sedlacek, C.J., Lebedeva, E.V., Han, P., Bulaev, A., Pjevac, P., Daebeler, A., Romano, S., Albertsen, M., Stein, L.Y., Daims, H., Wagner, M., 2017. Kinetic analysis of a complete nitrifier reveals an oligotrophic lifestyle. Nature 549, 269–272.
Koch, H., van Kessel, M.A.H.J., Lücker, S., 2019. Complete nitrification: insights into the ecophysiology of comammox Nitrospira. Appl. Microbiol. Biotechnol. 103, 177–189.
Kowal, P., Mehrani, M.-J., Sobotka, D., Ciesielski, S., Stense, D., Mąkinia, J., 2021. Coexistence of Canonical Nitrifiers and Comammox Bacteria during Biomass Washout Experiments at Decreasing Solids Retention Times (in preparation).
Lawson, C.E., Lücker, S., 2018. Complete ammonia oxidation: an important control on nitrification in engineered ecosystems? Curr. Opin. Biotechnol. 50, 158–165.
Lu, X., Pereira, D.S., Al-Hazmi, T., E, H., Majtacz, J., Zhou, Q., Xie, L., Makinia, J., 2018. Model-based evaluation of N2O production pathways in the anammox-enriched granular sludge cultivated in a sequencing batch reactor. Environ. Sci. Technol. 52, 2800–2809.
Makinia, J., Rosenwinkel, K.H., Spering, V., 2006. Comparison of two model concepts for simulation of nitrogen removal at a full-scale biological nutrient removal pilot plant. J. Environ. Eng. 132, 476–487.
Makinia, J., Zaborowska, E., 2020. Mathematical Modelling and Computer Simulation of Activated Sludge Systems, second ed. IWA, UK.
Metcalf, Eddy, 2014. Wastewater Engineering: Treatment and Resource Recovery, fifth ed. McGraw-Hill, New York, United States.
Noriega-Hevia, G., Mateo, O., Maciá, A., Lardín, C., Pastor, L., Serralta, J., Bouzas, A., 2020. Experimental sulphide inhibition calibration method in nitrification processes: a case-study. J. Environ. Manag. 274, 111191.
Palomo, A., Pedersen, A.G., Fowler, S.J., Dechesne, A., Sicheritz-Pontén, T., Smets, B.F., 2018. Comparative genomics sheds light on niche differentiation and the evolutionary history of comammox Nitrospira. ISME J. 12, 1779–1793.

Park, M.-R., Park, H., Chandran, K., 2017. Molecular and kinetic characterization of planktonic Nitrospira spp. selectively enriched from activated sludge. Environ. Sci. Technol. 51, 2720–2728.

Qian, F., Wang, J., Shen, Y., Wang, Y., Wang, S., Chen, X., 2017. Achieving high performance completely autotrophic nitrogen removal in a continuous granular sludge reactor. Biochem. Eng. J. 118, 97–104.

Razavi, S., Jakeman, A., Saltelli, A., Prieur, C., Iooss, B., Borgonovo, E., Plischke, E., Lo Piano, S., Iwanaga, T., Becker, W., Tarantola, S., Guillaume, J.H.A., Jakeman, J., Gupta, H., Melillo, N., Rabitti, G., Chabridon, V., Duan, Q., Sun, X., Smith, S., Sheikholeslami, R., Hosseini, N., Asadzadeh, M., Puy, A., Kucherenko, S., Maier, H. R., 2021. The Future of Sensitivity Analysis: an essential discipline for systems modeling and policy support. Environ. Model. Software 137, 104954.

Roots, P., Wang, Y., Rosenthal, A.F., Griffin, J.S., Sabba, F., Petrovich, M., Yang, F., Kozak, J.A., Zhang, H., Wells, G.F., 2019. Comammox Nitrospira are the dominant ammonia oxidizers in a mainstream low dissolved oxygen nitrification reactor. Water Res. 157, 396–405.

Sun, Z., Liu, C., Cao, Z., Chen, W., 2018. Study on regeneration effect and mechanism of high-frequency ultrasound on biological activated carbon. Ultrason. Sonochem. 44, 86–96.

van Kessel, M.A.H.J., Speth, D.R., Albertsen, M., Nielsen, P.H., Op den Camp, H.J.M., Kartal, B., Jetten, M.S.M., Lücker, S., 2015. Complete nitrification by a single microorganism. Nature 528, 555.

Wu, Lina, Shen, Mingyu, Li, Jin, Huang, Shan, Li, Zhi, Yan, Zhibin, Peng, Yongzhen, 2019. Cooperation between partial-nitrification, complete ammonia oxidation (comammox), and anaerobic ammonia oxidation (anammox) in sludge digestion liquid for nitrogen removal. Environ. Pollut. 254.

Wu, X., Yang, Y., Wu, G., Mao, J., Zhou, T., 2016. Simulation and optimization of a coking wastewater biological treatment process by activated sludge models (ASM). J. Environ. Manag. 165, 235–242.

Yu, L., Chen, S., Chen, W., Wu, J., 2020. Experimental investigation and mathematical modeling of the competition among the fast-growing “r-strategists” and the slow-growing “K-strategists” ammonium-oxidizing bacteria and nitrite-oxidizing bacteria in nitrification. Sci. Total Environ. 702, 135049.

Zhang, D., Su, H., Antwi, P., Xiao, L., Liu, Z., Li, J., 2019. High-rate partial-nitritation and efficient nitrifying bacteria enrichment/out-selection via pH-DO controls: efficiency, kinetics, and microbial community dynamics. Sci. Total Environ. 692, 741–755.

Zhou, X., Liu, X., Huang, S., Cui, B., Liu, Z., Yang, Q., 2018. Total inorganic nitrogen removal during the partial/complete nitrification for treating domestic wastewater: removal pathways and main influencing factors. Bioresour. Technol. 256, 285–294.

Zhu, A., Guo, J., Ni, B.-J., Wang, S., Yang, Q., Peng, Y., 2015. A novel protocol for model calibration in biological wastewater treatment. Sci. Rep. 5, 8493.

Paper III

M-J Mehrani, F Bagherzadeh, M Zheng, P Kowal, D Sobotka, J Makinia. 2022. Application of a hybrid mechanistic/machine learning model for prediction of nitrous oxide (N_2O) production in a nitrifying sequencing batch reactor. **Process Safety and Environmental Protection,** 162, 1015-1024.

https://doi.org/10.1016/j.psep.2022.04.058

Process Safety and Environmental Protection 162 (2022) 1015–1024

Contents lists available at ScienceDirect

Process Safety and Environmental Protection

journal homepage: www.elsevier.com/locate/psep

Application of a hybrid mechanistic/machine learning model for prediction of nitrous oxide (N_2O) production in a nitrifying sequencing batch reactor

Mohamad-Javad Mehrani[a,*], Faramarz Bagherzadeh[b], Min Zheng[c], Przemyslaw Kowal[a], Dominika Sobotka[a], Jacek Mąkinia[a]

[a] Faculty of Civil and Environmental Engineering, Gdansk University of Technology, ul. Narutowicza 11/12, 80-233 Gdansk, Poland
[b] Faculty of Mechanical Engineering, Gdansk University of Technology, ul. Narutowicza 11/12, 80-233 Gdansk, Poland
[c] Australian Centre for Water and Environmental Biotechnology, The University of Queensland, St Lucia, QLD 4072, Australia

ARTICLE INFO

Article history:
Received 6 September 2021
Received in revised form 25 February 2022
Accepted 24 April 2022
Available online 30 April 2022

Keywords:
Prediction accuracy
Mechanistic model
Machine learning
Nitrous oxide
Nitrification
GHG mitigation

ABSTRACT

Nitrous oxide (N_2O) is a key parameter for evaluating the greenhouse gas emissions from wastewater treatment plants. In this study, a new method for predicting liquid N_2O production during nitrification was developed based on a mechanistic model and machine learning (ML) algorithm. The mechanistic model was first used for simulation of two 15-day experimental trials in a nitrifying sequencing batch reactor. Then, model predictions (NH_4-N, NO_2-N, NO_3-N, MLSS, MLVSS) along with the recorded online measurements (DO, pH, temperature) were used as input data for the ML models. The data from the experiments at 20 °C and 12 °C, respectively, were used for training and testing of three ML algorithms, including artificial neural network (ANN), gradient boosting machine (GBM), and support vector machine (SVM). The best predictive model was the ANN algorithm and that model was further subjected to the 95% confidence interval analysis for calculation of the true data probability and estimating an error range of the data population. Moreover, Feature Selection (FS) techniques, such as Pearson correlation and Random Forest, were used to identify the most relevant parameters influencing liquid N_2O predictions. The results of FS analysis showed that NH_4-N, followed by NO_2-N had the highest correlation with the liquid N_2O production. With the proposed approach, a prompt method was obtained for enhancing prediction of the liquid N_2O concentrations for short-term studies with the limited availability of measured data.

1. Introduction

Nitrous oxide (N_2O) is one of the most significant greenhouse gases (GHGs) with an extremely high global warming potential (GWP), which is almost 300 times higher than that of carbon dioxide (IPCC, 2014). Wastewater treatment plants (WWTPs) are responsible for 3–5% of worldwide anthropogenic N_2O emissions (Mannina et al., 2019). In WWTPs, N_2O is primarily produced during biological nitrogen removal processes, including autotrophic nitritation (aerobic ammonium oxidation to nitrite) and heterotrophic denitritation (reduction of nitrite) (Su et al., 2019).

Moreover, carbon footprint (CF) is a measure of GHG emissions (Delre et al., 2019). The amount of N_2O produced in wastewater treatment operations has a significant impact on the overall CF of WWTPs (Maktabifard et al., 2020). High shares of N_2O emissions in the CF have been observed in biological nutrient removal (BNR) plants (Koutsou et al., 2018). Hence, an accurate estimation of N_2O can help in better understanding of the process behavior and consequently, mitigation and control of this GHG in WWTPs. An N_2O emission factor is a vital indicator of the long-term sustainability of WWTPs and environmental protection (Chen et al., 2020a; Vasilaki et al., 2019).

Mathematical models are a strong tool for process simulation, prediction, and optimization (Wisniewski et al., 2018). There are two possible approaches for N_2O modeling, including mechanistic models and machine learning (ML) techniques. In the area of wastewater treatment, the Activated Sludge Models (ASMs) (Henze et al., 2006) are the most common mechanistic models, which mathematically describe a hypothetical base for biological wastewater treatment processes. There has been a growing number of successful applications of mechanistic modeling for N_2O prediction

* Corresponding author.
E-mail address: mohammad-javad.mehrani@pg.edu.pl (M.-J. Mehrani).

https://doi.org/10.1016/j.psep.2022.04.058
0957-5820/

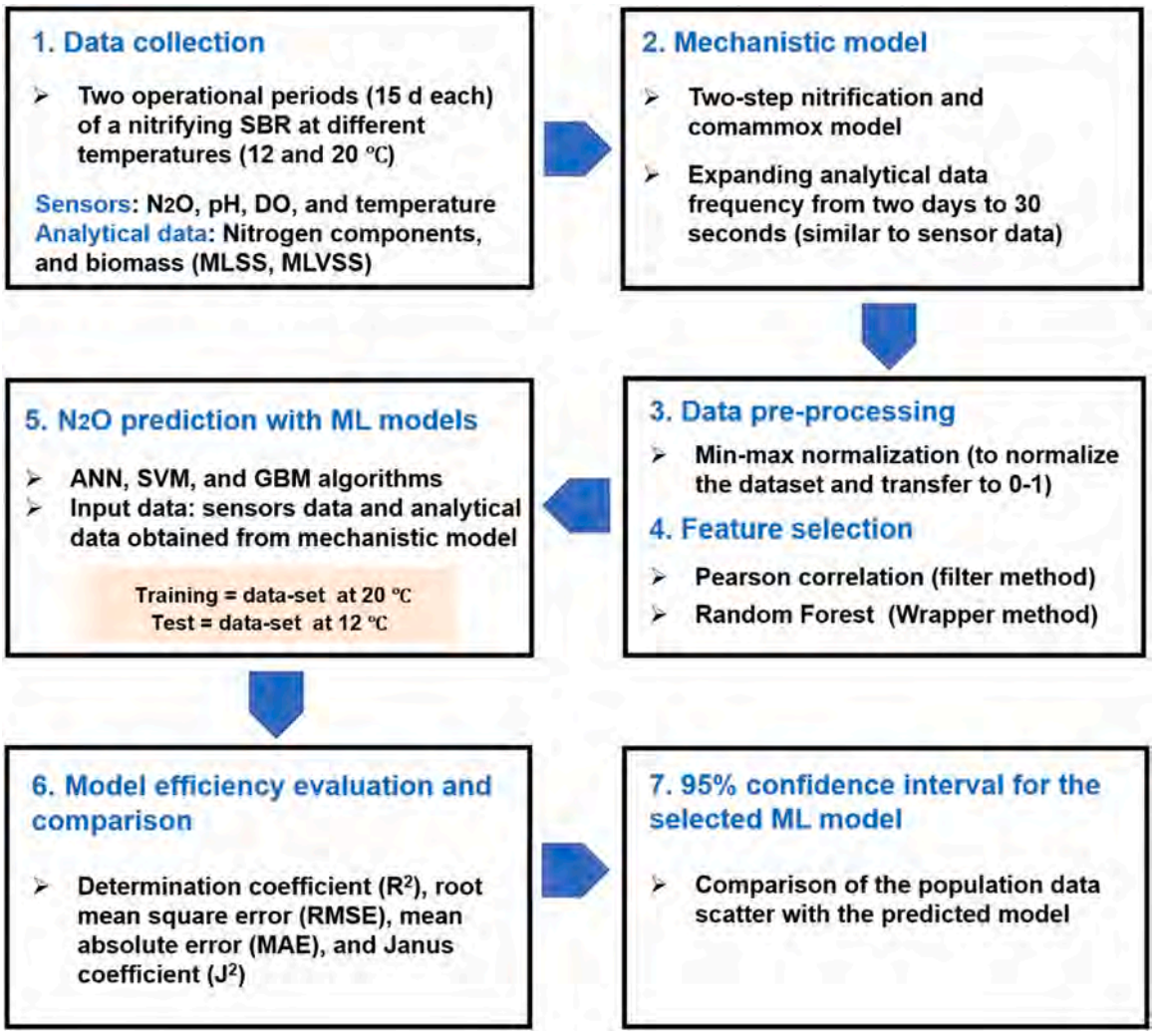

Fig. 1. The procedure of the implementation, training and test, and comparison of prediction ML models.

in real WWTPs (Massara et al., 2018; Su et al., 2019; Wang et al., 2016; Zaborowska et al., 2019). However, these models have a few limitations. First of all, prediction of N_2O requires an extensive knowledge of biological nitrogen transformations for model identification and calibration (Zaborowska et al., 2019). No generic mechanistic model is available, while various expansions and modifications have been added to the existing models (Vasilaki et al., 2019; Chen et al., 2020b). In addition, the traditional mechanistic models are over parameterized, highly sensitive to the changes in operational condition, and demand extensive efforts for calibration and validation. A calibration procedure for N_2O is especially challenging as N_2O is only an intermediate in the nitrogen transformation chain and its contribution to the nitrification process is low (Hwangbo et al., 2021).

On the other hand, ML is a tool for data analysis that can learn from input data and make decisions accordingly without any process equations and pathways (Al-Jamimi et al., 2018). ML algorithms recognize a specific pattern (during a training process) based on defined data (input data) for the prediction and/or classification purposes, which results in a more accurate output (Bagherzadeh et al., 2021; Osarogiagbon et al., 2021). In WWTPs, the ML prediction models have primarily been used for modeling influent/effluent wastewater characteristics. Those models are mainly artificial neural network (ANN) (Ryan et al., 2004; Shaahmadi et al., 2017) and support vector machine (SVM) (Alejo et al., 2018; Shaahmadi et al., 2017; Vasilaki et al., 2020b), while gradient boosting machine (GBM) has been used less frequently (Bagherzadeh et al., 2021). In addition, there are very limited studies on hybrid models (mechanistic models combined with the ML techniques) for forecasting influent/effluent wastewater components (Haimi et al., 2013; Hvala and Kocijan, 2020), but there has been no such a hybrid model applied for N_2O prediction yet.

In terms of N_2O, a predictive ML model of N_2O emission, based on experimental data from an anoxic/aerobic bioreactor with ANN, was proposed by Sun et al. (2017). Moreover, two algorithms, including random forest (RF) and SVM, were used by Vasilaki et al. (2020b) to determine N_2O emission factors. The SVM models performed better than RF in the training of the model to predict the expected range of N_2O emission in WWTPs. Very recently, data-driven-based models, including long short-term memory (LSTM) and deep neural network, have been used to predict liquid N_2O concentrations by big data from a full-scale WWTP (Hwangbo et al., 2021).

In this study, a predictive hybrid model for liquid N_2O production was developed based on the data from a laboratory-scale nitrifying sequencing batch reactor (SBR). The new model overcame limitations of the pure mechanistic models or ML algorithms. This approach includes two major steps: **i)** mechanistic model simulation for expanding the short-term experimental data into an extensive data set with a very small interval (similar to the recordings of a liquid N_2O sensor, and **ii)** liquid N_2O predictions using three powerful ML algorithms (ANN, SVM, and GBM) to achieve a highly accurate model by producing input data from the previous step. To the

Table 1
Statistical summary report of the input and output data used for the ML algorithms.

Data	Function	Mechanistic model predictions					Online measurements			
		NH_4-N (mg N/L)	NO_3-N (mg N/L)	NO_2-N (mg N/L)	MLSS (mg/L)	MLVSS (mg/L)	DO (mg O_2/L)	Temp (℃)	pH -	N_2O (mg N/L)
Training data	Min	2.00	4.86	4.92	545.4	350.9	0.20	18.74	7.11	0.00
	Max	49.06	37.29	12.97	2151.0	1351.0	2.22	21.51	8.35	0.57
	Mean	31.81	29.45	8.44	1176.5	744.54	0.61	20.08	7.55	0.15
Testing data	Min	0.00	19.22	0.00	545.4	350.9	0.150	11.74	7.09	0.00
	Max	119.30	127.40	53.33	2151	1351.0	2.17	13.11	8.65	0.11
	Mean	38.89	93.11	22.57	1176	744.54	0.65	12.29	7.45	0.07

best of our knowledge, this hybrid approach has been used for the first time for N_2O prediction in short-term studies. This research demonstrates a prompt method for enhancing prediction of liquid N_2O concentrations with the limited availability of measured data.

2. Materials and methods

The modeling procedure includes two separate steps for the mechanistic model and ML algorithms. The first step was carried out for expanding the data-set, i.e., converting the communication interval of analytical data similar to the sensor data. The complete process of calibration and validation of the mechanistic model using GPS-X 8.0 software can be found in our previous study (Mehrani et al., 2021). In the second step, liquid N_2O concentrations were predicted by three ML algorithms based on the data generated by the mechanistic model. The diagram in Fig. 1 presents the full modeling/prediction approach.

2.1. Data collection for simulation

Two series of long-term washout experimental trials were carried out in the SBR. The experiments aimed at washing out NOB at decreasing solids retention times (SRTs) from 4d to 3d. The inoculum biomass was taken from the "Czajka" WWTP in Warsaw, Poland during winter and summer periods. The working volume of the SBR was 10 L and the reactor was operated for 15 days at the temperatures typical for winter and summer conditions, i.e., 12 °C and 20 °C. The temperature was kept constant during the experiment with a tolerance of ± 1.5 for 20 ℃ and ± 1.0 for 12 ℃.

The experiments at 20 °C and 12 °C were selected for training and testing the ML algorithms, respectively (Table 1). The initial mixed liquid suspended solids (MLSS) and volatile fraction (MLVSS) concentrations were approximately 2000 mg/L and 1200 mg/L for the experiment at 12 °C, and 2500 mg/L and 1500 mg/L for the experiment at 20 °C.

The SBR was fed with ammonium-rich synthetic wastewater, including tracer elements, but without organic substrate (Mehrani et al., 2021). The volumetric nitrogen loading rates (NLRs) were kept stable at 0.02 ± 0.01 and 0.05 ± 0.01 g N/(L·d) at 12 °C and 20 °C, respectively. During the experiments, pH, temperature, DO concentration, and liquid N_2O concentration were recorded every 30 s by online sensors (Table 1).

2.2. Simulations with a mechanistic model

For both experiments, simulations with the mechanistic model (two-step nitrification with comammox) were run with a communication time of 30 s (similar to the online sensor data). GPS-X 8.0 software (Hydromantis, 2021) was used as a simulation platform. The details of calibration and validation of the mechanistic model can be found in the previous study (Mehrani et al., 2021).

Simulation results, including nitrogen species (NH_4-N, NO_2-N, and NO_3-N) and biomass components (MLSS, MLVSS), were selected as input data (> 50k data for each parameter) of the ML algorithms. Table 1 shows a brief representation of the acquiesced input data set from the mechanistic model and online sensors data, separately for the training and testing data sets.

2.3. Data pre-processing for ML algorithms

Before ML prediction, the data obtained from the mechanistic model and online sensors were subjected to data engineering, i.e., cleaning the information with care taken to the missing or irregular records (Halim et al., 2021; Ranjan et al., 2021). Moreover, input data for training and testing the models were normalized and scaled between 0.0 and 1.0 values as:

$$\mathrm{Xn} = \frac{Xi - Xmin}{Xmax - Xmin} \tag{1}$$

where Xn is normalized data, Xmax, and Xmin are the maximum and minimum values of the considered variable, and Xi is the value of the variable in each record. The normalization helps assign relevant weights for the ML models considering the value of each feature.

2.4. Feature selection for ML algorithms

Pearson correlation. Pearson correlation coefficient (PCC) is a feature selection (FS) filter method and is considered one of the most straightforward FS strategies. The PCC defines the linear relationship between two variables that range from + 1 to − 1, with 1 indicating total positive correlation, 0 indicating no correlation, while − 1 showing the negative correlation (Ali et al., 2021; Alver and Altaş, 2017). The PCC is computed as:

$$\sigma_{ij} = \frac{Cov(f_i, f_j)}{\sqrt{Var(f_i)Var(f_j)}} \tag{2}$$

where σ_{ij} is a correlation coefficient between a given feature f_i and all other features of the data set f_j, *Cov* is covariance, and *Var* is a variance.

Random Forest. The random forest (RF) is a ML filter method for ranking input variables according to their significance (Breiman, 2001). In this technique, several decision trees are created using random feature extraction and data set observations. The trees are de-correlated as a result of this random collection of records and features (bootstrapping). Each bootstrap is used to train a tree when there is a T number of trees in total (Breiman, 2001; Masmoudi et al., 2020). A small portion of data in each bootstrap is kept out of the box (oob_i) to evaluate the feature importance. Moreover, feeding the input feature f observations randomly to the tree will result in oob_i^f. Ultimately, the tree is able to predict the new values of the box by applying the mean squared error, $MSE(oob_i^f)$, and the feature importance is calculated as:

$$I(f) = \frac{1}{T}\sum_{i=1}^{T}\frac{MSE(oob_i^f) - MSE(oob_i)}{MSE(oob_i)} \tag{3}$$

Higher importance values show that the feature is more relevant to the target, and it can improve the prediction output.

2.5. Prediction of liquid N_2O concentrations with ML models

After mechanistic modeling and data pre-processing, the ML algorithms were constructed for liquid N_2O prediction during the two experimental trials in the SBR. Python 3.8 open source programming language was used, while applying various libraries, such as Pandas, Matplotlib, Keras, and Scikitlearn. Each prediction algorithm is outlined in the following subsections and the details are given in the SI.

ANN algorithm. To locate the useful connection among dependent and independent variables, fully connected neural networks can be built up for prediction analysis (Yegnanarayana, 2009). For each neuron, a linear equation between its input and output is assumed. Due to the unpredictability of a non-linear model, more neurons are expected to anticipate the objective variable with a satisfactory precision (Eq. (4)):

$$y = \sigma(\beta_0 + \beta_1 X_1 + \beta_2 X_2 + ...+\beta_n X_n) \tag{4}$$

where y is the output of the ANN, σ is the sigmoid function, X_i is the input number in each neuron, β_0 is the sum of biases of each neuron, and β_i is the weight (trainable parameter) of the neuron.

An ANN is a multilayer perceptron (MLP) with three layers: input, hidden, and output (Kazemi et al., 2021). In a straightforward approach, the number of input layer neurons is the same as the size of a model dimensionality. To guarantee a smooth and precise link between the layers, the rectified linear unit (ReLU) technique was utilized for selecting a suitable number of the layers. The constructed ANN algorithm consists of seven input layers (MLSS was ignored due to a high correlation with MLVSS), three hidden layers with 10, 10, and 5 neurons respectively, and one neuron in the output layer. The optimization algorithm and the loss criterion were Adam and MSE, respectively.

SVM algorithm. The SVM is a versatile ML model that can do linear and nonlinear predictions, and even outlier detection (Vapnik et al., 1995; Géron, 2019). This method was originally designed to solve classification problems before being expanded to solve prediction problems. Since the cost function criteria for model building do not refer to attribute values that lie outside the margin, a model generated by the SVM is extremely depended on the subset of training data (Arshad et al., 2021). As shown in Fig S1, data points outside of the decision boundary will be ignored for developing the hyperplane (removing outliers). Similarly, the SVM model is only based on a subset of the training results (Vapnik et al., 1995). Any training data which are close to the model prediction (hyperplane) are ignored by the cost function method to prevent overfitting issues (Steinwart and Christmann, 2008).

SVM prediction (SVR) is a supervised learning model that uses the same SVM (classification) manner with minor editions. As it is difficult to predict a real number (infinite possibilities), a margin of error is considered for the prediction. The SVR transforms an input matrix to a higher dimensional feature space via a kernel. The following equation expresses the non-linear SVR function $F(x)$ in a mathematical format (Eq. 5) (Awad and Khanna, 2015; Park et al., 2021):

$$F(x) = \sum_{i=1}^{M} (\alpha_i - \alpha_i^*) \quad K(X_i, X) + \delta \tag{5}$$

where M is the number of training records, α_i , α_i^* are Lagrange multipliers, K is the transformation kernel that contains the dot product of mapped vectors of the support vectors (X_1 .... X_i), and δ is the sum of biases (Smola and Schölkopf, 2004).

GBM algorithm. The gradient boosting machine (GBM) is a kind of decision-tree ML model with a distinct ensemble formation of supportive technique (Ayyadevara, 2018). In this method, new trees are added to the ensemble sequentially based on the overall ensemble prediction error (Natekin and Knoll, 2013). The estimation error for the dependent variable shrinks continuously by adding new trees until it reaches the highest possible accuracy (Bagherzadeh et al., 2021). The algorithm produces a new decision tree to minimize the prediction error, and finally, the output of all trees will be aggregated:

$$Data \quad set = \{x^i, Y^i\} \quad {}^{N}_{i=1} \quad Minimizing \quad \left\| \sum_{i=1}^{N} L(F(x^i), Y^i) \right\| \tag{6}$$

where N is the number of records, x^i are independent variables, Y^i is the target variable in the training data set, L is the error function, and $F(x^i)$ is the model output (Xenochristou et al., 2020).

The ultimate goal of GBM is to develop one strong model from several weak and smaller learning models (decision tree models). Considering Eq. (6), the GBM algorithm takes the training data and tries to minimize the error value. Decision trees divide the data set at each branch (node) to maximize the entropy. Each tree has several nodes and will split the data set until fulfilling the given hyperparameters (maximum tree depth).

Adjusting the hyper-parameters is a crucial step in designing a GBM model. Therefore, after many trial-and-error attempts, the following values were used in this study: a learning rate of 0.05, the number of 2000 trees for the forest, subsampling of 0.8, a tree depth of 6, a min sample leaf of 50, and minimum split samples as a 600.

2.6. Evaluation and comparison of the efficiency of ML models

The model performance can be evaluated with statistical methods. The dependent variable data are assumed as $y_1, y_2...y_n$ with the mean value $\bar{y}$ and estimated values of this variable as $f_1, f_2...f_n$ (collectively known as y_i and f_i). Then the sum square of residuals (SS_{res}) and the total sum of squares (SS_{tot}) are calculated, and the coefficient of determination (R-squared) indicates "goodness-of-fit" between the predicted feature and real values. Moreover, the mean absolute error (MAE), root mean square error (RMSE), and Janus coefficient describe the model errors and accuracy (Eqs. (7)–(12)) (Hauduc et al., 2015; Verma et al., 2013):

$$SS_{tot} = \sum_i (y_i - \bar{y})^2 \tag{7}$$

$$SS_{res} = \sum_i (y_i - f_i)^2 \tag{8}$$

$$R^2 = 1 - \frac{SS_{res}}{SS_{tot}} \tag{9}$$

$$MAE = \frac{1}{n} \sum_i (y_i - f_i) \tag{10}$$

$$RMSE = \sqrt{\frac{SS_{res}}{n}} \tag{11}$$

$$J^2 = \sqrt{\frac{RMSE^2_{validation}}{RMSE^2_{calibration}}} \tag{12}$$

where y_i is the observed data in the data set, f_i is the model prediction, $\bar{y}$ is the mean value of the observed data, and n is the number of observation samples.

2.7. Calculation of the confidence interval for the selected ML model

The confidence interval (CI) is a valuable measure to indicate the estimated range of error. In this study, there is a large number of observations with a normal error distribution. Therefore, the 95% CI was calculated with a z-score (Eq. (13)), considering that the standard deviation of the population is known due to having a high number of records (Hogg, 2012):

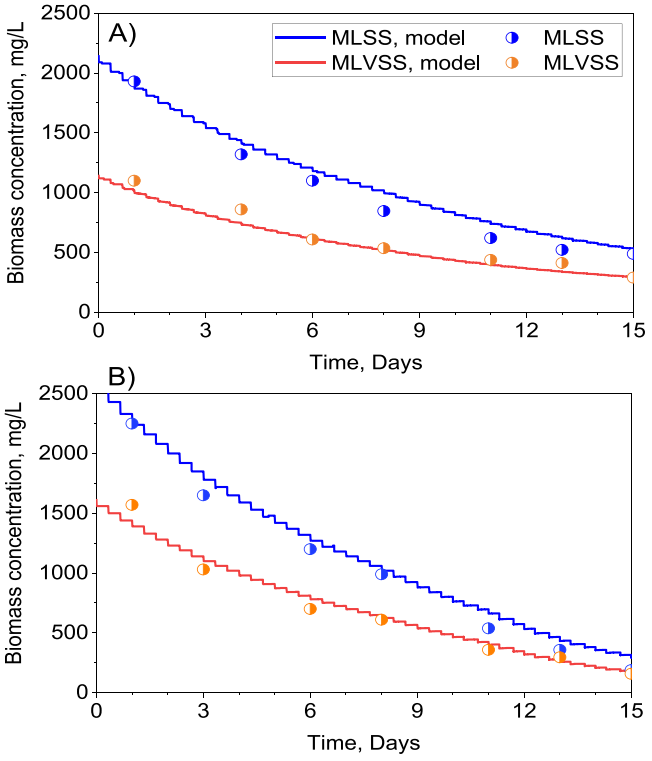

Fig. 2. Measured vs. predicted MLSS and MLVSS concentrations by the mechanistic model: A) Experiment at 12 °C, B) Experiment at 20 °C.

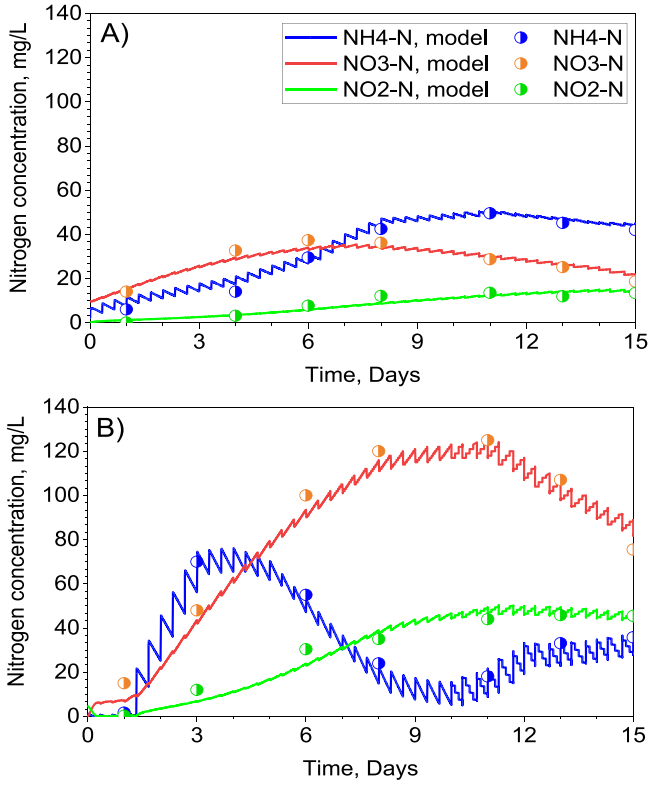

Fig. 3. Measured vs. predicted concentrations of nitrogen species by the mechanistic model: A) Experiment at 12 °C, B) Experiment at 20 °C.

$$CI = \bar{X} \pm z\frac{\sigma}{\sqrt{n}} \quad (13)$$

where $\bar{X}$ is the sample mean, z is the value from the standard normal distribution for the selected confidence level, σ is the standard deviation, and n is the total number of observations. If all the test points are within the 95% CI, it indicates a high level of precision (Abbas et al., 2018).

3. Results

3.1. Predictions of the mechanistic model (ML input data acquisition)

The results of predicted biomass concentrations (MLSS and MLVSS) and nitrogen species by the calibrated mechanistic model are shown in Fig. 2 and Fig. 3, respectively. The MLSS and MLVSS concentrations revealed a decreasing trend in both experiments due to the continuous biomass washout conditions (Fig. 2). Concerning the nitrogen species, in the experiment at 12 °C (Fig. 3a), NO_3-N started to dilute after the first week resulting from biomass and NOB washout, while NO_2-N stabilized at around 12–15 mg N/L to the end of the experiment. In the experiment at 20 °C (Fig. 3b), the NLRs were approximately doubled (0.05 ± 0.01 g N/(L·d)) in response to the higher activity of bacteria at higher temperature and NO_3-N dilution started after 10 days resulting from biomass and NOB washout, while NO_2-N stabilized at around 40–45 mg N/L. The NO_3-N and NO_2-N production were more than double in Fig. 3b in comparison to Fig. 3a based on higher activity of bacteria in higher temperature.

3.2. Feature selection for ML algorithms

Fig. 4 shows a heatmap of the PCC between the variables (N species, biomass components, and online measurements) and N_2O concentration (target variable). The highest positive and negative correlation, 0.82 and −0.56, was obtained for NH_4-N and NO_2-N, respectively. The biomass components (MLSS and MLVSS) with the correlation factor of 0.48 were the next highest correlated variables. However, both parameters (MLSS and MLVSS) had a perfect correlation of 1.0 between each other, and thus only one of them (MLSS) was considered in the final subset of features to avoid multicollinearity issues.

The results of the RF method were in line with the Pearson correlation concerning the highest importance level of the nitrogen species with the target variable (Fig. 5). The maximum importance levels were obtained for NH_4-N (0.71) and NO_2-N (0.37). Moreover, among the online measurements, DO concentration had the highest correlation with N_2O concentration for both examined methods.

3.3. ML modeling results

3.3.1. Model predictions against training data

All three examined prediction models were trained and tested based on the data from the experiment at 20 °C and 12 °C, respectively. The comparative results for all the training models are shown in Fig. 6a. The overall performance of the models was within an acceptable range (Table 2) The noisy data points were not predicted accurately as they were treated as outliers.

Each algorithm required a specific approach and trial-and-error attempt to obtain the optimum parameter set, which ensured a high prediction accuracy. The ANN model was developed after looping over 300 epochs on the training data set. The SVM model was built with the regularization parameter (C=1), and SVR epsilon tube (epsilon=0.1). For the GBM, the following setting was selected: 4000 estimators, the learning rate of 0.01, min. sample leaf of 40, min. sample split of 30, and max. depth of 40.

3.3.2. Model predictions against test data

The trained prediction models were tested by another data set (experiment at 12 °C) (Fig. 6b). The SVM and GBM were overfitted,

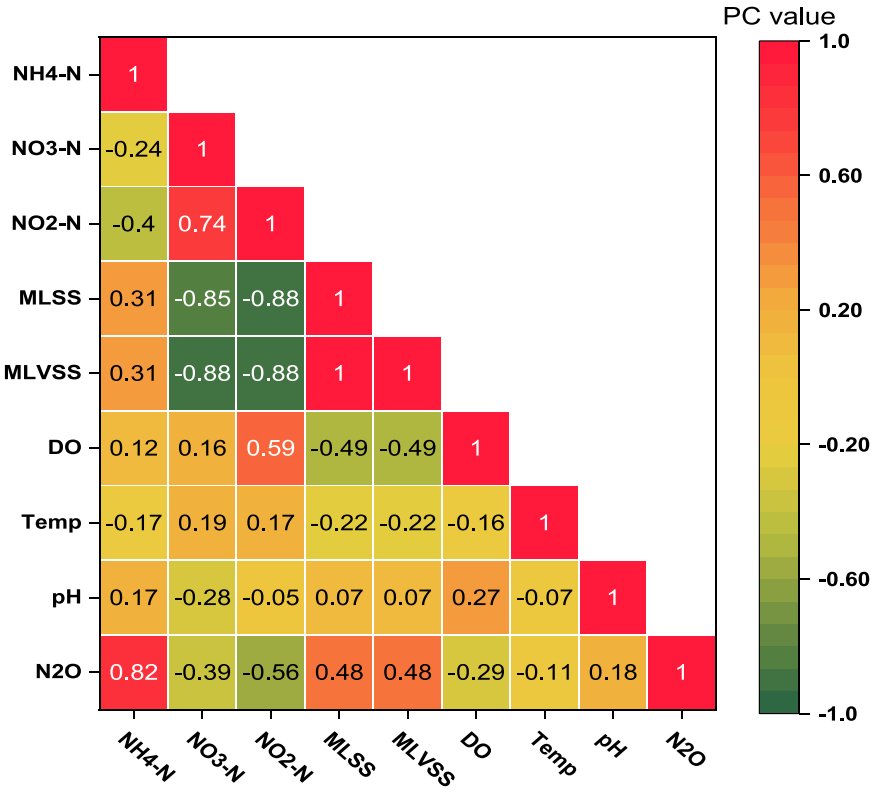

Fig. 4. Heatmap of Pearson correlation coefficient for input data with the target variable (N_2O).

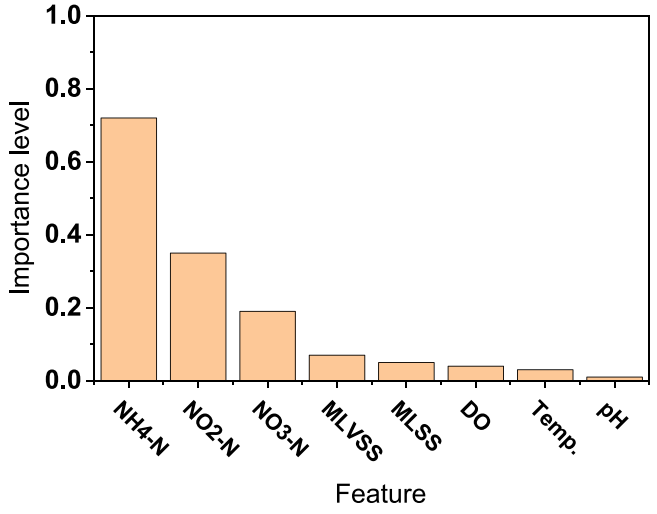

Fig. 5. RF feature selection importance level of the features related to N_2O production.

even though they were able to capture the train data patterns. On the other hand, the ANN demonstrated its versatility under the different operational conditions and process patterns. As shown in Fig. 6b, the SVM overestimated the N_2O peak with a 6-day delay, and the GBM failed to predict any distinguishable climax.

3.3.3. Model efficiency evaluation and comparison

Table 2 presents the efficiency and error of each prediction algorithm. The ANN had the highest coefficient of determination, i.e., $R^2_{Train=}0.93$, $R^2_{Test=}0.67$, and the lowest error indexes. These measures confirm that the ANN is the best model for predicting liquid N_2O concentrations during the experimental trials under different operational conditions. The SVM failed to predict the N_2O concentrations of unseen test data and the GBM partially detected the pattern

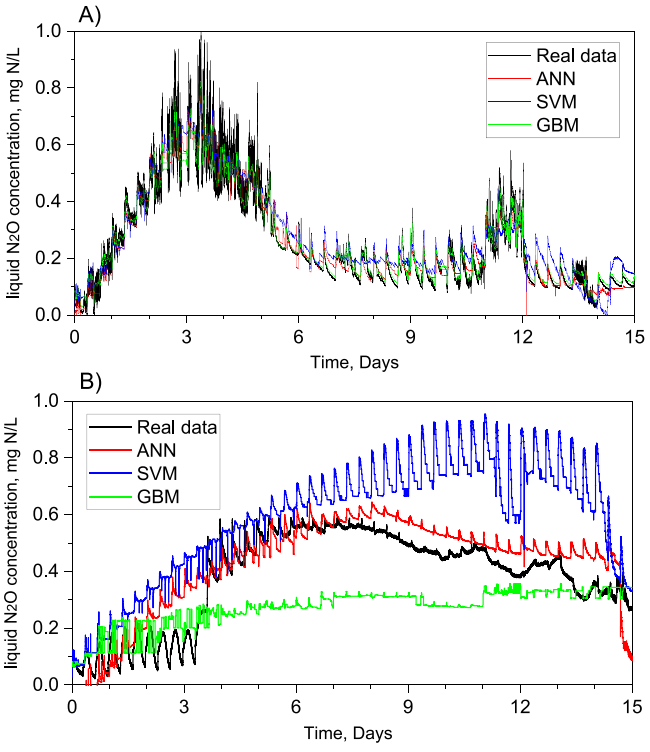

Fig. 6. Training and test results of the prediction models, (A) Train data (experiment at 20 °C), and (B) Test data (experiment at 12 °C).

of the real data at the beginning and end of the experiment. The high values of R^2_{Train} and low values of R^2_{Test} show that both SVM and GBM are overfitted and failed to predict the target variable. Among all the examined models, the ANN had also the best J^2, i.e., closest value to

Table 2
Model efficiency criteria for the examined prediction models.

Model	Training data				Test data				
	R^2	MSE	RMSE	MAE	R^2	MSE	RMSE	MAE	J^2
ANN	**0.92**	**0.002**	**0.048**	**0.006**	**0.67**	**0.012**	**0.09**	**0.002**	**1.87**
SVM	0.88	0.003	0.062	0.12	0.06	0.057	0.239	0.23	3.71
GBM	0.97	0.007	0.077	1.23	0.12	0.027	0.266	0.11	3.45

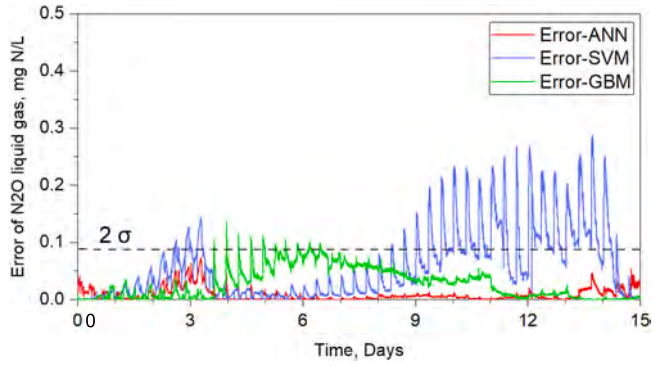

Fig. 7. Prediction errors of liquid N_2O concentrations for the examined prediction models from the test data (σ is the standard deviation of the test data set).

1.0. This confirms the ability of that model in finding data patterns under a highly dynamic behavior of the online measurements.

In Fig. 7, it can be seen that at the beginning of the experimental trial (days 2–4), the model outputs had considerable errors due to a sudden increase in N_2O production. After 4 days, when the stability in N_2O production was achieved, the errors (except for the SVM) became more stable. The ANN model output error was below the doubled standard deviation (2 σ) during the entire experiment, which indicated a valid and proper prediction (Fig. 7). Moreover, the variance of the prediction error in the ANN model was significantly lower than the SVM and GBM for the test data.

3.3.4. Confidence interval for the selected model (ANN)

The result of CI was evaluated based on the z-score as there was a large number of population and the Gaussian shape of the error distribution. Overall, the data values are mostly within the error range of ± 0.13 N_2O mg/L as an upper and lower band of 95% CI (Fig. 8). Moreover, the variance of ANN model prediction is located in the confidence region (95% CI), showing its accuracy. This confirms that the ANN model predicted the measured data with 95% of the observed uncertainty.

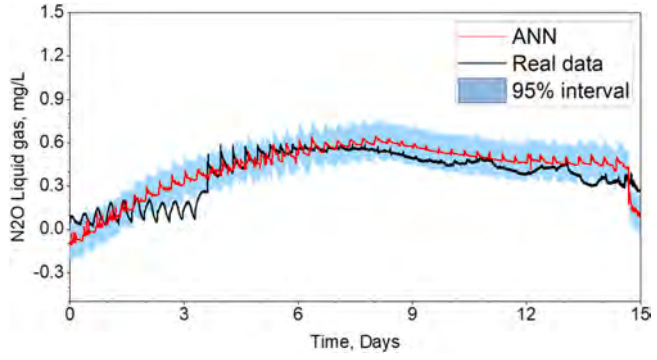

Fig. 8. Measured data, ANN model predictions and 95% confidence interval of the predictions.

3.3.5. Effect of mechanistic modeling (data acquisition) on the prediction performance

For evaluation of the effect of the mechanistic model on the ML prediction performance, the models were fed with the direct experimental data (without mechanistic modeling). It can be seen in the SI (Fig. S4) that only the SVM could train the model with the acceptable accuracy (R^2 =0.76), but failed to predict the test data set (R^2 =0.0). The ANN and GBM could not train the models nor predict the test data-set. Table S1 shows the efficiency and error for each prediction ML algorithm without considering the mechanistic model. Mechanistic modeling prior to the ML procedure had a significant impact on the accuracy of training and testing the N_2O prediction. In the ANN model, after applying mechanistic modeling before the ML prediction, the accuracy increased dramatically from R^2_{Test}= −0.06 (Table S1) to R^2_{Test}= 0.67 (Table 2). This improvement can be justified by the fact that ML models need a sufficiently large data-set first to train and then predict accurately the test data-set.

4. Discussion

Results of the feature selection analysis on N_2O production show that the behavior of NH_4-N and NO_2-N plays an important role in predicting N_2O accumulation during nitrification. This finding was supported by the results of other studies (Duan et al., 2020; Li et al., 2015; Song et al., 2020). Song et al. (2020) observed that NH_4-N and the sum of NO_2-N and NO_3-N had the highest effect on N_2O emissions in a feature selection study of a full-scale WWTP. Strong positive correlations between NH_4-N oxidation and N_2O production during nitrification were also reported in a pilot-scale SBR (Li et al., 2015) and full-scale SBR (Duan et al., 2020). Moreover, in the study of (Duan et al., 2020), a strong positive correlation was also found between liquid N_2O and NO_2-N concentration (Pearson correlation of 0.93).

Furthermore, Duan et al. (2020) observed that N_2O emission exhibited a clear pattern that followed the DO profile in an intermittent aeration mode (Pearson correlation of 0.74). In the present study, a weak negative correlation (−0.29) was also found between the DO concentration and N_2O production during continuous aeration at the low DO setpoint of 0.6 mg O_2/L. It should be emphasized, however, that the well-established favorable conditions for liquid N_2O production comprise low DO and high NO_2-N concentrations (Mannina et al., 2017; Massara et al., 2018; Peng et al., 2014; Vasilaki et al., 2020a).

In the present study, the observed correlation of N_2O production with pH and temperature was lower than other evaluated parameters. N_2O production presented a weak positive correlation of 0.18 with pH which was kept in the range of 7.0–7.5 (Fig. 4). Law et al. (2011) reported that N_2O production fluctuated with pH in the range of 6.0 and 8.5 while keeping the pH between 6.4 and 7.0 reduced N_2O production in a partial nitrification system with aerobic conditions (Law et al., 2011). It can be seen in Fig. 5 that the online measurement data (temperature, DO, and pH) had a lower importance level than nitrogen species and biomass concentrations for the prediction of N_2O production. Vasilaki et al. (2020a) found that under similar DO and pH concentrations, the average liquid N_2O conditions can vary substantially.

The trend of N_2O production was different in experiments for train and test of ML Algorithms. However, the ANN model successfully predict the N_2O production in a test experiment (Fig. 6a,b). This higher production of N_2O (up to 1.0 mg N/L) in the first week of train experiment (Fig. 6a) can due to higher NLR of 0.05 ± 0.01 g N/(L.d) in compare to the test experiment (0.02 ± 0.01 g N/(L.d)) (Fig. 6b).

Table 3 presents various N_2O prediction studies with different modeling approaches (mechanistic and ML) in lab-scale, pilot-scale, or full-scale WWTPs. The mechanistic models were mostly used for the prediction of lab-scale or pilot-scale systems, while the ML

Table 3
Summary of different studies on N_2O prediction in lab-scale or full-scale WWTP.

Prediction method	Model / Algorithm	Model Accuracy	System	Remarks	References
Mechanistic	A mathematical model based on AOB and HB processes	na	Lab- and pilot-scale	The model result showed that the contribution of heterotrophs to N_2O production decreased with the increasing DO concentrations.	(Wang et al., 2016)
	ASM2d-N_2O	na	Full-scale	N_2O hotspots (important rise and falls) were predicted theoretically by an extended ASM considering all the biological pathways for N_2O production.	(Massara et al., 2018)
	ASM2d	R^2 = 0.65	Lab-scale and pilot-scale	The model was used as a tool for assessing the multivariable problem of N_2O mitigation in a combined N-P activated sludge system.	(Zaborowska et al., 2019)
	Mathematical model (two-step nitrification, four step HD)	R^2 = 0.83–0.99	Batch experiment	In the best-fit model, which combined two-step nitrification and denitrification pathways, the contribution of heterotrophs to N_2O production was stronger than autotrophs.	(Domingo-Félez et al., 2017)
	ASM-ICE	R^2 = 0.94–0.98	Batch experiment	The model predicted that N_2O accumulation resulted from a faster drop of the N_2O reduction rate than the NO_2-N reduction rate.	(Ding et al., 2017)
	Extended ASM model	R^2_{Test}= 0.88	Full-scale	The integrated N_2O model, considering the nitrification/denitrification pathways, could predict N_2O production.	(Ni et al., 2015)
	Extended ASM model	R^2 = 0.10–0.53 RMSE= 0.4–1.14	Full-scale	Imbalanced distribution of flow rate between the two treatment lines did not result in a substantial increase in N_2O emissions for the particular WWTP and operational parameters, according to the N_2O simulation results.	(Solís et al., 2022)
	Extended ASM model	R^2 (NSE)= 0.3–0.33 RMSE= 0.38–0.41	Full-scale	The model estimated the N_2O in terms of liquid and gaseous N_2O emissions. This extended model indicated the essential function of heterotrophs. The N_2O emission factor (EF) for the examined plant was between 0.9% and 0.94% of the influent TN-load.	(Maktabifard et al., 2022)
Machine Learning	Back Propagation-ANN	R^2_{Test}= 0.81–94 MSE= 0.1–0.8	Full-scale / pilot-scale	The model was a convenient and feasible method for the prediction of N_2O emissions in a nitrifying-denitrifying system.	(Sun et al., 2017)
	DNN and LSTM	R^2_{DNN}= 0.86 R^2_{LSTM}= 0.94	Full-scale	In a comparative study, the LSTM-based forecasting model performed better than the DNN-based model in terms of model goodness-of-fit	(Hwangbo et al., 2021)
	SVM	na	Full-scale	The model predicted that N_2O emissions accounted for 7.6% of the total NH_4-N load (on average) in a sidestream SBR. N_2O was correlated with DO, influent NH_4-N load, and pH.	(Vasilaki et al., 2020a)
Hybrid method	Extended ASM1 and three different ML algorithms (ANN, SVM, and GBM)	ANN model: R^2_{Train}= 0.92 R^2_{Test}= 0.67 $RMSE_{Train}$= 0.048 $RMSE_{Test}$= 0.09	Lab-scale	NH_4-N and NO_2-N had the highest correlation with N_2O production. ANN revealed the best performance among other algorithms.	This study

na: not available, AOB: Ammonia oxidation bacteria, HB: heterotrophic bacteria, HD: heterotrophic denitrification, DNN: deep neural network, SVM: support vector machines, ANN: artificial neural network, CSTR: continuously stirred tank reactor, ASM-ICE: Activated Sludge Model for Indirect Coupling of Electrons, NSE: Nash-Sutcliff coefficient.

methods considered data from full-scale systems. In general, the accuracy of N_2O prediction was higher for the pure ML models than the pure mechanistic models, and the developed hybrid model of this study revealed one of the highest prediction accuracies in comparison with the studies shown in Table 3.

An accurate prediction of N_2O can play a significant role in the mitigation of N_2O from WWTPs (Solís et al., 2022; Maktabifard et al., 2022). Hence, the proposed approach, i.e., expanding a data set by a mechanistic model and prediction with ML algorithms, can be useful for the limited amounts of data collected during N_2O measurement campaigns towards a mitigation of this hazardous gas from the WWTPs. With sufficiently big data set, the ML algorithms can ensure predictions with a satisfactory level of performance (without expanding the data by a mechanistic model).

The present approach still has some limitations. Only the limited experimental data from a lab-scale system were considered, while the hybrid model still requires validation based on experimental data from full-scale WWTPs. Furthermore, nitrogen transformations were only evaluated with respect to nitrification, whereas denitrification may also be an important source of N_2O production in full-scale WWTPs. Expanding the input data of ML algorithms by external software, such as GPS-X, requires experiments to validate the mechanistic model. Furthermore, applicability of the hybrid models still requires further validation with more variety of data-sets.

For future studies, a comparison between mechanistic modeling and ML predictions for liquid N_2O production and gas N_2O emission in a bigger data set is suggested. Future ML algorithms can be developed for prediction of specific N_2O production pathways, although this function is now applicable only by mechanistic models. In addition, estimation of an N_2O emission factor, EF_{N2O}, can be another interesting and useful application for full-scale WWTPs. This factor plays a critical role in determining the WWTP carbon footprint (Maktabifard et al., 2020).

5. Conclusions

A hybrid model, combining mechanistic and ML (ANN) models, accurately predicted the liquid N_2O concentrations during two 15-day experimental trials in a nitrifying SBR. This approach is novel in comparison with the previous attempts for finding a predictive model of N_2O production during nitrification. The hybrid model successfully predicted unknown test data with an acceptable coefficient of determination (R^2_{TEST} = 0.67), showing its versatility in terms of variable operating conditions and the ability to generalize process patterns more accurately than the other two examined models (SVM, GBM). On the other hand, the SVM overfitted in the estimation of the test data and GBM failed to predict an acceptable model. Moreover, accounting for the level of uncertainty for the ANN model, the predicted values with more than 95% accuracy are reliable enough for delivering valuable information regarding the phenomenon for further research and practical applications. A hybrid modeling concept that combines mechanistic models of WWTPs (e.g., ASMs) with ML can be further expanded to predict N_2O production/emission in full-scale WWTPs for N_2O mitigation strategies.

Declaration of Competing Interest

The authors declare that they have no known competing financial interests or personal relationships that could have appeared to influence the work reported in this paper.

Acknowledgment

This work was supported by the Polish National Science Center, Poland under project no. UMO-2017/27/B/NZ9/01039.

Appendix A. Supporting information

Supplementary data associated with this article can be found in the online version at doi:10.1016/j.psep.2022.04.058.

References

Abbas, M.H., Norman, R., Charles, A., 2018. Neural network modelling of high pressure CO_2 corrosion in pipeline steels. Process Saf. Environ. Prot. 119, 36–45.
Al-Jamimi, H.A., Al-Azani, S., Saleh, T.A., 2018. Supervised machine learning techniques in the desulfurization of oil products for environmental protection: A review. Process Saf. Environ. Prot. 120, 57–71.
Alejo, L., Atkinson, J., Guzmán-Fierro, V., Roeckel, M., 2018. Effluent composition prediction of a two-stage anaerobic digestion process: machine learning and stoichiometry techniques. Environ. Sci. Pollut. Res. 25, 21149–21163.
Ali, M.M.M., Li, Z., Zhao, H., Rawashdeh, A., Al Hassan, M., Ado, M., 2021. Characterization of the health and environmental radiological effects of TENORM and radiation hazard indicators in petroleum waste –Yemen. Process Saf. Environ. Prot. 146, 451–463.
Alver, A., Altaş, L., 2017. Characterization and electrocoagulative treatment of landfill leachates: A statistical approach. Process Saf. Environ. Prot. 111, 102–111.
Arshad, U., Taqvi, S.A.A., Buang, A., Awad, A., 2021. SVM, ANN, and PSF modelling approaches for prediction of iron dust minimum ignition temperature (MIT) based on the synergistic effect of dispersion pressure and concentration. Process Saf. Environ. Prot. 152, 375–390.
Awad, M., Khanna, R., 2015. Support vector regression. In: Awad, M., Khanna, R. (Eds.), Efficient Learning Machines: Theories, Concepts, and Applications for Engineers and System Designers. Apress, Berkeley, CA, pp. 67–80.
Ayyadevara V.K., 2018, Gradient Boosting Machine. In: Pro Machine Learning Algorithms. Apress, Berkeley, CA.
Bagherzadeh, F., Mehrani, M.-J., Basirifard, M., Roostaei, J., 2021. Comparative study on total nitrogen prediction in wastewater treatment plant and effect of various feature selection methods on machine learning algorithms performance. Journal of Water Process Engineering 41.
Bagherzadeh, F., Shojaei Nouri, A., Mehrani, M.-J., Thennadil, S., 2021. Prediction of energy consumption and evaluation of affecting factorsin a full-scale WWTP using a machine learning approachFaramarz. Process Safety and Environmental Protection 154, 458–466. https://doi.org/10.1016/j.psep.2021.08.040
Breiman, L., 2001. Random forests. Mach. Learn. 45, 5–32.
Chen, K.H., Wang, H.C., Han, J.L., Liu, W.Z., Cheng, H.Y., Liang, B., Wang, A.J., 2020a. The application of footprints for assessing the sustainability of wastewater treatment plants: a review. J. Clean. Prod. 277, 124053.
Chen, H., Zeng, L., Wang, D., Zhou, Y., Yang, X., 2020b. Recent advances in nitrous oxide production and mitigation in wastewater treatment. Water Res 184, 116168.
Delre, A., ten Hoeve, M., Scheutz, C., 2019. Site-specific carbon footprints of Scandinavian wastewater treatment plants, using the life cycle assessment approach. J. Clean. Prod. 211, 1001–1014.
Ding, X., Zhao, J., Hu, B., Li, X., Ge, G., Gao, K., Chen, Y., 2017. Mathematical modeling of nitrous oxide (N2O) production in anaerobic/anoxic/oxic processes: Improvements to published N2O models. Chem. Eng. J. 325, 386–395.
Domingo-Félez, C., Pellicer-Nàcher, C., Petersen, M.S., Jensen, M.M., Plósz, B.G., Smets, B.F., 2017. Heterotrophs are key contributors to nitrous oxide production in activated sludge under low C-to-N ratios during nitrification—Batch experiments and modeling. Biotechnol. Bioeng. 114, 132–140.
Duan, H., van den Akker, B., Thwaites, B.J., Peng, L., Herman, C., Pan, Y., Ni, B.-J., Watt, S., Yuan, Z., Ye, L., 2020. Mitigating nitrous oxide emissions at a full-scale wastewater treatment plant. Water Res. 185, 116196.
Géron, A., 2019. Hands-On Machine Learning with Scikit-Learn, Keras, and TensorFlow, second ed., O'Reilly Media, Inc., 1005 Gravenstein Highway North, Sebastopol, CA, pp. 95472.
Haimi, H., Mulas, M., Corona, F., Vahala, R., 2013. Data-derived soft-sensors for biological wastewater treatment plants: An overview. Environ. Model. Softw. 47, 88–107.
Halim, S.Z., Quddus, N., Pasman, H., 2021. Time-trend analysis of offshore fire incidents using nonhomogeneous Poisson process through Bayesian inference. Process Saf. Environ. Prot. 147, 421–429.
Hauduc, H., Neumann, M.B., Muschalla, D., Gamerith, V., Gillot, S., Vanrolleghem, P.A., 2015. Efficiency criteria for environmental model quality assessment: A review and its application to wastewater treatment. Environ. Model. Softw. 68, 196–204.
Henze, M., Gujer, W., Mino, T., van Loosedrecht, M., 2006. Activated Sludge Models ASM1, ASM2, ASM2d and ASM3. IWA Publishing,.
Hogg, Rv, 2012. Introduction to Mathematical Statistics. Pearson.
Hvala, N., Kocijan, J., 2020. Design of a hybrid mechanistic/Gaussian process model to predict full-scale wastewater treatment plant effluent. Comput. Chem. Eng. 140, 106934.

Hwangbo, S., Al, R., Chen, X., Sin, G., 2021. Integrated Model for Understanding N2O Emissions from Wastewater Treatment Plants: A Deep Learning Approach. Environ. Sci. Technol. 55, 2143–2151.
Hydromantis, 2021. ⟨https://www.hydromantis.com/GPSX⟩. Canada.
IPCC, 2014, Intergovernmental Panel on Climate Change Fifth Assessment Report.
Kazemi, P., Bengoa, C., Steyer, J.-P., Giralt, J., 2021. Data-driven techniques for fault detection in anaerobic digestion process. Process Saf. Environ. Prot. 146, 905–915.
Koutsou, O.P., Gatidou, G., Stasinakis, A.S., 2018. Domestic wastewater management in Greece: greenhouse gas emissions estimation at country scale. J. Clean. Prod. 188, 851–859.
Law, Y., Lant, P., Yuan, Z., 2011. The effect of pH on N2O production under aerobic conditions in a partial nitritation system. Water Res. 45, 5934–5944.
Li, P., Wang, S., Peng, Y., Liu, Y., He, J., 2015. The synergistic effects of dissolved oxygen and pH on N2O production in biological domestic wastewater treatment under nitrifying conditions. Environ. Technol. 36, 1623–1631.
Maktabifard, M., Zaborowska, E., Makinia, J., 2020. Energy neutrality versus carbon footprint minimization in municipal wastewater treatment plants. Bioresour. Technol. 300, 122647.
Maktabifard, M., Blomberg, K., Zaborowska, E., Mikola, A., Mąkinia, J., 2022. Model-based identification of the dominant N2O emission pathway in a full-scale activated sludge system. J. Clean. Prod. 336, 130347.
Mannina, G., Capodici, M., Cosenza, A., Di Trapani, D., van Loosdrecht, M.C.M., 2017. Nitrous oxide emission in a University of Cape Town membrane bioreactor: The effect of carbon to nitrogen ratio. J. Clean. Prod. 149, 180–190.
Mannina, G., Rebouças, T.F., Cosenza, A., Chandran, K., 2019. A plant-wide wastewater treatment plant model for carbon and energy footprint: model application and scenario analysis. J. Clean. Prod. 217, 244–256.
Masmoudi, S., Elghazel, H., Taieb, D., Yazar, O., Kallel, A., 2020. A machine-learning framework for predicting multiple air pollutants' concentrations via multi-target regression and feature selection. Sci. Total Environ. 715, 136991.
Massara, T.M., Solís, B., Guisasola, A., Katsou, E., Baeza, J.A., 2018. Development of an ASM2d-N2O model to describe nitrous oxide emissions in municipal WWTPs under dynamic conditions. Chem. Eng. J. 335, 185–196.
Mehrani, M.-J., Lu, X., Kowal, P., Sobotka, D., Mąkinia, J., 2021. Incorporation of the complete ammonia oxidation (comammox) process for modeling nitrification in suspended growth wastewater treatment systems. J. Environ. Manag. 297, 113223.
Natekin, A., Knoll, A., 2013. Gradient boosting machines, a tutorial. Front. Neurorobotics 7.
Ni, B.-J., Pan, Y., van den Akker, B., Ye, L., Yuan, Z., 2015. Full-scale modeling explaining large spatial variations of nitrous oxide fluxes in a step-feed plug-flow wastewater treatment reactor. Environ. Sci. Technol. 49, 9176–9184.
Osarogiagbon, A.U., Khan, F., Venkatesan, R., Gillard, P., 2021. Review and analysis of supervised machine learning algorithms for hazardous events in drilling operations. Process Saf. Environ. Prot. 147, 367–384.
Park, J., Forman, B.A., Lievens, H., 2021. Prediction of active microwave backscatter over snow-covered terrain across western colorado using a land surface model and support vector machine regression. IEEE J. Sel. Top. Appl. Earth Obs. Remote Sens. 14, 2403–2417.
Peng, L., Ni, B.-J., Erler, D., Ye, L., Yuan, Z., 2014. The effect of dissolved oxygen on N2O production by ammonia-oxidizing bacteria in an enriched nitrifying sludge. Water Res. 66, 12–21.
Ranjan, K.G., Prusty, B.R., Jena, D., 2021. Review of preprocessing methods for univariate volatile time-series in power system applications. Electr. Power Syst. Res. 191, 106885.
Ryan, M., Müller, C., Di, H.J., Cameron, K.C., 2004. The use of artificial neural networks (ANNs) to simulate N2O emissions from a temperate grassland ecosystem. Ecol. Model. 175, 189–194.
Shaahmadi, F., Anbaz, M.A., Bazooyar, B., 2017. Analysis of intelligent models in prediction nitrous oxide (N2O) solubility in ionic liquids (ILs). J. Mol. Liq. 246, 48–57.
Smola, A.J., Schölkopf, B., 2004. A tutorial on support vector regression. Stat. Comput. 14, 199–222.
Song, M.J., Choi, S., Bae, W.B., Lee, J., Han, H., Kim, D.D., Kwon, M., Myung, J., Kim, Y.M., Yoon, S., 2020. Identification of primary effecters of N2O emissions from full-scale biological nitrogen removal systems using random forest approach. Water Res. 184, 116144.
Solís, B., Guisasola, A., Pijuan, M., Corominas, L., Baeza, J.A., 2022. Systematic calibration of N2O emissions from a full-scale WWTP including a tracer test and a global sensitivity approach. Chem. Eng. J. 435, 134733.
Steinwart, I., Christmann, A., 2008. Support Vector Machines. Springer, New York.
Su, Q., Domingo-Félez, C., Jensen, M.M., Smets, B.F., 2019. Abiotic Nitrous Oxide (N2O) Production Is Strongly pH Dependent, but Contributes Little to Overall N2O Emissions in Biological Nitrogen Removal Systems. Environ. Sci. Technol. 53, 3508–3516.
Sun, S., Bao, Z., Li, R., Sun, D., Geng, H., Huang, X., Lin, J., Zhang, P., Ma, R., Fang, L., Zhang, X., Zhao, X., 2017. Reduction and prediction of N2O emission from an Anoxic/Oxic wastewater treatment plant upon DO control and model simulation. Bioresour. Technol. 244, 800–809.
Vasilaki, V., Conca, V., Frison, N., Eusebi, A.L., Fatone, F., Katsou, E., 2020a. A knowledge discovery framework to predict the N2O emissions in the wastewater sector. Water Res. 178, 115799.
Vasilaki, V., Danishvar, S., Mousavi, A., Katsou, E., 2020b. Data-driven versus conventional N2O EF quantification methods in wastewater; how can we quantify reliable annual EFs? Comput. Chem. Eng. 141, 106997.
Vasilaki, V., Massara, T.M., Stanchev, P., Fatone, F., Katsou, E., 2019. A decade of nitrous oxide (N2O) monitoring in full-scale wastewater treatment processes: A critical review. Water Res. 161, 392–412.
Vapnik, V., Guyon, I., Hastie, T., 1995. Support vector machines. Mach. Learn 20, 273–297.
Verma, A., Wei, X., Kusiak, A., 2013. Predicting the total suspended solids in wastewater: A data-mining approach. Eng. Appl. Artif. Intell. 26, 1366–1372.
Wang, Q., Ni, B.-J., Lemaire, R., Hao, X., Yuan, Z., 2016. Modeling of Nitrous Oxide Production from Nitritation Reactors Treating Real Anaerobic Digestion Liquor. Sci. Rep. 6, 25336.
Wisniewski, K., Kowalski, M., Makinia, J., 2018. Modeling nitrous oxide production by a denitrifying-enhanced biologically phosphorus removing (EBPR) activated sludge in the presence of different carbon sources and electron acceptors. Water Res. 142, 55–64.
Xenochristou, M., Hutton, C., Hofman, J., Kapelan, Z., 2020. Water Demand Forecasting Accuracy and Influencing Factors at Different Spatial Scales Using a Gradient Boosting Machine. Water Resour. Res. 56 e2019WR026304.
Yegnanarayana, B., 2009. Artificial Neural Networks. PHI Learning Pvt. Ltd.
Zaborowska, E., Lu, X., Makinia, J., 2019. Strategies for mitigating nitrous oxide production and decreasing the carbon footprint of a full-scale combined nitrogen and phosphorus removal activated sludge system. Water Res. 162, 53–63.

Paper IV

M-J Mehrani, M Azari, B Teichgraber, P Jagemann, J Schoth, M Denecke, J Mąkinia. 2022. Performance evaluation and model-based optimization of the mainstream deammonification in an integrated fixed-film activated sludge reactor. **Bioresource Technology,** 351, 126942.
https://doi.org/10.1016/j.biortech.2022.126942

Bioresource Technology 351 (2022) 126942

Contents lists available at ScienceDirect

Bioresource Technology

journal homepage: www.elsevier.com/locate/biortech

Performance evaluation and model-based optimization of the mainstream deammonification in an integrated fixed-film activated sludge reactor

Mohamad-Javad Mehrani [a,b], Mohammad Azari [c,*], Burkhard Teichgräber [d], Peter Jagemann [d], Jens Schoth [d], Martin Denecke [a], Jacek Mąkinia [b]

[a] Department of Urban Water- and Waste Management, University of Duisburg-Essen, Universitätsstraße 15, 45141, Essen, Germany
[b] Faculty of Civil and Environmental Engineering, Gdansk University of Technology, Ul. Narutowicza 11/12, 80-233, Gdansk, Poland
[c] Department of Aquatic Environmental Engineering, Institute for Water and River Basin Management, Karlsruhe Institute of Technology (KIT), Gotthard-Franz-Str. 3, Karlsruhe 76131, Germany
[d] EMSCHERGENOSSENSCHAFT and LIPPEVERBAND, Kronprinzenstrasse 24, 45128, Essen, Germany

HIGHLIGHTS

- Mainstream pilot-scale deammonification was simulated under seasonal temperature.
- Intermittent aeration strategy plays an important role in stable NOB suppression.
- The aeration was set to the optimized values (DO = 0.2 mgO_2/L, on/off ratio = 0.05).
- The nitrogen removal efficiency can enhance from 30% to > 50% (at optimized values).
- The nitrogen removal rate increased up to 25 gN/m^3d by optimized aeration values.

GRAPHICAL ABSTRACT

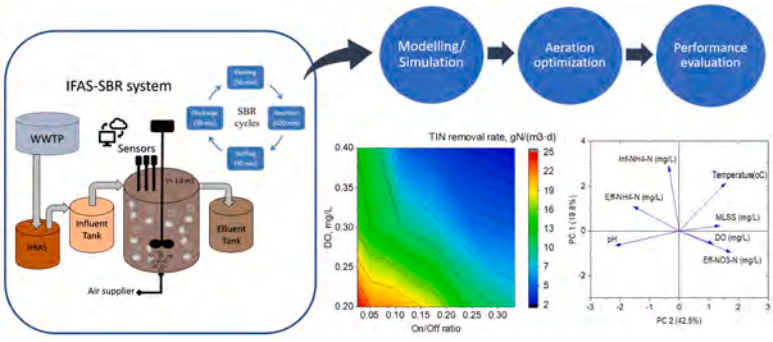

ARTICLE INFO

Keywords:
Optimization
Mainstream deammonification
Anammox
IFAS
Simulation

ABSTRACT

This study aimed to model and optimize mainstream deammonification in an integrated fixed-film activated sludge (IFAS) pilot plant under natural seasonal temperature variations. The effect of gradually decreasing temperature on the performance was evaluated during a winter season and a transition period to summer conditions, and the correlation of the performance parameters was investigated using principal component analysis (PCA). The optimization of intermittent aeration in the long-term (30 days) dynamic conditions with on/off ratio and dissolved oxygen (DO) set-point control was used to maximize the N-removal rate (NRR) and N-removal efficiency (NRE). Optimization results (DO set-point of 0.2–0.25 mgO_2/L, and on/off ratio of 0.05)

Abbreviations: IFAS, Integrated fixed-film activated sludge; PCA, Principal component analysis; NRR, N-removal rate; NRE, N-removal efficiency; Anammox, Anaerobic ammonium oxidation; WWTP, Wastewater treatment plant; MBBR, Moving bed biofilm reactor; SRT, Solid retention time; C/N, carbon to nitrogen ratio; DOE, Design of experiment; CFD, Computational fluid dynamic; SBR, Sequencing batch reactor; PN, Partial nitrification; HET, Heterotrophic denitrifiers; HRAS, High-rate activated sludge; IBC, Intermediate bulk container; TSS, Total suspended solids; TN, Total nitrogen; ML(V)SS, Mixed liquor (volatile) suspended solids; TIN, Total inorganic nitrogen; ASM2d, Activated Sludge Model No. 2d; SA, Sensitivity Analysis; ADM1, Anaerobic Digestion Model No. 1; FNA, Free nitrous acid; MAE, Mean absolute error.

* Corresponding author.
E-mail address: mohammad.azari@kit.edu (M. Azari).

https://doi.org/10.1016/j.biortech.2022.126942
Received 10 January 2022; Received in revised form 25 February 2022; Accepted 1 March 2022
Available online 4 March 2022

increased the NRE and NRR of total inorganic N (daily average) from 30% to > 50% and 15 gN/m^3d to 25 gN/m^3d, respectively. This novel long-term optimization strategy is a powerful tool for enhancing the efficiency in mainstream deammonification.

1. Introduction

Deammonification, also termed partial nitrification/anaerobic ammonium oxidation (anammox) or PN/A, is a sustainable and energy-efficient nitrogen removal process in wastewater treatment plants (WWTPs) (Gu et al., 2020). This process has widely been developed for sidestream treatment, such as anaerobic sludge digester liquors, but recently it has also been examined for treating wastewater in the mainstream (Izadi et al., 2021). However, the mainstream applications are facing numerous technical challenges, including stable PN and nitrite-oxidizing bacteria (NOB) suppression, sufficient anammox bacteria retention, a high carbon to nitrogen ratio (C/N), and influence of low temperature (Han et al., 2016; Gu et al., 2020).

The integrated fixed-film activated sludge (IFAS) process by combining flocs and biofilm can upgrade existing floccular activated sludge systems. The IFAS process produces less sludge, uses less energy, and brings a lower carbon footprint (Waqas et al., 2020). Moreover, IFAS is more robust than moving bed biofilm reactors (MBBRs) to achieve a more energy-efficient N-removal (Lemaire and Christensson, 2021; Malovanyy et al., 2015).

The key to efficient WWTP management is process optimization, which may be accomplished by searching for the best process conditions, such as aeration strategy, solid retention time (SRT), influent concentrations, and flow rates. Multi-objective optimization is a section of multiple criteria decision-making that assesses more than one objective function at the same time on a target (Newhart et al., 2019; Qiao & Zhang, 2018). NOB suppression is one of the most crucial challenges in deammonification systems (Mehrani et al., 2020; Gao & Xiang, 2021). An intermittent aeration strategy was reported as an effective solution for NOB diminishing (Miao et al., 2016; Van Hulle et al., 2010). Therefore, optimized intermittent aeration (switching between aerobic and anoxic phases) can enhance NOB suppression while reducing energy consumption and decreasing N_2O production (Al-Hazmi et al., 2021). Leix et al., (2017) optimized the deammonification process based on an aeration strategy, pH, and feeding parameters to enhance performance using a design of experiment (DOE) method. In other studies, the optimization of aeration parameters in IFAS was carried out using a combined experimental and computational fluid dynamic (CFD) approach (Xu et al., 2020; Zhou et al., 2019). In addition, based on model predictions, Al-Hazmi et al., (2021) optimized the aeration strategy (on/off cycles, frequency, and ratio) of a lab-scale granular deammonification sequencing batch reactor (SBR).

Nevertheless, there is still limited information for optimizing intermittent aeration and correlating related operational parameters in deammonification systems to suppress the NOB and to reach a higher nitrogen removal efficiency (NRE) and nitrogen removal rate (NRR) (Xu et al., 2020).

This study aims to model a stable long-term deammonification process for mainstream wastewater treatment (pilot-scale) to evaluate the following issues: i) estimation of the kinetic parameters for deammonification under dynamic temperature and C/N; ii) principal component analysis (PCA) to evaluate the correlation of the operational parameters on the system efficiency, and iii) model-based multi-objective optimization of the intermittent aeration strategy (DO concentration and on/off time) for maximizing the NRR and NRE. Additionally, most of the past studies on aeration strategy optimization were carried out in short-term operational conditions (batch tests or one cycle of a long-term experiment). On the contrary and as an initiative, this study investigates optimal aeration settings under the long-term (30 days) dynamic conditions.

2. Materials and methods

2.1. Experimental data for modeling purpose

2.1.1. Reactor setup

A one-stage pilot deammonification system (working volume of 1 m^3) was employed using an integrated fixed activated sludge (IFAS) process in a SBR. The reactor was installed at the WWTP Emschermündung near Dinslaken, Germany (EGLV) to treat real municipal wastewater. Biofilm carriers (AnoxKaldnes™ K3, Veolia) with a filling ratio of 20 % were used to provide conditions for anammox growth and accumulation. The reactor was previously seeded with anammox-rich sludge from a stably operating full-scale sidestream treatment reactor at Kamen-Körnebach WWTP near Dortmund, Germany (EGLV).

The reactor was initially operated with almost 12-hour batch cycles consisting of filling, reaction, sedimentation, and discharge phases. 120 L of wastewater were fed for 30 min into the reactor in the first phase, and the reaction phase lasted 620 min in total. To provide an intermittent aeration regime, the stage was divided into 20-minute on/off cycles. The aeration was on for 4 min and was off for 16 min as initial parameters, based on a former lab-scale study (Azari et al., 2020). During the aeration switched on phase, the DO concentration was initially set to 0.4 mg O_2/L (subject to the change as a control strategy parameter). To achieve a proper sludge settling and avoid biomass loss in the effluent, the sedimentation phase had been optimized at 30 min with no aeration or mixing. During the discharge phase (30 min), 120 L of the reactor content was discharged into the effluent container. Regular sampling (at least three times a week) was carried out in the influent tank, inside of the reactors, and in the effluent tank. The schematic layout of the SBR cycles can be found in supplementary materials (see supplementary material). To maintain a steady operation of deammonification, avoiding high organic loads and limiting the activity of heterotrophic denitrifiers (HET) are necessary (Hausherr et al., 2021). Hence, a carbon removal step, using a high-rate activated sludge (HRAS) reactor, was applied before the deammonification reactor, which can also capture the carbon for further energy recovery (Guven et al., 2019; Jimenez et al., 2015). The system also consisted of a 1 m^3 influent intermediate bulk container (IBC), into which the HRAS effluent was discharged and kept until it was pumped into the deammonification reactor.

Online sensors for DO, NO_3-N, NH_4-N, temperature, pH, and total suspended solids (TSS) (WTW, Xylem Analytics Germany Sales GmbH & Co) were installed on the top of the SBR, and the measurement outputs were sent to the central control unit via an SC1000 controller.

2.1.2. Analytical methods and calculations

Concentrations of ammonium (NH_4-N), nitrate (NO_3-N), nitrite (NO_2– N), total nitrogen (TN), and chemical oxygen demand (COD) were determined photometrically with DR3800 and corresponding cuvette tests (Hach-Lange, Germany). All samples were filtered through a 0.45 μm fiber filter before the analysis. The gravimetric technique was also used for total mixed liquor suspended solids measurement (MLSS) and its volatile fraction (MLVSS) to estimate the fraction of biomass in flocs and biofilm. MLSS concentration of flocs was also used for calibration of the TSS sensor for online monitoring (approximately in the range 3.0–4.0 g/L) during the experiment.

The calculated total inorganic nitrogen (TIN) comprised the sum of NH_4-N, NO_2– N, and NO_3-N. The process performance was assessed in terms of the NRE and NRR. The NRE was measured as the percentage of nitrogen removed in terms of both NH_4-N and TIN (Eq. (1)), and the NRR was determined for TIN (Eq. (2)).

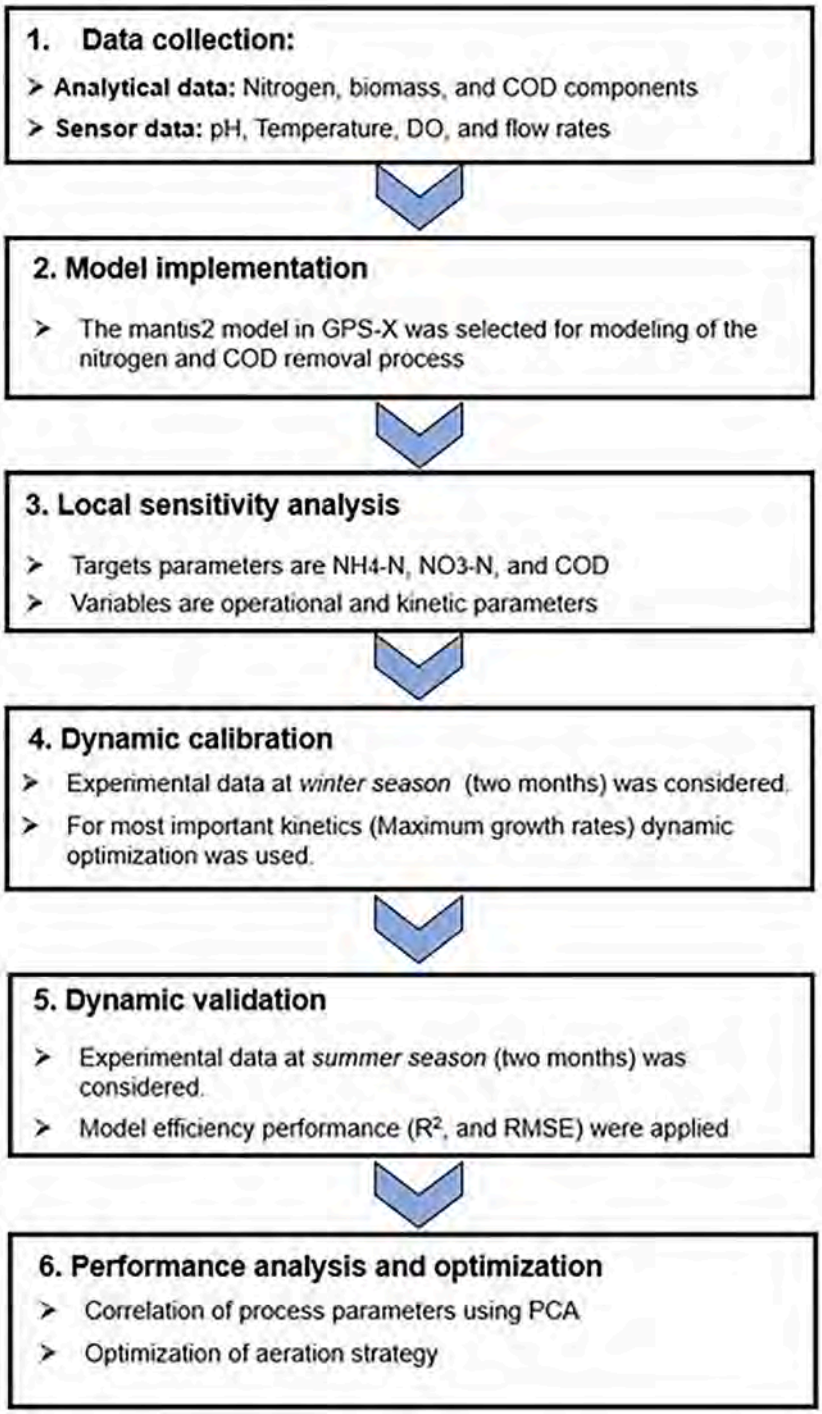

Fig. 1. Modelling, performance analysis, and optimization of the deammonification procedure.

$$NRE = \frac{N_i - N_e}{N_i} \times 100 \quad (1)$$

$$NRR = \frac{Q \times (N_i - N_e)}{V} \quad (2)$$

where N_i is nitrogen concentration in the influent (g/m^3), N_e is nitrogen concentration in the effluent (g/m^3), Q is a flow rate (L/d), and V is a volume of the system (L). The NRE and NRR are calculated as % and g N/m^3d, respectively.

2.2. Biokinetic model and simulation platform

The GPS-X (Hydromantis, Canada) is an open simulation and analysis platform for different wastewater treatment systems compatible with a sensitivity analysis (SA) (section 2.4.1) and optimization based on the Nelder-Mead simplex method (section 2.4.2) (Chang, 2012). The Mantis2 model, implemented in GPS-X 8.0, was used for modeling the studied pilot-scale deammonification system. The core model structure is based on the Activated Sludge Model No. 2d (ASM2d) (Henze et al., 1999) and Anaerobic Digestion Model No. 1 (ADM1) (Batstone et al., 2002). The model was extended to incorporate two-step nitrification and anammox processes (Abou-Elela et al., 2016; Sean et al., 2020). This

Table 1
Initial values of the kinetic parameters.

Bacteria	Kinetic parameter	Unit	Initial values
AOB	μ_{AOB}	1/d	1.01
	$K_{NH4,AOB}$	mg N/L	0.675
	$K_{O,AOB}$	mg O_2/L	0.30
	b_{AOB}	1/d	0.15
NOB	μ_{NOB}	1/d	0.31
	$K_{NO2,NOB}$	mg N/L	0.057
	$K_{O,NOB}$	mg O_2/L	0.2
	b_{NOB}	1/d	0.05
AMX	μ_{AMX}	1/d	0.03
	$K_{NH4,AMX}$	mg N/L	0.07
	$K_{NO2,AMX}$	mg N/L	0.05
	$K_{O,AMX}$	mg O_2/L	0.01
	b_{AMX}	1/d	0.003
HET	μ_{HET}	1/d	2.0
	$K_{NH4,HET}$	mg N/L	0.01
	$K_{NO3,HET}$	mg N/L	0.2
	$K_{NO2,HET}$	mg N/L	0.2
	$K_{O,HET}$	mg O_2/L	0.2
	b_{HET}	1/d	0.6

AOB: ammonia oxidation bacteria, NOB: nitrite oxidation bacteria, AMX: Anammox, HET: Heterotroph bacteria, K: half saturation coefficient, μ: maximum specific growth rate, b: specific decay rate,.

model has been used to simulate and optimize different wastewater treatment systems, especially deammonification systems (Pekyavas et al., 2020; Puchongkawarin et al., 2015; Sean et al., 2020). The IFAS-SBR reactor contains two different technologies of IFAS and SBR. However, GPS-X has IFAS and SBR reactors separately and cannot run them in a single system. Hence, this modeling study was carried out by applying an advanced SBR and assuming the apparent kinetics for the biochemical processes (Baeten et al., 2019).

2.3. Initial conditions

For dynamic calibration and validation of the models, the initial biomass concentrations for MLSS, MLVSS, and other microorganisms are needed (Yu et al., 2020). In this study, the microbiological tool was used to estimate the initial values of MLSS, MLVSS as well as ammonia-oxidizing bacteria (AOB), NOB, anammox bacteria (AMX), and HET initial population (relative abundance) using 16S rRNA gene high-throughput amplicon sequencing, based on previous assays (Azari et al., 2021). An example of 16S rRNA gene high-throughput amplicon sequencing results in the same period of the modelling study can be found in the supplementary material (see supplementary material). Also, Table 1 shows the initial kinetic parameters selected for sensitivity analysis and calibration procedure.

2.4. Simulation, validation, and optimization procedures

Calibration and validation are crucial steps in the modeling process that examine the model prediction capacity and reliability under various operating conditions. In this study, the mantis2 model (section 2.2) was first calibrated based on the data from a winter period (60 days) and then validated with another 60 days dataset from a summer period of the IFAS-SBR reactor. The calibration procedure was started with SA to find out the most sensitive parameters to optimize the kinetic parameters. Then, based on SA results, optimization of kinetic parameters based on experimental observation was done, and then, model performance with different performance criteria (R^2, RMSE, and MAE) was checked. Moreover, validation of the calibrated model with different periods of experimental observation were done to show the validity of the model. Fig. 1 shows the whole simulation/optimization procedure, and the most critical steps are discussed in the following subsections.

2.4.1. Sensitivity analysis

Sensitivity analysis is a method for determining the influence of one or more uncertain variables on some important results or quantities in mathematical models (Hong et al., 2019). In this study, 19 kinetic parameters targeting the N components (NH_4-N, NO_3-N) and COD concentrations were subjected to SA under the phase dynamic mode in GPS-X. Table 1 shows the initial values for the kinetic parameters under investigation. The uncertainty of 20% (±10% of the modified value) was assigned to each evaluated parameter (Lu et al., 2018). The ratio of the percentage change ($\Delta y_{i,j}/y_i$) in the *i-th* output variable (y_i) to the percentage change ($\Delta x_j/x_j$) in the *j-th* model parameter (x_j) was defined as the normalized sensitivity coefficient ($S_{i,j}$):.

$$S_{i,j} = \left|\frac{\Delta y_{i,j}}{y_i}.\frac{x_j}{\Delta x_j}\right| \quad (3)$$

The following classification determines the impact of each modified parameter on the specific model result: i) low influential ($S_{i,j} < 0.25$), ii) influential ($0.25 \le S_{i,j} < 1.0$), iii) high influential ($1.0 \le S_{i,j} < 2.0$), and iv) extremely influential ($S_{i,j} \ge 2.0$).

2.4.2. Selection of the kinetic parameters based on optimization in GPS-X

Parameter Optimizer uses the Nelder-Mead simplex method with different objective functions to search for the parameter values with the minimum variance between measured data and model predictions (Chang, 2012). The optimization method was repeated until all sizes of the measured parameters decreased below the parameter tolerance (Lu et al., 2018).

Based on the SA results, high and extremely sensitive ($S_{i,j} \ge 1.0$) kinetic parameters were selected for estimation using the GPS-X optimization utility, and the least influential parameters ($S_{i,j} < 1.5$), were determined based on the literature in Table 1 (Mehrani et al., 2021; Yu et al., 2020; Al-Hazmi et al. 2021).

2.4.3. Comparison of model efficiencies

Various evaluation measures can be used to assess the model efficiency (goodness-of-fit), including the coefficient of determination (R^2), root mean square error (RMSE), and mean absolute error (MAE) which are frequently used. The RMSE measures the overall error in the same unit as the response variable, while the MAE assesses the quality of a predicted fluctuation and unbiasedness (Eq. 4–8). The R^2 measures the goodness-of-fit of a model based on experimental observations with a linear relationship. A model with accurate prediction has higher R^2 values (up to 1.0) (Hauduc et al., 2015).

$$SS_{tot} = \sum_i (y_i - \bar{y})^2$$

$$SS_{res} = \sum_i (y_i - f_i)^2$$

$$R^2 = 1 - \frac{SS_{res}}{SS_{tot}}$$

$$MAE = \frac{1}{n}\sum_i (y_i - f_i)$$

$$RMSE = \sqrt{\frac{SS_{res}}{n}} \quad (8)$$

where n is the total number of records, and i = 1, 2,..n is the number of observations. Also, SS_{res} is a residual sum of squares, and SS_{tot} is a total sum of squares of residuals, considering to y_i as a predicted value ,f_i as an observed value, and $\bar{y}$ as an average value.

2.4.4. Aeration optimization strategy

Optimization of the aeration strategy to minimize TIN concentration was carried out by defining several scenarios for DO concentrations

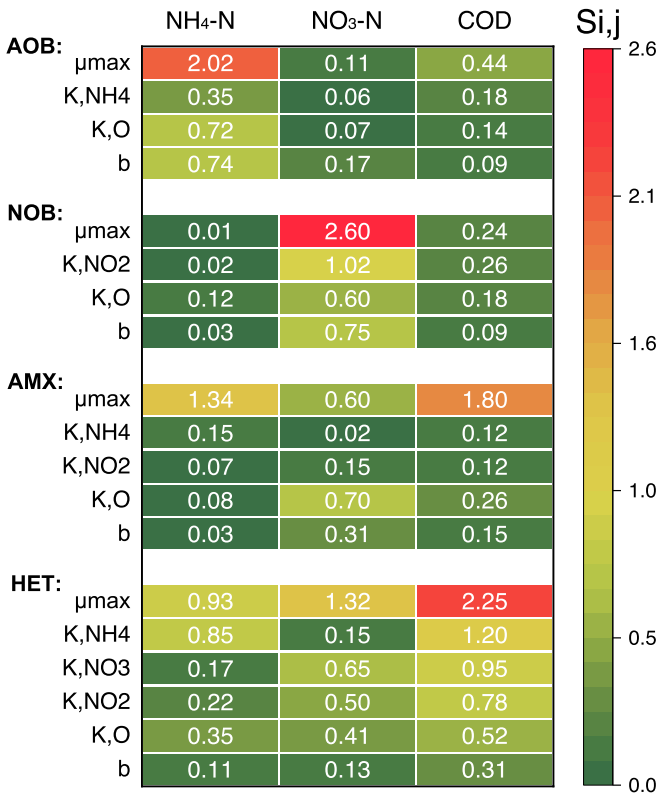

Fig. 2. Sensitivity analysis of the N components and COD by different kinetic parameters.

(0.2–0.4 mg O_2/L) and on/off ratio (0.02–0.3) in the intermittent aeration. The sum of the aeration and non-aeration periods was fixed on 20 min in the 12-hour reaction cycle of SBR, e.g., the on/off ratio of 0.05 refers to 1 min on and 19 min off periods (optimized values). Optimization was carried out using the GSP-X optimizer utility in the long-term during the calibrated period. The results were evaluated in terms of maximizing daily averages of NRR and NRE (calculated based on TIN) as the optimization target variable. All 18 defined scenarios for the analysis were presented (see supplementary material).

2.4.5. Correlation of process parameters using PCA

PCA is a useful analytical tool to understand the link between process parameters and reactor performance and classify data based on their stated variables in a variety of domains. PCA creates a new set of variables, and the old variables are transformed orthogonally. Different environmental effects are represented by arrows, with the length of the arrow indicating the degree of the factor. A positive correlation between two corresponding environmental elements is indicated by an acute angle between two arrows, and a negative correlation by an obtuse angle (Chen et al., 2021).

The fundamental goal of this multivariate method is to highlight those factors that improve the relative description of other objects, create specific groupings based on similarities, and classify variables (Rezaali et al., 2020). To reduce redundancy, the result contains two or three principal components (PC), which are a linear mixture of the original data plus orthogonal eigenvectors (Ringnér, 2008), to compare statistical relationships between operational parameters (MLSS, temperature, pH and DO), influent/effluent NH_4-N, and effluent NO_3-N. The two-dimensional (2D) PCA was created by OriginPro 2021 (OriginLab Corp) with a statistically significant level ($p < 0.05$).

Table 2
List of the kinetic parameters adjusted during calibration.

Bacteria	parameter	Unit	Initial value (Table 1)	Adjusted value
AOB	μ_{AOB}	1/d	1.01	0.5
	$K_{O,AOB}$	mg O_2/L	0.30	0.35
NOB	μ_{NOB}	1/d	0.31	0.3
	$K_{O,NOB}$	mg O_2/L	0.2	0.23
HET	μ_{HET}	1/d	2.0	1.0
AMX	μ_{AMX}	1/d	0.03	0.025

AOB: Ammonia oxidation bacteria, NOB: Nitrite oxidation bacteria, HET: Heterotroph bacteria, AMX: Anammox, K: half-saturation coefficient, μ: Maximum specific growth rate, and b: Decay rate.

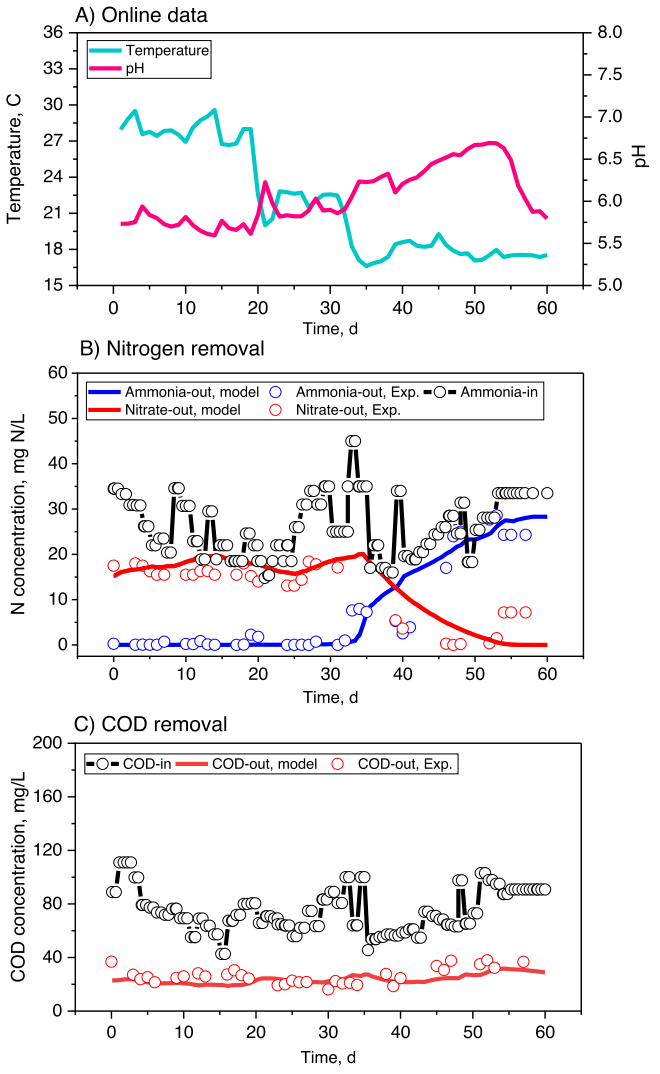

Fig. 3. Calibration results during the winter season (with temperature adaptation in the first 20 days of calibration period): A) online variables, B) concentrations of N components, and C) COD concentrations.

3. Results and discussion

3.1. Sensitivity analysis

Fig. 2 shows the sensitivity coefficients for all 19 kinetic parameters related to AOB, NOB, anammox (AMX), and heterotroph bacteria (HET)

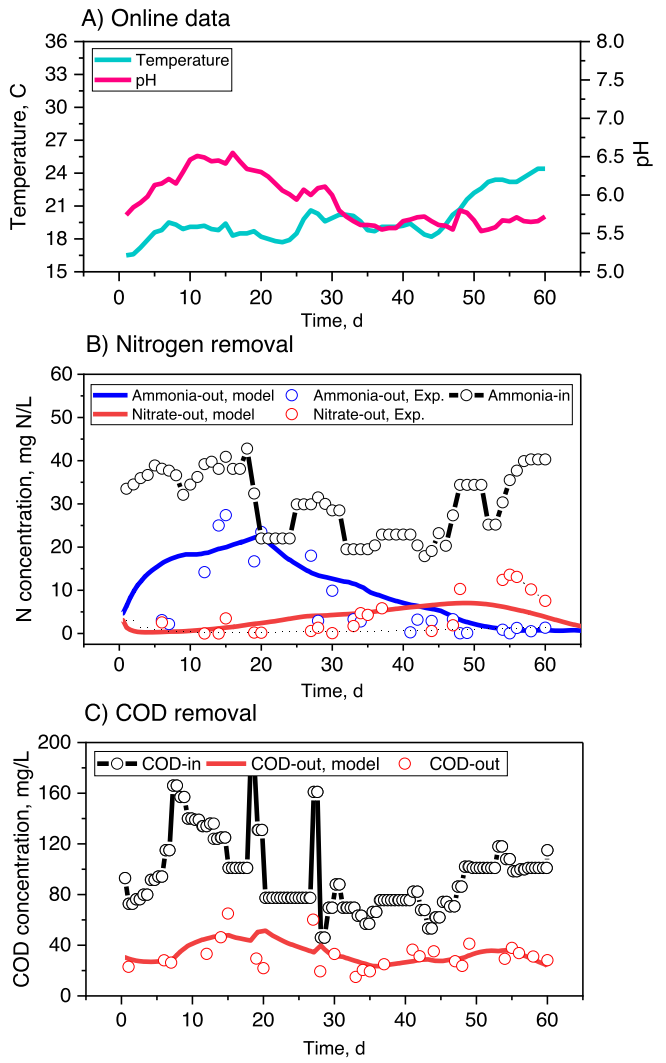

Fig. 4. Validation results during the summer season (without temperature adaptation), A) online variables, B) concentrations of N components, and C) COD concentrations.

concerning three state variables in the effluent tank (NH_4-N, NO_3-N, and COD). The μ of AOB, NOB, and HET were extremely influential ($S_{i,j} \geq 2$) for NH_4-N, NO_3-N, and COD, respectively. Next, high influential parameters ($1.0 \leq S_{i,j} < 2.0$) comprised $K_{NO2\text{-}N}$ of NOB for NO_3-N, μ_{AMX} for NH_4-N and COD, μ_{HET} for NO_3-N, and $K_{NH4\text{-}N}$ of HET for COD. The μ_{AMX} was the most influential kinetic parameter concerning the behavior of NH_4-N, with the $S_{i,j}$ ranging from 1.3 to 1.8. On the other hand, the decay rates of AMX and HET were among the least influential parameters.

3.2. Model calibration (parameter estimation)

Overall, μ of all the bacterial groups and *Ko* of AOB and NOB were among the highly influential parameters (Si,j > 1.0) and were thus selected for estimation in the calibration procedure, while the remaining parameters were kept constant based on the results of previous studies (Yu et al., 2020; Al-Hazmi et al., 2021). Table 2 presents the adjusted values of the kinetic parameters.

Table 3
A summary of the model efficiency measures during the calibration and validation phases.

State variables	Calibration phase			Validation phase		
	R^2	RMSE	MAE	R^2	RMSE	MAE
NH_4-N	0.85	2.29	2.75	0.79	3.67	4.02
NO_3-N	0.78	3.47	3.61	0.74	4.10	4.81
COD	0.88	2.36	2.95	0.76	3.72	3.45

The experimental data and calibrated model predictions for the most important variables in the system (NH_4-N, NO_3-N, and COD) are shown in Fig. 3. The temperature was 27–30 °C during the first 20 days, which was the adaptation period. Subsequently, the temperature was not controlled, and the reactor was kept at ambient temperature, decreasing to 16 °C (Fig. 3a). The pH value was kept in the range of 5.7–6.7 (with an average of 6.2 and a standard deviation of 2.5 mg/L) throughout the operation (Fig. 3a). Other studies also demonstrated the possibility of nitrification in low pH conditions in biofilm reactors (Tarre et al., 2007). Another study also proved that the acidic operation of a nitrifying bioreactor in the pH range of 5 – 6 can generate ppm level free nitrous acid (FNA), as an inhibitor for the suppression of NOB activity (Li et al., 2020). Besides, the inhibitory effect of FNA on anammox bacteria is not comprehensively understood. But it is shown that active anammox bacteria may sustain in various acidic aquatic environments with pH 3.9 – 6.5 (Nie et al., 2018).

The influent NH_4-N concentration during calibration was in the range of 18–45 mg/L with the average and standard deviation of 30 mg/L and 2.3 mg/L, respectively. The calibrated model simulated the effluent concentration of NH_4-N and NO_3-N very well (Fig. 3b). There was a stable operation of the system in the first 30 days for NH_4-N removal with an NH_4-N effluent concentration of < 1 mg/L. In the same period, NO_3-N production occurred with a concentration of up to 20 mg/L. The nitrifier population is subjected to substantial changes because of the reduction of μ_{AOB} and μ_{NOB} which is the function of the temperature. Due to the operational and natural conditions, the temperature decreased to ambient condition (Fig. 3b). In the same period, the negligible concentration of NH_4-N in the effluent started to increase, and consequently, NO_3-N decreased to zero. As shown in Fig. 3c, COD in the influent was always below 120 mg/L with the average and standard deviation of 80 mg/L and 2.0 mg/L. COD removal was stable (60–70%) during the entire calibration period and was not subjected to any change after dropping the temperature.

Comparing the adjusted model parameters (Table 2) implies that μ_{AOB} was reduced by approximately 50% and there was only a slight change in μ_{NOB} compared to the initial values (Table 1). The adjusted values for μ_{AOB} (0.5 1/d) and μ_{NOB} (0.3 1/d) are in accordance with the results of other studies (Park et al., 2017; Zhang et al., 2019). Neither $K_{O,AOB}$, nor $K_{O,NOB}$ was subjected to any significant change after calibration and remained in the reported range (Mehrani et. al. 2021). Moreover, μ_{HET} was reduced from its initial value of 2.0 1/d to 1.0 1/d and μ_{AMX} was modified from 0.03 to 0.025 1/d.

3.3. Model validation

For model validation, a different set of experimental data was examined (April-June). Fig. 4 shows the observed data and model predictions of NH_4-N, NO_3-N, and COD during the validation phase. The temperature during the validation period was more stable (varied averagely between 16 and 19.5 °C) up to the last 10 days of the simulation period. From day 45 of validation, the temperature increased naturally up to 24 °C during the summer conditions (June) in Germany.

During the validation period, the minimum and maximum influent NH_4-N concentrations were 18 and 44 mg/L with the average and standard deviation of 30 mg/L and 2.5 mg/L. The NH_4-N concentration in the effluent gradually reduced after day 20 of the validation and from day 40 to 60 of validation, the NH_4-N in the effluent was stable (<5 mg/L). The validated model could predict this gradual decrease and stability (Fig. 4b). The NO_3-N concentration was kept below 10 mg N/L and the model predicted it accurately. By increasing the temperature in summer, NO_3-N increased by 5 mg N/L and NH_4-N decreased to nearly zero

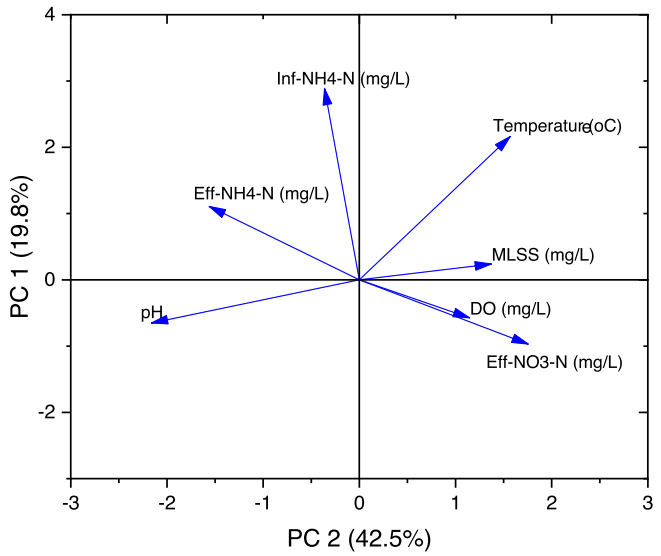

Fig. 5. Relationship between operational parameters and N components by PCA.

(Fig. 4b). Concerning the COD, the influent concentration in the first 30 days of the validation period was fluctuated up to 160 mg/L for a few days (average and standard deviation as 90 mg/L and 3.1 mg/L). The validated model could fit the measurements of the COD in the effluent as well (Fig. 4c).

3.4. Model efficiency evaluation

Numerical values for all the model efficiency measures (R^2, RMSE, MAE) are listed in Table 3. The model appears to have a high goodness-of-fit ($R^2 > 0.8$) in the calibration phase for all the evaluated variables (NH_4-N, NO_3-N, and COD). Moreover, a reasonable goodness-of-fit ($R^2 > 0.7$) was achieved for all the variables in the validation phase, revealing the accurate performance of the model.

3.5. Correlation of process parameters by PCA

PCA was employed as a useful analytical method to explore the link between process parameters. PC1 axis with 42.5% variance is more significant criterion rather than the PC2 axis (19.8%) for comparing various parameters correlation. The arrows reflect several environmental factors, while the length of the arrow is representing the degree of the element (Fig. 5). The effluent NO_3-N was closely correlated with the DO value, showing the importance of the aeration strategy for efficient NOB suppression. MLSS showed a positive correlation with NO_3-N, while a direct negative correlation between NO_3-N and NH_4-N in the effluent can be seen. Both pH and temperature were less correlated with the effluent NO_3-N.

3.6. Optimization of the aeration strategy

Fig. 6 shows the optimization of the aeration strategy including the DO values (0.2 to 0.4 mg/L) and on/off ratio (0.05–0.3) considering on daily average of NRR and NRE, NH4-N, and COD removal efficiency. Overall, the optimum values for DO and on/off ratio were obtained 0.2–0.25 mg O_2/L and 0.05 (Aeration pump is 1.0 min on per each the

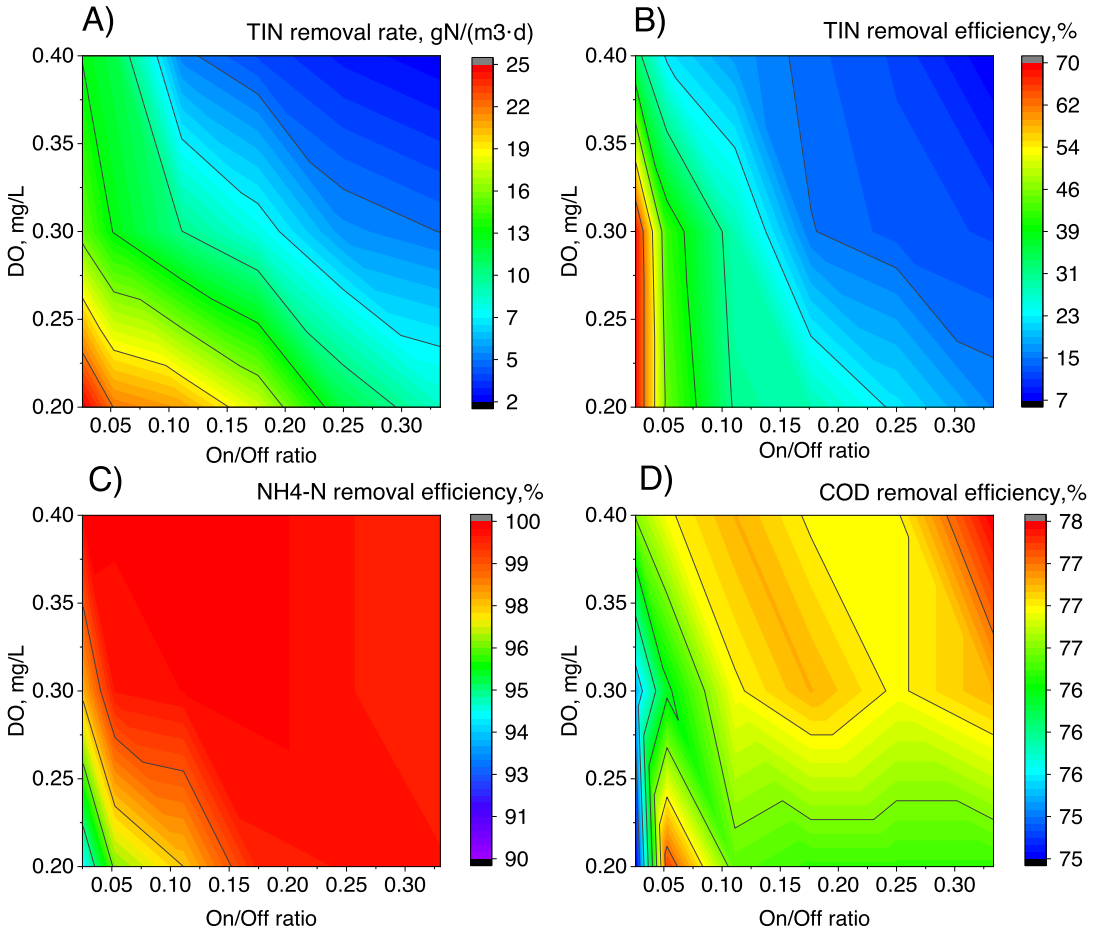

Fig. 6. Optimization of the aeration strategy, A) NRR for TIN, B) NRE for TIN, C) NRE for NH_4-N, and D) COD removal efficiency (all results as the daily average).

Table 4
Summary of different aeration strategy optimization techniques and results in different N removal systems and the comparison with this study.

Optimization method	Optimization factors	Optimization target	Process (System)	Remarks
Experimental (Lochmatter et al., 2013)	DO set-point and aeration type (intermittent or alternating high/low DO)	Maximizing the N and P removal efficiency	N-DN (SBR)	The maximum NRE was achieved using intermittent aeration rather than alternatively high/low DO. Intermittent aeration with anoxic periods and without mixing between aeration pulses was significantly better for N-removal (78.3%) with the lowest COD loading rate examined.
Data-driven (Asadi et al., 2017)	DO set point	Reducing energy consumption without affecting the effluent quality	N-DN (WWTP)	The optimization caused increasing the effluent quality such as BOD, and TSS up to 18% (even better than actual values).
RSM (Leix et al., 2017)	DO set-point (including change in anoxic and aeration modes) and stripping effects.	Maximizing the NRR and minimizing N_2O emissions	PN/A (SBR)	The most appropriate condition was intermittent aeration with equally distributed aerated (5.5 min) and unaerated phases (6.5 min) at a moderate aeration intensity (44 L/h).
CFD (Zhou et al., 2019)	DO set-point and aeration intensity	Maximizing the TN removal and reactor stability	PN/A (bioreactor)	An optimized low DO of 0.2 mg O_2/L and high aeration intensity (0.17 cm/s) resulted in denitrifying bacteria growth and high TN removal (82.1%) and a persistent biofilm structure.
Experimental (Yang et al., 2020)	DO set-point	Efficient N removal, and stable AOB and anammox activity	PN/A (IFAS)	The optimized DO was in a range of 0.24–0.28 mg O_2/L, caused the stable AOB activity and enhanced ammonia and TN removal. When the DO was in the range of 0.28–0.35 mg O_2/L, the anammox activity was inhibited and a considerable amount of free nitrous acid (FNA) was accumulated (21.70 μg/L).
Experimental (Xu et al, 2020)	DO set-point and anoxic/aerobic ratio	Maximizing the NRR, NRE, and NOB suppression	PN/A (IFAS)	For NOB suppression, the DO value was more significant than the anoxic period. By optimizing the intermittent aeration (low DO of 0.5 mg O_2/L and anoxic time of 20 min), the NRR was enhanced by 40%, a steady and high NRE (80–89%) was achieved, and NOB was more inhibited with a low DO level (0.5 mg O_2/L), rather than a high DO of 1.5–1.8 mg O_2/L.
Mechanistic model (Al-Hazmi et al., 2021)	DO set-point, on/off frequently, and on/off ratio	Maximizing the AUR, minimizing the NPR and N2O emission	PN/A (SBR)	High AUR to low NPR values (NPR/AUR = 0.07–0.08) and limited N_2O emissions ($E_{N2O} < 2\%$) were achieved at the optimized aeration parameters (DO set-point = 0.7 mg O_2/L, on/off ratio of 2, and on/off frequency of 6–7 h^{-1}).
Mechanistic model (long-term optimization (this study)	DO set-point and on/off ratio	Maximizing the NRR and NRE for TIN and NOB suppression	PN/A (IFAS-SBR)	Aeration optimization was done in a long-term 30 days of the operation. The optimized values of DO (0.2–0.25 mg O_2/L), and on/off ratio of 0.05 (1 min on and 19 min off) could enhance the daily average values from 30% to > 50% (NRE), and from 15 g N/m^3.d to ~ 25 g N/m^3.d (NRR).

PN/A: partial nitrification/anammox (deammonification), N-DN: nitrification–denitrification, NRR: N removal rate, NRE: N removal efficiency, TIN: total inorganic nitrogen, RSM: response surface methodology, CFD: computational fluid dynamics, AUR: ammonium utilization rate, NPR: nitrate production rate.

20 min cycle), respectively to achieve the highest NRR and NRE of the system. By decreasing of DO and on/off ratio (up to 0.2–0.25 mg/L and 0.05), the current levels of NRE and NRR could increase from the daily average of 30% to > 50% and from 15 g N/m^3.d to approximately 25 g N/m^3d, respectively (Fig. 6a,b). However, the optimization did not have a significant individual effect on NH_4-N and COD removal efficiently (Fig. 6c,d).

Moreover, Table 4 provided a summary of recent optimization studies in N removal systems and a comparison of them with this study. As stated, most of the past studies on aeration strategy optimization were carried out in short-term operational conditions while this study investigated optimization under the long-term period of 30 days. The DO set-point and aeration on/off times were two important optimization factors, while maximizing the NRR and NRE, stable suppression of NOB, and mitigation of N_2O production were among the most important optimization target in such studies.

Lochmatter et al., (2013) optimized an aeration strategy and reported that highest NRE can be achieved by intermittent aeration rather than DO setpoint. Nevertheless, Asadi et al., 2017 and Zhou et al., (2019) built optimize-based models on DO setpoint and aeration intensity. Furthermore, Leix et al., (2017) optimized intermittent aeration mode (stripping effect and aerated/unaerated phases) to maximize the NRR and minimize N_2O emissions using the response surface methodology (RSM).

Yang et al., (2020) noted that the optimized DO (0.24–0.28 mg O_2/L) could enhance ammonia and TN removal with the stable AOB activity in a deammonification process in an IFAS system. Xu et al., (2020) revealed that optimization of the intermittent aeration (low DO of 0.5 mg O_2/L and anoxic time of 20 min), can improve the NRR by 40% and achieved a high NRE (80–89%). Very recently, Al-Hazmi et al., (2021), optimized aeration (DO set-point, on/off frequently, and ratio) of the deammonification process in a laboratory-scale SBR. High ammonia utilization rate (AUR), low nitrite production rate (NPR), and limited N_2O emissions (N_2O emission factor < 2%) were achieved at the optimized aeration parameters (DO set-point = 0.7 mg O_2/L, aeration on/off ratio of 2, and on/off frequency of 6–7 h^{-1}). The optimized aeration value of this study (DO set-point of 0.2–0.25 mgO_2/L, and on/off ratio of 0.05) are in range within the reported range of Zhou et al., (2019), and Yang et al., (2020). This low DO value and on/off ratio not only can enhance the NRE and NRR value (up to 50%), but also can improve the reactor performance, and energy saving of the system (Hreiz et al., 2015; Wang et al., 2022).

In the end, some recent intermittent aeration strategies in successful deammonification systems were compared (see supplementary material). The DO ranges are between 0.2 and 0.5 mg O_2/L and aeration time varies between 2 and 40 min. In an intermittent aeration system, NOB inhibition was related to the DO concentration, anoxic time, and parameters, such as the type of NOB species (Bao et al., 2017). A recent study showed that a 15-minute anoxic interval suppressed NOB activity, which could be due to the high concentrations of free ammonia in the influent (Qiu et al., 2019). Besides, high nitrite accumulation could be sustained at a high DO (>1.5 mg O_2/L) under intermittent aeration (Regmi et al., 2014).

To summarize, the outcomes of this modelling and optimization study provided insights into the operational condition of mainstream deammonification systems under dynamic temperature and COD: N ratio and the effect of intermittent aeration optimization on N-removal efficiency and NOB suppression performance.

4. Conclusions

A mechanistic model for the mainstream deammonification process in temperature variations was successfully verified using real pilot-scale data. The aeration strategy optimization showed by decreasing the DO set-point and on/off ratio to 0.2 mg O_2/L and 0.05, respectively, the NRR and NRE increased up to 25 g N/m^3.d and > 50%. PCA results confirmed that the DO set-point and on/off ratio are the most crucial parameters in the suppression of NOB. Overall, the novel long-term optimization strategy of this research is a powerful tool for enhancing the efficiency and the effluent quality of the mainstream deammonification.

CRediT authorship contribution statement

Mohamad-Javad Mehrani: Conceptualization, Investigation, Methodology, Formal analysis, Visualization, Data curation, Software, Validation, Writing – original draft. **Mohammad Azari:** Conceptualization, Investigation, Methodology, Data curation, Visualization, Writing – review & editing. **Burkhard Teichgräber:** Resources, Project administration, Writing – review & editing. **Peter Jagemann:** Resources, Project administration, Funding acquisition, Writing – review & editing. **Jens Schoth:** Conceptualization, Methodology, Writing – review & editing. **Martin Denecke:** Resources, Project administration, Funding acquisition, Writing – review & editing. **Jacek Mąkinia:** Resources, Methodology, Supervision, Funding acquisition, Writing – review & editing.

Declaration of Competing Interest

The authors declare that they have no known competing financial interests or personal relationships that could have appeared to influence the work reported in this paper.

Acknowledgments

Special acknowledgements are given to (a) Integrated Development Program of Gdańsk University of Technology for the grant (POWR.03.05.00-00.Z044/17) for an internship program, (b) Landesamt für Natur, Umwelt und Verbraucherschutz Nordrhein-Westfalen for financial support of this study with the grant (Az.: 17-04.02.01-9a/2017), and (c) Emschergenossenschaft und Lippeverband (EGLV) and University of Duisburg-Essen due to the technical supports.

Appendix A. Supplementary data

Supplementary data to this article can be found online at https://doi.org/10.1016/j.biortech.2022.126942.

References

Abou-Elela, S.I., Hamdy, O., El Monayeri, O., 2016. Modeling and simulation of hybridanaerobic/aerobic wastewater treatment system. Int. J. Environ. Sci. Tech. 13 (5), 1289–1298.

Al-Hazmi, H.E., Lu, X., Majtacz, J., Kowal, P., Xie, L., Makinia, J., 2021. Optimization of the aeration strategies in a deammonification sequencing batch reactor for efficient nitrogen removal and mitigation of N2O production. Environ. Sci. Tech. 55 (2), 1218–1230.

Asadi, A., Verma, A., Yang, K., Mejabi, B., 2017. Wastewater treatment aeration process optimization: A data mining approach. J. Environ. Manage. 203, 630–639.

Azari, M., Aslani, A., Denecke, M., 2020. The effect of the COD: N ratio on mainstream deammonification in an integrated fixed-film activated sludge sequencing batch reactor. Chemosphere 259, 127426. https://doi.org/10.1016/j.chemosphere.2020.127426.

Azari, M., Jurnalis, A., Denecke, M., 2021. The influence of aeration control and temperature reduction on nitrogen removal and microbial community in two anammox-based hybrid sequencing batch biofilm reactors. J. Chem. Tech. Biotech. 96 (12), 3358–3370.

Baeten, J.E., Batstone, D.J., Schraa, O.J., van Loosdrecht, M.C.M., Volcke, E.I.P., 2019. Modelling anaerobic, aerobic and partial nitritation-anammox granular sludge reactors - A review. Water Res. 149, 322–341.

Batstone, D.J., Keller, J., Angelidaki, I., Kalyuzhnyi, S.V., Pavlostathis, S.G., Rozzi, A., Sanders, W.T.M., Siegrist, H.A., Vavilin, V.A., 2002. The IWA anaerobic digestion model no 1 (ADM1). Water Science and technology 45 (10), 65–73.

Chang, K.-H., 2012. Stochastic Nelder-Mead simplex method – A new globally convergent direct search method for simulation optimization. Euro.J. Opera. Res. 220 (3), 684–694.

Chen, J., Zhou, X., Cao, X., Li, S., 2021. Optimizing anammox capacity for weak wastewater in an AnSBBR using aerobic activated sludge as inoculation. J. Environ. Manage. 280, 111649.

Gao, D., Xiang, T., 2021. Deammonification process in municipal wastewater treatment: Challenges and perspectives. Bioresour. Tech. 320, 124420.

Gu, J., Zhang, M., Liu, Y., 2020. A review on mainstream deammonification of municipal wastewater: Novel dual step process. Bioresour. Tech. 299, 122674.
Guven, H., Ersahin, M.E., Dereli, R.K., Ozgun, H., Isik, I., Ozturk, I., 2019. Energy recovery potential of anaerobic digestion of excess sludge from high-rate activated sludge systems co-treating municipal wastewater and food waste. Energy 172, 1027–1036.
Han, M., Vlaeminck, S.E., Al-Omari, A., Wett, B., Bott, C., Murthy, S., De Clippeleir, H., 2016. Uncoupling the solids retention times of flocs and granules in mainstream deammonification: A screen as effective out-selection tool for nitrite oxidizing bacteria. Bioresour. Tech. 221, 195–204.
Hausherr, D., Niederdorfer, R., Morgenroth, E., Joss, A., 2021. Robustness of mainstream anammox activity at bench and pilot scale. Sci. Total Environ. 796, 148920. https://doi.org/10.1016/j.scitotenv.2021.148920.
Henze, M., Gujer, W., Mino, T., Matsuo, T., Wentzel, M.C., Marais, G.V.R., Van Loosdrecht, M.C., 1999. Activated sludge model no. 2d, ASM2d. Water science and technology 39 (1), 165–182.
Hong, Y., Liao, Q., Bonhomme, C., Chebbo, G., 2019. Physically-based urban stormwater quality modelling: An efficient approach for calibration and sensitivity analysis. J. Environ. Manage. 246, 462–471.
Hreiz, R., Latifi, M.A., Roche, N., 2015. Optimal design and operation of activated sludge processes: State-of-the-art. Chem. Eng. J. 281, 900–920.
Izadi, P., Izadi, P., Eldyasti, A., 2021. Towards mainstream deammonification: Comprehensive review on potential mainstream applications and developed sidestream technologies. J. Environ. Manage. 279, 111615.
Jimenez, J., Miller, M., Bott, C., Murthy, S., De Clippeleir, H., Wett, B., 2015. High-rate activated sludge system for carbon management – Evaluation of crucial process mechanisms and design parameters. Water Res. 87, 476–482.
Leix, C., Drewes, J.E., Ye, L., Koch, K., 2017. Strategies for enhanced deammonification performance and reduced nitrous oxide emissions. Bioresour. Tech. 236, 174–185.
Lemaire, R., Christensson, M., 2021. Lessons Learned from 10 Years of ANITA Mox for Sidestream Treatment. Processes 9 (5), 863.
Li, J., Xu K., Liu, T., Bai, G., Liu, Y. 2020. Chengwen Wang, Min Zheng. 2020. Achieving Stable Partial Nitritation in an Acidic Nitrifying Bioreactor. *Environmental Science & Technology* 54 (1), 456-463.
Lochmatter, S., Gonzalez-Gil, G., Holliger, C., 2013. Optimized aeration strategies for nitrogen and phosphorus removal with aerobic granular sludge. Water Res. 47 (16), 6187–6197.
Malovanyy, A., Trela, J., Plaza, E., 2015. Mainstream wastewater treatment in integrated fixed film activated sludge (IFAS) reactor by partial nitritation/anammox process. Bioresour. Tech. 198, 478–487.
Mehrani, M.-J., Lu, X., Kowal, P., Sobotka, D., Mąkinia, J., 2021. Incorporation of the complete ammonia oxidation (comammox) process for modeling nitrification in suspended growth wastewater treatment systems. J. Environ. Manage. 297, 113223.
Mehrani, M.-J., Sobotka, D., Kowal, P., Ciesielski, S., Makinia, J., 2020. The occurrence and role of Nitrospira in nitrogen removal systems. Bioresour. Tech. 303, 122936.
Miao, Y., Zhang, L., Yang, Y., Peng, Y., Li, B., Wang, S., Zhang, Q., 2016. Start-up of single-stage partial nitrification-anammox process treating low-strength swage and its restoration from nitrate accumulation. Bioresour. Tech. 218, 771–779.
Newhart, K.B., Holloway, R.W., Hering, A.S., Cath, T.Y., 2019. Data-driven performance analyses of wastewater treatment plants: A review. Water Res. 157, 498–513.
Nie, S., Lei, X., Zhao, L., Wang, Y.i., Wang, F., Li, H.u., Yang, W., Xing, S., 2018. Response of activity, abundance, and composition of anammox bacterial community to different fertilization in a paddy soil. Biology and Fertility of Soils 54 (8), 977–984.
Park, M.-R., Park, H., Chandran, K., 2017. Molecular and kinetic characterization of planktonic nitrospira spp. selectively enriched from activated sludge. Environ. Sci. Tech. 51 (5), 2720–2728.
Pekyavas, G., Dereli, R.K., Yangin-Gomec, C., 2020. Comparative assessment of modeling and experimental data of ammonia removal from pre-digested chicken manure. J. Environ. Sci. Health, Part A 55 (11), 1333–1338.
Puchongkawarin, C., Gomez-Mont, C., Stuckey, D.C., Chachuat, B., 2015. Optimization-based methodology for the development of wastewater facilities for energy and nutrient recovery. Chemosphere 140, 150–158.
Qiao, J., Zhang, W., 2018. Dynamic multi-objective optimization control for wastewater treatment process. Neural Computing and Applications 29 (11), 1261–1271.
Qiu, S., Hu, Y., Liu, R., Sheng, X., Chen, L., Wu, G., Hu, H., Zhan, X., 2019. Start up of partial nitritation-anammox process using intermittently aerated sequencing batch reactor: Performance and microbial community dynamics. Sci. Total Environ. 647, 1188–1198.
Regmi, P., Miller, M.W., Holgate, B., Bunce, R., Park, H., Chandran, K., Wett, B., Murthy, S., Bott, C.B., 2014. Control of aeration, aerobic SRT and COD input for mainstream nitritation/denitritation. Water Res. 57, 162–171.
Rezaali, M., Karimi, A., Moghadam Yekta, N., Fouladi Fard, R., 2020. Identification of temporal and spatial patterns of river water quality parameters using NLPCA and multivariate statistical techniques. Int. J. Environ. Sci. Tech. 17 (5), 2977–2994.
Ringnér, M., 2008. What is principal component analysis? Nature Biotech. 26 (3), 303–304.
Sean, W.-Y., Chu, Y.-Y., Mallu, L.L., Chen, J.-G., Liu, H.-Y., 2020. Energy consumption analysis in wastewater treatment plants using simulation and SCADA system: Case study in northern Taiwan. J. Clean. Prod. 276, 124248.
Tarre, S., Shlafman, E., Beliavski, M., Green, M., 2007. Changes in ammonia oxidiser population during transition to low pH in a biofilm reactor starting with Nitrosomonas europaea. Water Sci. Tech. 55 (8–9), 363–368.
Van Hulle, S.W.H., Vandeweyer, H.J.P., Meesschaert, B.D., Vanrolleghem, P.A., Dejans, P., Dumoulin, A., 2010. Engineering aspects and practical application of autotrophic nitrogen removal from nitrogen rich streams. Chem. Eng. J. 162 (1), 1–20.
Waqas, S., Bilad, M.R., Man, Z., Wibisono, Y., Jaafar, J., Indra Mahlia, T.M., Khan, A.L., Aslam, M., 2020. Recent progress in integrated fixed-film activated sludge process for wastewater treatment: A review. J. Environ. Manage. 268, 110718.
Wang, L., Gu, W., Liu, Y., Liang, P., Zhang, X., Huang, X., 2022. Challenges, solutions and prospects of mainstream anammox-based process for municipal wastewater treatment. Sci. Total Environ. 820, 153351.
Xu, Z., Zhang, L., Gao, X., Peng, Y., 2020. Optimization of the intermittent aeration to improve the stability and flexibility of a mainstream hybrid partial nitrification-anammox system. Chemosphere 261, 127670.
Yang, S., Xu, S., Boiocchi, R., Mohammed, A., Li, X., Ashbolt, N.J., Liu, Y., 2020. Long-term continuous partial nitritation-anammox reactor aeration optimization at different nitrogen loading rates for the treatment of ammonium rich digestate lagoon supernatant. Process Biochem. 99, 139–146.
Yu, L., Chen, S., Chen, W., Wu, J., 2020. Experimental investigation and mathematical modeling of the competition among the fast-growing “r-strategists” and the slow-growing “K-strategists” ammonium-oxidizing bacteria and nitrite-oxidizing bacteria in nitrification. Sci. Total Environ. 702, 135049. https://doi.org/10.1016/j.scitotenv.2019.135049.
Zhang, Q., Li, Z., Snowling, S., Siam, A., El-Dakhakhni, W., 2019. Predictive models for wastewater flow forecasting based on time series analysis and artificial neural network. Water Sci. Tech. 80 (2), 243–253.
Zhou, J.h., Yu, H.c., Ye, K.q., Wang, H.y., Ruan, Y.j., Yu, J.m. 2019. Optimized aeration strategies for nitrogen removal efficiency: application of end gas recirculation aeration in the fixed bed biofilm reactor. Environmental Science and Pollution Research, 26(27), 28216-28227.